

AD-776 374

A THEORY FOR SUBSONIC AND TRANSONIC  
FLOW OVER A CONE - WITH OR WITHOUT  
SMALL YAW ANGLE

Jain-Ming Wu, et al

Tennessee University Space Institute

Prepared for:

Army Missile Command

December 1973

DISTRIBUTED BY:

**NTIS**

National Technical Information Service  
U. S. DEPARTMENT OF COMMERCE  
5285 Port Royal Road, Springfield Va. 22151

#### DISPOSITION INSTRUCTIONS

DESTROY THIS REPORT WHEN IT IS NO LONGER NEEDED. DO NOT RETURN IT TO THE ORIGINATOR.

#### DISCLAIMER

THE FINDINGS IN THIS REPORT ARE NOT TO BE CONSTRUED AS AN OFFICIAL DEPARTMENT OF THE ARMY POSITION UNLESS SO DESIGNATED BY OTHER AUTHORIZED DOCUMENTS.

ACCESSION For	
NTIS	White Section <input checked="" type="checkbox"/>
DGC	Buff Section <input type="checkbox"/>
UNANNOUNCED	<input type="checkbox"/>
JUSTIFICATION.....	
BY.....	
DISTRIBUTION/AVAILABILITY CODES	
Dist.	AVAIL. and/or SPECIAL
A	

#### TRADE NAMES

USE OF TRADE NAMES OR MANUFACTURERS IN THIS REPORT DOES NOT CONSTITUTE AN OFFICIAL INDORSEMENT OR APPROVAL OF THE USE OF SUCH COMMERCIAL HARDWARE OR SOFTWARE.

## DOCUMENT CONTROL DATA - R &amp; D

(Security classification of title, body of abstract and indexing annotation must be entered when the overall report is classified)

1. ORIGINATING ACTIVITY (Corporate author) US Army Missile Research, Development and Engineering Laboratory US Army Missile Command Redstone Arsenal, Alabama 35809		2a. REPORT SECURITY CLASSIFICATION Unclassified	
		2b. GROUP NA	
3. REPORT TITLE  A THEORY FOR SUBSONIC AND TRANSONIC FLOW OVER A CONE — WITH AND WITHOUT SMALL YAW ANGLE			
4. DESCRIPTIVE NOTES (Type of report and inclusive dates) Technical Report			
5. AUTHOR(S) (First name, middle initial, last name)  Jain-Ming Wu and Robert C. Lock			
6. REPORT DATE December 1973		7a. TOTAL NO. OF PAGES 82	7b. NO. OF REFS 0
8a. CONTRACT OR GRANT NO.  b. PROJECT NO. (DA) 1M262303A214  c. AMC Management Structure Code No. 522C.11.21405  d.		9a. ORIGINATOR'S REPORT NUMBER(S)  RD-74-2  9b. OTHER REPORT NO(S) (Any other numbers that may be assigned this report)	
10. DISTRIBUTION STATEMENT  Approved for public release; distribution unlimited.			
11. SUPPLEMENTARY NOTES  None		12. SPONSORING MILITARY ACTIVITY  Same as No. 1	
13. ABSTRACT <p>The primary purpose of this work was to develop an accurate method of calculating the surface pressure distribution over a conical forebody for a wide range of free-stream Mach numbers, which includes subsonic, transonic, and low supersonic flow.</p> <p>The theoretical approach used was similar to the one previously proposed by Wu and Aoyama. The nondimensionalized small disturbance transonic flow equation was linearized to a variable coefficient elliptic form. A transformation was introduced to further reduce the governing equation to a Laplace form, which yields an integral equation for the transformation function. A first-order solution was obtained by an iterative procedure. The effect due to the small angle of attack has been included by adding the linearized cross flow contribution.</p> <p>Surface pressure distributions calculated by the present method for very slender cones at zero and small angles of attack agree very well with experimental measurements for all Mach numbers up to the shock attachment Mach number.</p> <p>Reproduced by NATIONAL TECHNICAL INFORMATION SERVICE U S Department of Commerce Springfield VA 22151</p> <p>85</p>			

DD FORM 1473  
1 NOV 65REPLACES DD FORM 1473, 1 JAN 64, WHICH IS  
OBSOLETE FOR ARMY USE.UNCLASSIFIED  
Security Classification

**UNCLASSIFIED**  
**Security Classification**

14. KEY WORDS	LINK A		LINK B		LINK C	
	ROLE	WT	ROLE	WT	ROLE	WT
First-order solutions						
Subsonic and transonic flow						
Yaw angle						
Conical flow						

**UNCLASSIFIED**  
**Security Classification**

## CONTENTS

	Page
Section I. INTRODUCTION . . . . .	3
Section II. FIRST ORDER SOLUTION FOR FLOW OVER A CONE . . . .	5
Section III. CALCULATION OF FOREBODY PRESSURE DRAG . . . . .	23
Section IV. COMPARISON OF PRESENT METHOD WITH EXPERIMENTAL RESULTS AND OTHER THEORIES . . . . .	26
Section V. CONCLUSIONS AND RECOMMENDATIONS . . . . .	58
REFERENCES . . . . .	59
Appendix A. DETAILS OF THE NUMERICAL ITERATION PROCEDURE . . .	60
Appendix B. COMPUTER PROGRAM AND SAMPLE OUTPUT . . . . .	69

## PREFACE

This report was prepared by the University of Tennessee Space Institute under US Army Contract No. DAAH01-71-C-1078. The contract was initiated under DA Project No. 1M262303A214 and AMC Management Structure Code No. 522C.11.21405. The technical effort was under the direction of Dr. D. J. Spring of the Aerodynamics Group, Aeroballistic Directorate, US Army Missile Research, Development and Engineering Laboratory, US Army Missile Command, Redstone Arsenal, Alabama.

## Section I. INTRODUCTION

The cone is a very basic aerodynamic shape, yet no single theory exists which predicts accurately the pressure distribution on the surface of a cone for all Mach numbers. Subsonic compressible flow theories [1,2,3] exist which predict accurately the pressure distribution on a body of revolution for all subsonic Mach numbers not too close to one. Supersonic flow theories [3,4] exist which predict accurately the pressure distributions on a body of revolution for a wide range of supersonic Mach numbers above the shock attachment Mach number. Several approximate transonic flow theories exist (such as Yoshihara [5], Leiter and Oswatitsch [6], Spreiter and Alksne [7], and Wu and Aoyama [8]), which predict the pressure distributions on a body of revolution for sonic freestream flow, except Wu and Aoyama's method was intended for various ranges of transonic Mach numbers. A comparison of various transonic theories was given by Wu and Aoyama [9].

It was observed that calculations of the pressure distribution on a cone using the previously developed method of Wu and Aoyama [8] were in very good agreement with experimental data except near the shoulder of the cone. Thus the method is very promising to extended to low Mach number flow. Further investigations of that method showed that at a particular fixed location on the cone surface, the variation of the pressure coefficient with Mach number showed a correct trend for all Mach numbers up to the shock attachment Mach number. The only deficiencies seemed to be at low subsonic Mach numbers where the experimentally determined pressure coefficients were constantly lower than the Wu-Aoyama calculated values, and near the cone shoulder, where the experimental values were again lower than the theoretical values. Both of these deficiencies, however, were attributed to the fact that Wu and Aoyama had neglected one term in their solution because of problems encountered in their numerical iteration scheme.

The subsonic theory,<sup>11</sup> on the other hand, showed very good agreement with data for low Mach numbers, but the theoretical pressure coefficient at a fixed position on the cone surface displayed an incorrect trend with Mach number near a Mach number of unity. This deficiency was attributed to the Prandtl-Glauert form of the governing equation which becomes inadequate near a Mach number of one.

In view of the previous observations, it was decided that accounting for the neglected term in the previous Wu and Aoyama calculation might improve the solution near the cone shoulder and perhaps improve the subsonic solution as well. Therefore, a modified approach was taken for

this investigation. This improved and more consistent inviscid flow theory has been employed to predict the surface pressure distribution on a conical forebody at zero and small angles of yaw for subsonic and transonic Mach numbers up to the supersonic shock attachment Mach number. Unlike the original solution of Wu and Aoyama, no terms in the present analysis were explicitly neglected. In view of the observation of the fact that the solutions agree very well with data even to a very low subsonic flow, the current method, though it is only a first-order approximation, provides a means of solution from subsonic to transonic Mach numbers. Thus, incorporating this supersonic conical theory when the shock attached to the body, one can solve the entire Mach number range with continuity.

## Section II. FIRST ORDER SOLUTION FOR FLOW OVER A CONE

The nondimensional transonic small perturbation equation can be written as [8]:

$$\left[ (1 - M_\infty^2) - (\gamma + 1) M_\infty^2 \phi_{\bar{x}} \right] \phi_{\bar{x}\bar{x}} + \phi_{\bar{r}\bar{r}} + \frac{\phi_{\bar{r}}}{\bar{r}} + \frac{\phi_{\theta\theta}}{\bar{r}^2} = 0 \quad (1)$$

where all lengths are normalized with respect to the axial length of the cone (Figure 1) and all perturbation velocities are normalized with respect to the free-stream velocity,  $U_\infty$ . Thus,

$$\bar{x} = \frac{x}{L}, \quad \bar{r} = \frac{r}{L}$$

and

$$\phi_{\bar{x}} = \frac{u}{U_\infty}, \quad \phi_{\bar{r}} = \frac{v}{U_\infty}, \quad \frac{\phi_{\theta}}{\bar{r}} = \frac{w}{U_\infty}.$$

In transonic flow over a cone, the sonic velocity is fixed very close to the shoulder and the flow on the surface over the entire conical forebody is subsonic, provided the shock wave is not yet attached to the cone [1]. Hence, the coefficient of  $\phi_{\bar{x}\bar{x}}$  can be expected to remain greater than zero.

Using the same linearization technique as Wu and Aoyama originally proposed [8], let

$$f^2(\bar{x}) \equiv (1 - M_\infty^2) - (\gamma + 1) M_\infty^2 \phi_{\bar{x}} \quad (2)$$

and assume  $f(\bar{x})$  is a known function. The value will be determined later. By this process, Equation (1) is linearized to the form

$$f^2 \phi_{\bar{x}\bar{x}} + \phi_{\bar{r}\bar{r}} + \frac{1}{\bar{r}} \phi_{\bar{r}} + \frac{1}{\bar{r}^2} \phi_{\theta\theta} = 0 \quad (3)$$

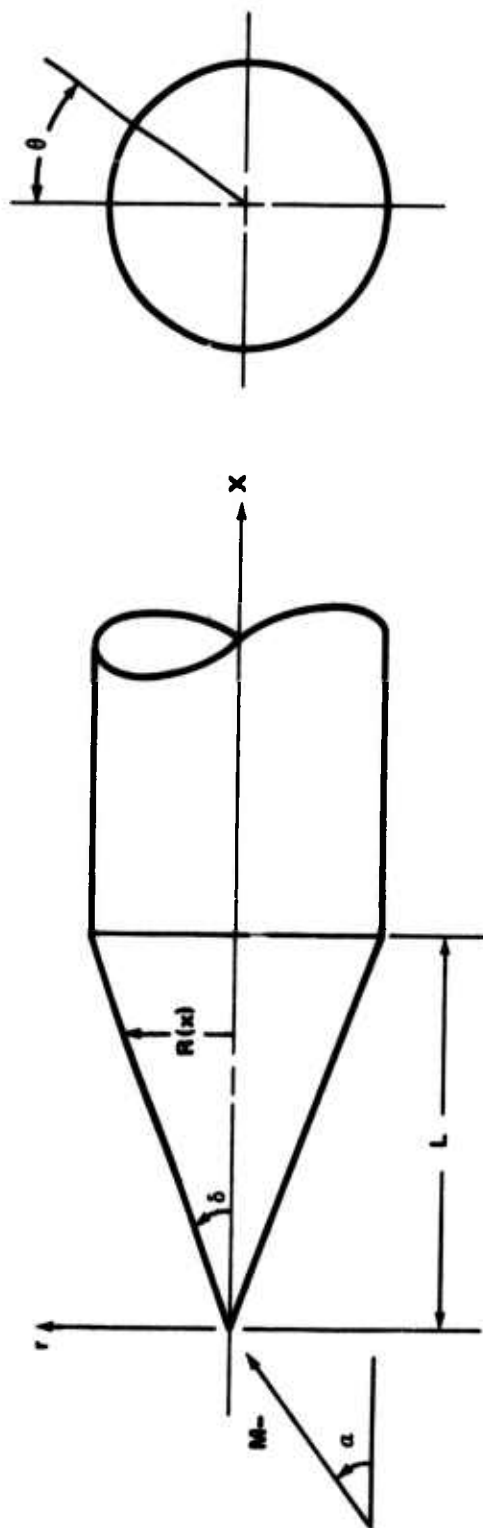


Figure 1. Nomenclature of cone cylinder.

Now introduce a new independent variable,  $\xi$ , defines as\*

$$\frac{f[\bar{x}(\xi)]}{\beta} = \frac{d\bar{x}}{d\xi} ,$$

or

$$\bar{x}(\xi) = \frac{1}{\beta} \int_0^{\xi} f(t) dt . \quad (4)$$

By using a chain rule

$$\frac{\partial}{\partial \bar{x}} = \frac{\partial}{\partial \xi} \frac{\partial \xi}{\partial \bar{x}} ; \frac{\partial^2}{\partial \bar{x}^2} = \left( \frac{\partial \xi}{\partial \bar{x}} \right)^2 \frac{\partial^2}{\partial \xi^2} + \frac{\partial^2 \xi}{\partial \bar{x}^2} \frac{\partial}{\partial \xi} ,$$

Equation (3) is reduced to

$$\beta^2 \phi_{\xi\xi} - \beta f'(\bar{x}) \phi_{\xi} + \frac{1}{r} \frac{\partial}{\partial r} (\bar{r} \phi_{\bar{r}}) + \frac{1}{r^2} \phi_{\theta\theta} = 0 . \quad (5a)$$

In order to solve this equation, it is realized that  $f'(\bar{x})$  is very small. In fact,  $f'(\bar{x})$  is zero for the low subsonic compressible flow case, between as the free-stream Mach number is very less than unity,

$$f(\bar{x}) \rightarrow \beta = \sqrt{1 - M_{\infty}^2} ,$$

which is a constant. The term containing  $\phi_{\xi}$  contributes only as the Mach number approaches unity. Therefore, an approximation method may be employed.

Rewrite Equation (5a) as

$$\beta^2 \phi_{\xi\xi} - K(\epsilon) \phi_{\xi} + \frac{1}{r} \frac{\partial}{\partial r} (\bar{r} \phi_{\bar{r}}) + \frac{1}{r^2} \phi_{\theta\theta} = 0 \quad (5b)$$

---

\*The factor,  $\beta = \sqrt{1 - M_{\infty}^2}$ , can be absorbed in the transformation of coordinates as in the original report [1]. However, it behaves as a constant in transformation; thus, it will not affect the final result.

where  $K(\epsilon)$  is a higher order small function. Assume that the complete solution may be expressed as

$$\phi = \phi_0 + \phi_1 + \dots \quad (6)$$

where  $\phi_0$  is the first-order solution corresponding to  $K(\epsilon) = 0$ , and  $\phi_1$  is the second-order solution.  $\phi_0$  and  $\phi_1$  satisfy the following equations:

$$\beta^2 \phi_0_{\xi\xi} + \frac{1}{\bar{r}} \frac{\partial}{\partial \bar{r}} \left( \bar{r} \phi_{0\bar{r}} \right) + \frac{1}{\bar{r}^2} \phi_{0\theta\theta} = 0 \quad (7a)$$

and

$$\beta^2 \phi_1_{\xi\xi} + \frac{1}{\bar{r}} \frac{\partial}{\partial \bar{r}} \left( \bar{r} \phi_{1\bar{r}} \right) + \frac{1}{\bar{r}^2} \phi_{1\theta\theta} = K(\epsilon) \phi_{0\xi} \quad (7b)$$

A method of successive approximation can be set up to obtain the complete solution. In this study, only the first approximation is treated and yields a very satisfactory result.\* From here on, the subscript 0 for the first-order solution is dropped for simplicity.

The contribution due to the cross flow is assumed to be small if the angle of attack is small. Let  $\phi_a$  be the axial flow component and  $\phi_c$  be the cross flow contribution; then it is assumed that the non-dimensional perturbation velocity potential,  $\phi$ , is composed of

$$\phi(\xi, \bar{r}, \theta) = \phi_a(\xi, \bar{r}) + \phi_c(\xi, \bar{r}, \theta) \quad (8)$$

The linearized cross flow solution for slender bodies of revolution according to [1] is:

$$\phi_c(\xi, \bar{r}, \theta) = \sin \alpha \cos \theta \frac{\bar{R}^2(\xi)}{\bar{r}} \quad (9)$$

---

\*It was observed that the transformation function,  $f$ , is nearly constant, which accounts for a small value of  $f'$ ; hence, good agreement with data results even for the first approximation.

where

$$\bar{R}(\xi) = \frac{R(\xi)}{L} ,$$

and the general solution of Equation (7a) for the axial flow is [1]:

$$\phi_a(\xi, \bar{r}) = -\frac{1}{4\pi} \int_0^{\xi^*} \frac{F(t)}{\sqrt{(\xi - t)^2 + \beta \bar{r}^2}} dt \quad (10)$$

where  $\xi^*$  is the value attained by  $\xi$  at the shoulder of the cone (at  $\bar{x} = 1$ ), and  $F(t)$  is the source distribution which can be determined from the boundary conditions.

Van Dyke [3] shows that Equation (10) can be expressed by the following first-order approximation:

$$\phi_a(\xi, \bar{r}) = \frac{F(\xi)}{2\pi} \ln \bar{r} + G(\xi) \quad (11)$$

where

$$G(\xi) = \frac{F(\xi)}{2\pi} \ln \frac{\beta}{2\sqrt{\xi(\xi^* - \xi)}} + \frac{1}{4\pi} \int_0^{\xi^*} \frac{F(\xi) - F(t)}{|\xi - t|} dt \quad (12)$$

Hence,

$$\begin{aligned} \phi_a(\xi, \bar{r}) &= \frac{F(\xi)}{2\pi} \ln \bar{r} + \frac{F(\xi)}{2\pi} \ln \frac{\beta}{2\sqrt{\xi(\xi^* - \xi)}} \\ &+ \frac{1}{4\pi} \int_0^{\xi^*} \frac{F(\xi) - F(t)}{|\xi - t|} dt \quad (13) \end{aligned}$$

The boundary condition for inviscid flow requires tangential flow on the surface of the cone. In terms of the untransformed variables, this boundary condition is expressed as:

$$\begin{aligned} \left. \frac{\partial \phi_a(\bar{x}, \bar{r})}{\partial \bar{r}} \right|_{\text{on the body}} &= \frac{d\bar{R}(\bar{x})}{d\bar{x}} \\ &= \tan \delta \approx \delta \quad (14) \end{aligned}$$

for small angles where  $\delta$  is the half angle of the cone measured in radians.

Because  $\bar{r}$  was affected little by the transformation, the boundary condition in terms of the transformed variables [10] becomes:

$$\frac{\partial \phi_a}{\partial \bar{r}}(\xi, \bar{r}) \approx \delta \quad \text{on the body} \quad (15)$$

Now the source distribution  $F(\xi)$  can be found by differentiation of Equation (11) with respect to  $\bar{r}$ .

$$\frac{\partial \phi_a(\xi, \bar{r})}{\partial \bar{r}} = \frac{F(\xi)}{2\pi \bar{r}} \quad ; \quad (16)$$

hence,

$$F(\xi) = 2\pi \bar{r} \frac{\partial \phi_a}{\partial \bar{r}} \quad (17)$$

Now on the body

$$\bar{r} = \bar{R} \quad , \quad (18)$$

and from Equation (14)

$$\delta \approx \frac{d\bar{R}}{d\bar{x}} \quad , \quad (19)$$

which implies

$$\bar{R}(\xi) = \delta \bar{x}(\xi) \quad . \quad (20)$$

By substituting Equations (15), (18), and (20) into Equation (17), we obtain:

$$F(\xi) = 2\pi \delta^2 \bar{x}(\xi) \quad . \quad (21)$$

Now by substituting Equation (4) into Equation (21), we obtain:

$$F(\xi) = \frac{2\pi\delta^2}{\beta} \int_0^{\xi} f(t)dt \quad (22)$$

Substitution of Equation (22) into Equation (13) gives the following expression for the axial flow velocity potential in terms of the unknown function,  $f(\xi)$ :

$$\begin{aligned} \phi_a(\xi, \bar{r}) = & \frac{(\ln \bar{r})\delta^2}{\beta} \int_0^{\xi} f(t)dt + \frac{\delta^2}{\beta} \int_0^{\xi} f(t)dt \left[ \ln \frac{\beta}{2\sqrt{\xi(\xi^* - \xi)}} \right] \\ & + \frac{\delta^2}{2\beta} \int_0^{\xi^*} \frac{\int_0^{\xi} f(t)dt - \int_0^t f(s)ds}{|\xi - t|} dt \quad (23) \end{aligned}$$

Combine Equations (20), (4), and (9); then the cross flow velocity potential may be expressed in terms of  $f(\xi)$  by:

$$\phi_c(\xi, \bar{r}, \theta) = \sin \alpha \cos \theta \frac{\delta^2}{\beta^2 \bar{r}} \left[ \int_0^{\xi} f(t)dt \right]^2 \quad (24)$$

Combination of Equations (8), (23), and (24) provides an expression for the total velocity potential which satisfies Equation (7a).

$$\begin{aligned} \phi(\xi, \bar{r}, \theta) = & \frac{(\ln \bar{r})\delta^2}{\beta} \int_0^{\xi} f(t)dt + \frac{\delta^2}{\beta} \int_0^{\xi} f(t)dt \left[ \ln \frac{\beta}{2\sqrt{\xi(\xi^* - \xi)}} \right] \\ & + \frac{\delta^2}{2\beta} \int_0^{\xi^*} \frac{\int_0^{\xi} f(t)dt - \int_0^t f(s)ds}{|\xi - t|} dt \\ & + \sin \alpha \cos \theta \frac{\delta^2}{\beta^2 \bar{r}} \left[ \int_0^{\xi} f(t)dt \right]^2 \quad (25) \end{aligned}$$

Now one is in a position to solve for the unknown function,  $f(\xi)$ . From Equation (2),

$$\phi_{\bar{x}} = \left[ \frac{(1 - M_{\infty}^2) - f^2(\xi)}{(\gamma + 1)M_{\infty}^2} \right] , \quad (26)$$

and from Equation (4),

$$\frac{d\xi}{d\bar{x}} = \frac{\beta}{f(\xi)} . \quad (27)$$

Thus, the chain rule gives:

$$\frac{\partial \phi}{\partial \bar{x}} = \frac{\partial \phi}{\partial \xi} \frac{\partial \xi}{\partial \bar{x}} \quad (28)$$

or

$$\frac{\partial \phi}{\partial \bar{x}} = \frac{\beta}{f(\xi)} \frac{\partial \phi}{\partial \xi} . \quad (29)$$

Another expression for  $\phi_{\bar{x}}$  can now be obtained by differentiation of Equation (25) with respect to  $\bar{x}$ . Then by equating the two expressions for  $\phi_{\bar{x}}$  an integral equation for  $f(\xi)$  is formed.

For the sake of orderliness when differentiating, Equation (25) can be rewritten as follows:

$$\phi(\xi, \bar{r}, \theta) = \phi_{a_1} + \phi_{a_2} + \phi_{a_3} + \phi_c , \quad (30)$$

and then one can differentiate each term separately to obtain:

$$\phi_{\bar{x}} = \frac{\beta}{f(\xi)} \left[ \frac{\partial \phi_{a_1}}{\partial \xi} + \frac{\partial \phi_{a_2}}{\partial \xi} + \frac{\partial \phi_{a_3}}{\partial \xi} + \frac{\partial \phi_c}{\partial \xi} \right] . \quad (31)$$

Term  $\phi_{a_3}$ :

$$\phi_{a_3} = \frac{\delta^2}{2\beta} \int_0^{\xi^*} \frac{\int_0^{\xi} f(t)dt - \int_0^{\xi} f(s)ds}{|\xi - t|} dt \quad (38)$$

or

$$\phi_{a_3}(\xi, \bar{r}) = \frac{\delta^2}{2\beta} I_0^{\xi^*} \quad , \quad (39)$$

where  $I_0^{\xi^*}$  is the subsonic slender body integral defined by Van Dyke [3]:

$$I_0^{\xi^*} = \int_0^{\xi^*} \frac{F(\xi) - F(t)}{|\xi - t|} dt \quad , \quad (40)$$

and the derivative of this integral is

$$\begin{aligned} I_0^{\xi^*'} &= \int_0^{\xi^*} \frac{F'(\xi) - F'(t)}{|\xi - t|} dt + \frac{F(\xi) - F(0)}{\xi - 0} \\ &+ \frac{F(\xi^*) - F(\xi)}{\xi^* - \xi} \quad . \end{aligned} \quad (41)$$

Now,

$$\frac{\partial \phi_{a_3}}{\partial \xi} = \frac{\delta^2}{2\beta} I_0^{\xi^*'} \quad . \quad (42)$$

From Equations (4), (38), (39), and (40),

$$\begin{aligned} F(\xi) &= \int_0^{\xi} f(t)dt \quad , \\ F(\xi^*) &= \int_0^{\xi^*} f(t)dt = \beta \quad , \end{aligned}$$

Consider now the terms on the right-hand side of Equation (30):

Term  $\phi_{a_1}$ :

$$\phi_{a_1} = \frac{(\ln \bar{r})\delta^2}{\beta} \int_0^{\xi} f(t)dt \quad ; \quad (32)$$

differentiation gives:

$$\frac{\partial \phi_{a_1}}{\partial \xi} = \frac{(\ln \bar{r})\delta^2}{\beta} f(\xi) \quad . \quad (33)$$

Term  $\phi_{a_2}$ :

$$\phi_{a_2} = \frac{\delta^2}{\beta} \int_0^{\xi} f(t)dt \left[ \ln \frac{\beta}{2\sqrt{\xi(\xi^* - \xi)}} \right] \quad ; \quad (34)$$

now,

$$\frac{d}{d\xi} \left[ \int_0^{\xi} f(t)dt \right] = f(\xi) \quad (35)$$

and

$$\frac{d}{d\xi} \left[ \ln \frac{\beta}{2\sqrt{\xi(\xi^* - \xi)}} \right] = - \frac{(\xi^* - 2\xi)}{2\xi(\xi^* - \xi)} \quad ; \quad (36)$$

therefore,

$$\begin{aligned} \frac{\partial \phi_{a_2}}{\partial \xi} &= f(\xi) \frac{\delta^2}{\beta} \ln \frac{\beta}{2\sqrt{\xi(\xi^* - \xi)}} \\ &\quad - \frac{\delta^2(\xi^* - 2\xi)}{2\beta\xi(\xi^* - \xi)} \int_0^{\xi} f(t)dt \quad . \quad (37) \end{aligned}$$

$$F'(\xi) = f(\xi) \quad ,$$

$$F(t) = \int_0^t f(s) ds \quad ,$$

$$F'(t) = f(t) \quad ,$$

$$F(0) = 0 \quad . \quad (43)$$

Combine Equations (41), (42), and (43) and obtain:

$$\frac{\partial \phi_a}{\partial \xi} = \frac{\delta^2}{2\beta} \int_0^{\xi^*} \frac{f(\xi) - f(t)}{|\xi - t|} dt + \frac{\delta^2}{2\beta\xi} \int_0^{\xi} f(t) dt + \frac{\delta^2}{2\beta} \left[ \frac{\beta - \int_0^{\xi} f(t) dt}{\xi^* - \xi} \right] . \quad (44)$$

Term  $\phi_c$ :

$$\phi_c = \sin \alpha \cos \theta \frac{\delta^2}{\xi^2 \bar{r}} \left[ \int_0^{\xi} f(t) dt \right]^2 ; \quad (45)$$

differentiation gives:

$$\frac{\partial \phi_c}{\partial \xi} = \frac{2f(\xi)\delta^2}{\xi^2 \bar{r}} \sin \alpha \cos \theta \int_0^{\xi} f(t) dt \quad . \quad (46)$$

Now combine Equations (31), (33), (37), (44), and (46) to obtain:

$$\begin{aligned} \phi_x(\xi, \bar{r}, \theta) = & \delta^2 \ln \bar{r} + \delta^2 \ln \frac{\beta}{2 \sqrt{\xi(\xi^* - \xi)}} \\ & - \frac{\delta^2(\xi^* - 2\xi)}{2\xi f(\xi)(\xi^* - \xi)} \int_0^{\xi} f(t) dt + \frac{\delta^2}{2f(\xi)} \int_0^{\xi^*} \frac{f(\xi) - f(t)}{|\xi - t|} dt \end{aligned}$$

$$\begin{aligned}
& + \frac{\delta^2}{2\xi f(\xi)} \int_0^\xi f(t) dt + \frac{\delta^2}{2f(\xi)} \left[ \frac{\beta - \int_0^\xi f(t) dt}{\xi^* - \xi} \right] \\
& + \frac{2\delta^2}{\beta \bar{r}} \sin \alpha \cos \theta \int_0^\xi f(t) dt \quad . \quad (47)
\end{aligned}$$

Equate Equations (26) and (47) to form an integral equation for  $f(\xi)$ :

$$\begin{aligned}
& \frac{(1 - M_\infty^2)}{(\gamma + 1)M_\infty^2} - \frac{f^2(\xi)}{(\gamma + 1)M_\infty^2} = \delta^2 \ln \bar{r} + \delta^2 \ln \frac{\beta}{2\sqrt{\xi(\xi^* - \xi)}} \\
& - \frac{\delta^2}{2\xi f(\xi)} \frac{(\xi^* - 2\xi)}{(\xi^* - \xi)} \int_0^\xi f(t) dt + \frac{\delta^2}{2f(\xi)} \int_0^{\xi^*} \frac{f(\xi) - f(t)}{|\xi - t|} dt \\
& + \frac{\delta^2}{2\xi f(\xi)} \int_0^\xi f(t) dt + \frac{\delta^2}{2f(\xi)} \left[ \frac{\beta - \int_0^\xi f(t) dt}{\xi^* - \xi} \right] \\
& + \frac{2\delta^2}{\beta \bar{r}} \sin \alpha \cos \theta \int_0^\xi f(t) dt \quad . \quad (48)
\end{aligned}$$

On the body,

$$\bar{r} = \bar{R}(\xi) \quad . \quad (49)$$

Substitute Equations (4) and (20) into Equation (49) to obtain an expression for  $\bar{r}$  on the body in terms of  $\xi$ :

$$\bar{r} \Big|_{\text{on the body}} = \frac{\delta}{\beta} \int_0^\xi f(t) dt \quad . \quad (50)$$

Substitute Equation (50) into Equation (48), multiply through by  $f(\xi)$ , and rearrange terms to obtain:

$$\begin{aligned}
f^3(\xi) = & \left(1 - M_\infty^2\right) f(\xi) + (\gamma + 1) M_\infty^2 \left[ -f(\xi) \delta^2 \ln \left( \frac{\delta}{\beta} \int_0^\xi f(t) dt \right) \right. \\
& - f(\xi) \delta^2 \ln \frac{\beta}{2 \sqrt{\xi(\xi^* - \xi)}} + \frac{\delta^2}{2\xi} \frac{(\xi^* - 2\xi)}{(\xi^* - \xi)} \int_0^\xi f(t) dt \\
& - \frac{\delta^2}{2} \int_0^{\xi^*} \frac{f(\xi) - f(t)}{|\xi - t|} dt - \frac{\delta^2}{2\xi} \int_0^\xi f(t) dt \\
& \left. - \frac{\delta^2}{2} \left( \frac{\beta - \int_0^\xi f(t) dt}{(\xi^* - \xi)} \right) - 2f(\xi) \delta \sin \alpha \cos \theta \right] . \quad (51)
\end{aligned}$$

Now factor a  $\delta^2/2$  term from some of the terms on the right-hand side of Equation (51), combine the two logarithmic terms, and obtain, finally:

$$\begin{aligned}
f^3(\xi) = & \left[ \left(1 - M_\infty^2\right) - 2\delta (\gamma + 1) M_\infty^2 \sin \alpha \cos \theta \right] f(\xi) \\
& + \frac{\delta^2}{2} (\gamma + 1) M_\infty^2 \left[ -2f(\xi) \ln \left( \frac{\delta \int_0^\xi f(t) dt}{2 \sqrt{\xi(\xi^* - \xi)}} \right) \right. \\
& + \frac{(\xi^* - 2\xi)}{\xi(\xi^* - \xi)} \int_0^\xi f(t) dt - \int_0^{\xi^*} \frac{f(\xi) - f(t)}{|\xi - t|} dt \\
& \left. - \frac{1}{\xi} \int_0^\xi f(t) dt - \left( \frac{\beta - \int_0^\xi f(t) dt}{(\xi^* - \xi)} \right) \right] . \quad (52)
\end{aligned}$$

The boundary conditions for Equation (52) are as follows:

a) The cone apex ( $\xi = 0$ ) is assumed to be a stagnation point for zero and small angles of attack. Thus, the total velocity (i.e., the

sum of the free-stream velocity and the perturbation velocity) has to be zero. Hence,

$$U_{\infty} + U_{\infty} \phi_{\bar{x}}(0) = 0 \quad (53)$$

or

$$\phi_{\bar{x}}(0) = -1 \quad (54)$$

It must be noted that Equation (54) is only approximately true since at the stagnation point the small disturbance assumption is violated. Hence, the present solution is not correct at the stagnation point. However, for a sharp slender cone, the stagnation region is very small and the error in the vicinity of the stagnation region does not affect the solution over the rest of the cone. Substitution of Equation (54) into Equation (2) gives the boundary condition on  $f(\xi)$  at the stagnation point, namely,

$$f(0) = \left[ \left( 1 - M_{\infty}^2 \right) + (\gamma + 1) M_{\infty}^2 \right]^{1/2} \quad (55)$$

b) The shoulder of the cone ( $\xi = \xi^*$ ) has been assumed as the location of the sonic velocity. It is here that the governing equation changes from elliptic to parabolic and hence it is expected that

$$f(\xi^*) = 0 \quad (56)$$

Now it is observed that a solution to the integral equation [Equation (52)] is dependent on a dimensional parameter,  $\xi$ . Since very little is known about this quantity except that it varies from zero at  $\bar{x} = 0$  to  $\xi^*$  at  $\bar{x} = 1$ , it is necessary to nondimensionalize Equation (52) with respect to  $\xi^*$  in order to have an independent variable which varies between zero and one.

The following transformation nondimensionalizes Equation (52) with respect to  $\xi^*$  to make it possible to solve for  $f(\xi)$  and at the same time eliminates  $\beta$  entirely from the equation, thus allowing real solutions for  $f(\xi)$  up to the supersonic shock attachment Mach numbers. Let

$$\bar{\xi} = \frac{\xi}{\beta \xi^{**}} \quad (57)$$

where  $\xi^{**}$  is the value of  $\xi/\beta$  at the shoulder of the cone such that  $0 \leq \bar{\xi} \leq 1$ . Thus,

$$\xi = \beta \xi^{**} \bar{\xi} \quad , \quad (58)$$

and at the shoulder

$$\xi^* = \beta \xi^{**} \quad . \quad (59)$$

The chain rule gives:

$$\frac{\partial}{\partial \xi} = \frac{\partial}{\partial \bar{\xi}} \frac{\partial}{\partial \xi} = \frac{1}{\beta \xi^{**}} \frac{\partial}{\partial \bar{\xi}} \quad (60)$$

and

$$\frac{\partial^2}{\partial \xi^2} = \frac{\partial}{\partial \bar{\xi}} \frac{\partial}{\partial \bar{\xi}} \left( \frac{1}{\beta \xi^{**}} \frac{\partial}{\partial \bar{\xi}} \right) = \frac{1}{\beta^2 \xi^{**2}} \frac{\partial^2}{\partial \bar{\xi}^2} \quad . \quad (61)$$

This transformation transforms Equation (7a) to:

$$\frac{\phi_{\bar{\xi}\bar{\xi}}}{\xi^{**2}} + \phi_{\bar{r}\bar{r}} + \frac{\phi_{\bar{r}}}{\bar{r}} + \frac{\phi_{\theta\theta}}{\bar{r}^2} = 0 \quad , \quad (62)$$

and Equation (2) becomes:

$$f^2(\bar{\xi}) = \left(1 - M_\infty^2\right) - (\gamma + 1) M_\infty^2 \phi_{\bar{x}} \quad ; \quad (63)$$

therefore,

$$\phi_{\bar{x}} = \frac{\left(1 - M_\infty^2\right) - f^2(\bar{\xi})}{(\gamma + 1) M_\infty^2} \quad . \quad (64)$$

Equation (4) can be rewritten:

$$f(\bar{\xi}) = \frac{1}{\xi^{**}} \frac{d\bar{x}}{d\bar{\xi}} \quad , \quad (65)$$

and integration of Equation (65) gives:

$$\bar{x}(\bar{\xi}) = \xi^{**} \int_0^{\bar{\xi}} f(s) ds \quad . \quad (66)$$

Now substitute Equations (58) and (59) into Equation (52) to get an integral equation which can be solved for  $f(\bar{\xi})$  by numerical iteration methods.

$$\begin{aligned} f^3(\bar{\xi}) = & \left[ \left( 1 - M_{\infty}^2 \right) - 2\delta (\gamma + 1) M_{\infty}^2 \sin \alpha \cos \theta \right] f(\bar{\xi}) \\ & + \frac{\delta^2}{2} (\gamma + 1) M_{\infty}^2 \left[ -2f(\bar{\xi}) \ln \left( \frac{\delta \int_0^{\bar{\xi}} f(\bar{t}) \beta \xi^{**} d\bar{t}}{2 \sqrt{\beta \xi^{**} \bar{\xi} (\beta \xi^{**} - \beta \xi^{**} \bar{\xi})}} \right) \right. \\ & + \frac{(\beta \xi^{**} - 2\beta \xi^{**} \bar{\xi})}{\beta \xi^{**} \bar{\xi} (\beta \xi^{**} - \beta \xi^{**} \bar{\xi})} \int_0^{\bar{\xi}} f(\bar{t}) \beta \xi^{**} d\bar{t} \\ & - \int_0^1 \frac{f(\bar{\xi}) - f(\bar{t})}{|\beta \xi^{**} \bar{\xi} - \beta \xi^{**} \bar{t}|} \beta \xi^{**} d\bar{t} - \frac{1}{\beta \xi^{**} \bar{\xi}} \int_0^{\bar{\xi}} f(\bar{t}) \beta \xi^{**} d\bar{t} \\ & \left. - \left( \frac{\beta - \int_0^{\bar{\xi}} f(\bar{t}) \beta \xi^{**} d\bar{t}}{(\beta \xi^{**} - \beta \xi^{**} \bar{\xi})} \right) \right] \quad . \quad (67) \end{aligned}$$

Cancel  $\beta$  and  $\xi^{**}$  terms and the final form of the integral equation for  $f(\bar{\xi})$  becomes:

$$f^3(\bar{\xi}) = \left[ \left( 1 - M_{\infty}^2 \right) - 2\delta (\gamma + 1) M_{\infty}^2 \sin \alpha \cos \theta \right] f(\bar{\xi})$$

$$\begin{aligned}
& + \frac{\delta^2}{2} (\gamma + 1) M_\infty^2 \left[ -2f(\bar{\xi}) \ln \left( \frac{\delta \int_0^{\bar{\xi}} f(\bar{\tau}) d\bar{\tau}}{2 \sqrt{\bar{\xi}(1 - \bar{\xi})}} \right) \right. \\
& + \frac{(1 - 2\bar{\xi})}{\bar{\xi}(1 - \bar{\xi})} \int_0^{\bar{\xi}} f(\bar{\tau}) d\bar{\tau} - \int_0^1 \frac{f(\bar{\xi}) - f(\bar{\tau})}{|\bar{\xi} - \bar{\tau}|} d\bar{\tau} \\
& \left. - \frac{1}{\bar{\xi}} \int_0^{\bar{\xi}} f(\bar{\tau}) d\bar{\tau} - \left( \frac{\frac{1}{\xi^{**}} - \int_0^{\bar{\xi}} f(\bar{\tau}) d\bar{\tau}}{(1 - \bar{\xi})} \right) \right] . \quad (68)
\end{aligned}$$

Where

$$f(0) = \left[ (1 - M_\infty^2) + (\gamma + 1) M_\infty^2 \right]^{1/2} , \quad (69)$$

$$f(1) = 0 , \quad (70)$$

keep in mind that

$$\bar{x}(\bar{\xi}) = \xi^{**} \int_0^{\bar{\xi}} f(\bar{\tau}) d\bar{\tau} , \quad (71)$$

$$\bar{x}(0) = 0 \quad (72)$$

at the shoulder

$$\bar{x}(1) = \xi^{**} \int_0^1 f(\bar{\tau}) d\bar{\tau} = 1 ; \quad (73)$$

thus,

$$\xi^{**} = \frac{1}{\int_0^1 f(\bar{\tau}) d\bar{\tau}} ; \quad (74)$$

repeating Equation (64),

$$\phi_x^- = \frac{(1 - M_\infty^2) - f^2(\bar{\xi})}{(\gamma + 1)M_\infty^2}, \quad (75)$$

and, finally, the pressure coefficient on the surface of the cone is given by [8]:

$$C_p = -2\phi_x^- - \delta^2 + (1 - 4 \sin^2 \theta) \sin^2 \alpha. \quad (76)$$

The pressure coefficient on the cone is then determined as in the following paragraphs.

Equation (68) is solved for  $f(\bar{\xi})$  by numerical iteration using the Wu-Aoyama solution as the first approximation. The iteration is halted when a particular test condition is satisfied.

The values of  $f(\bar{\xi})$  of the last iteration are then used to calculate  $\phi_x^-$  according to Equation (75), and the pressure coefficient,  $C_p$ , is calculated from Equation (76).

Solutions for  $C_p$  can be calculated for all Mach numbers from zero to the shock attachment Mach number.

A more detailed explanation of the numerical iteration technique is presented in Appendix A, along with a computer program listing in Appendix B.

The present procedure is more consistent than that used by Wu and Aoyama because both the source strength,  $F(\xi)$ , and the velocity,  $\phi_x^-(\xi, \bar{r}, \theta)$ , were obtained from Equation (11). Wu and Aoyama, on the other hand, used the approximate equation [Equation (11)] to determine the source strength,  $F(\xi)$ , but then used the more exact equation [Equation (10)] to solve for the velocity.

### Section III. CALCULATION OF FOREBODY PRESSURE DRAG

For zero angle of attack, the pressure,  $p$ , at an arbitrary section,  $\bar{x}$  (Figure 2), acts on the projected area,  $d\bar{S}(\bar{x})$ , to produce an elemental force in the axial direction. The free-stream pressure,  $p_\infty$ , acts at the base of the cone-cylinder combination to produce a force in the opposite direction. Hence, the total drag on the forebody can be calculated by integration of the net pressure  $(p - p_\infty)$ , which acts on each elemental area,  $d\bar{S}(\bar{x})$ .

$$D_1 = \int_{\bar{x}=0}^1 (p - p_\infty) d\bar{S}(\bar{x}) \quad . \quad (77)$$

Now

$$d\bar{S}(\bar{x}) = 2\pi\bar{R}(\bar{x})d\bar{R}(\bar{x}) = 2\pi\bar{R}(\bar{x}) \frac{d\bar{R}(\bar{x})}{d\bar{x}} d\bar{x} \quad (78)$$

and

$$\frac{d\bar{R}(\bar{x})}{d\bar{x}} = \tan \delta \approx \delta \quad (79)$$

for small angles; hence,

$$\bar{R}(\bar{x}) = \delta \bar{x} \quad , \quad (80)$$

and

$$d\bar{S}(\bar{x}) = 2\pi\delta^2 \bar{x}d\bar{x} \quad . \quad (81)$$

The net pressure force can be expressed in terms of the pressure coefficient

$$C_p = \frac{p - p_\infty}{q_\infty} \quad (82)$$

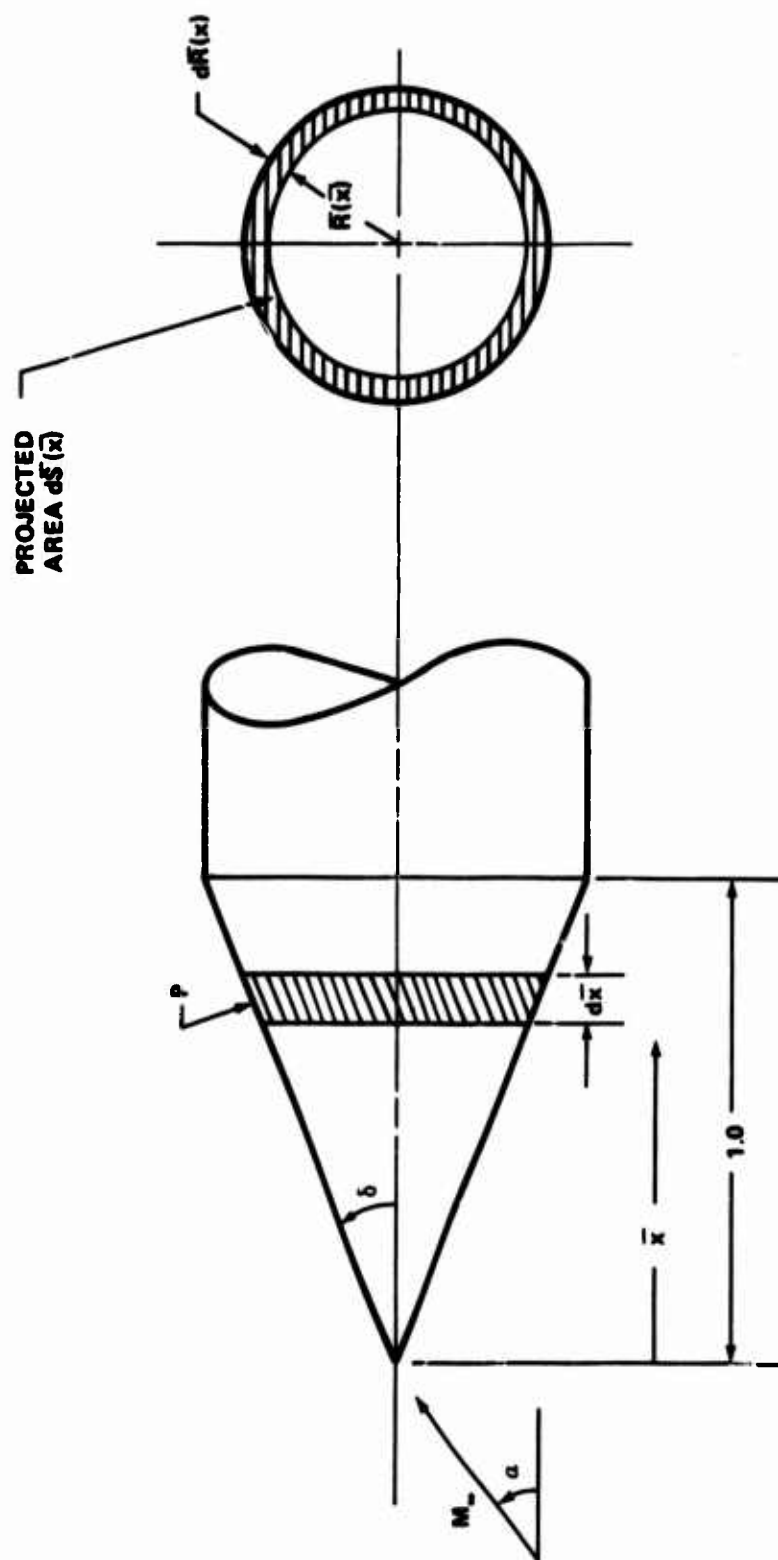


Figure 2. Nomenclature of cone cylinder for pressure drag calculations.

from which

$$p - p_{\infty} = C_p q_{\infty} \quad . \quad (83)$$

Therefore, substitution of Equations (81) and (83) into Equation (77) gives:

$$D_1 = 2\pi\delta^2 \int_{\bar{x}=0}^1 C_p q_{\infty} \bar{x} d\bar{x} \quad . \quad (84)$$

Now the drag coefficient based on the base area of the cone is:

$$C_{D_1} = \frac{D_1}{q_{\infty} \bar{S}(1)} \quad , \quad (85)$$

where the base area of the cone,  $\bar{S}(1)$ , can be expressed as

$$\bar{S}(1) = \pi \bar{R}^2(1) = \pi \delta^2 \quad . \quad (86)$$

Hence, Equations (84), (85), and (86) give:

$$C_{D_1} = 2 \int_0^1 C_p \bar{x} d\bar{x} \quad . \quad (87)$$

Liepmann and Roshko [1] shows that for slender bodies of revolution at small angles of attack, the cross flow contribution is approximately equal to  $\alpha^2$ .

Hence, the drag coefficient for small angle of attack is:

$$C_D = C_{D_1} + \alpha^2 \quad . \quad (88)$$

#### Section IV. COMPARISON OF PRESENT METHOD WITH EXPERIMENTAL RESULTS AND OTHER THEORIES

Surface pressure distributions calculated by the present method for a 5-degree half-angle cone are compared with other theoretical results and experimental data in Figure 3.  $\theta$  is assumed equal to zero when not specified. The results labeled SPII were calculated by the method due to Smith and Pierce[2] for a sharp cone with a cylindrical afterbody having the same diameter as the base of the cone. The results labeled SPI were calculated by the same method for a sharp cone with a cylindrical afterbody having a diameter approximately half as large as the base diameter of the cone. Note that the present results are in good agreement with the experimental data for all of the Mach numbers, although for Mach numbers near one the calculated values are a little lower than the data points. The previous Wu-Aoyama results, on the other hand, are quite high for the low subsonic Mach numbers, but agree with the experimental data for the transonic Mach number range, except near the shoulder. The error near the shoulder and the high values in the subsonic regime are probably due to the fact that this method neglects a term in the integral equation used to evaluate the pressure coefficient.

Consider now the two subsonic compressible calculations. Note that the results labeled SPI agree with data for the lower subsonic Mach numbers, while the results labeled SPII agree better than SPI for the Mach numbers above  $M_\infty = 0.6$ . This is probably due to the fact that as the Mach number increases, the flow on the cone surface takes on a higher kinetic energy, which helps the flow over the shoulder and causes the streamlines to behave as if the cone had a full-size cylindrical afterbody, regardless of the diameter of the real afterbody. Hence, one must be careful when using the subsonic solutions because of the significant differences in pressure distributions which result for different geometry inputs. The major disadvantage of the subsonic theories is that they cannot be used for Mach numbers greater than or equal to one.

Figure 4(a) shows the trend of the SPI pressure coefficients with Mach number, and Figure 4(b) shows the same trend for the SPII values. Note that as the Mach number increases, the curves seem to rotate about a common axial location ( $x/L \approx 0.72$  for SPI and  $x/L \approx 0.9$  for SPII). Figure 4(c) shows the behavior of the Wu-Aoyama solution with Mach number. As Mach number increases, the curves simply translate to higher pressure coefficient values. Figure 4(d) shows the variation of present method with Mach number. As Mach number increases, the curves seem to translate upwards as well as rotate to a flatter slope, approaching the value calculated at the shock attachment Mach numbers. From Figure 3 the trend of the experimental data is seen to be similar. The fact that the present method exhibits both the rotation of the subsonic solutions and the translation of the transonic solutions is very encouraging, and is necessary for a unified theory.

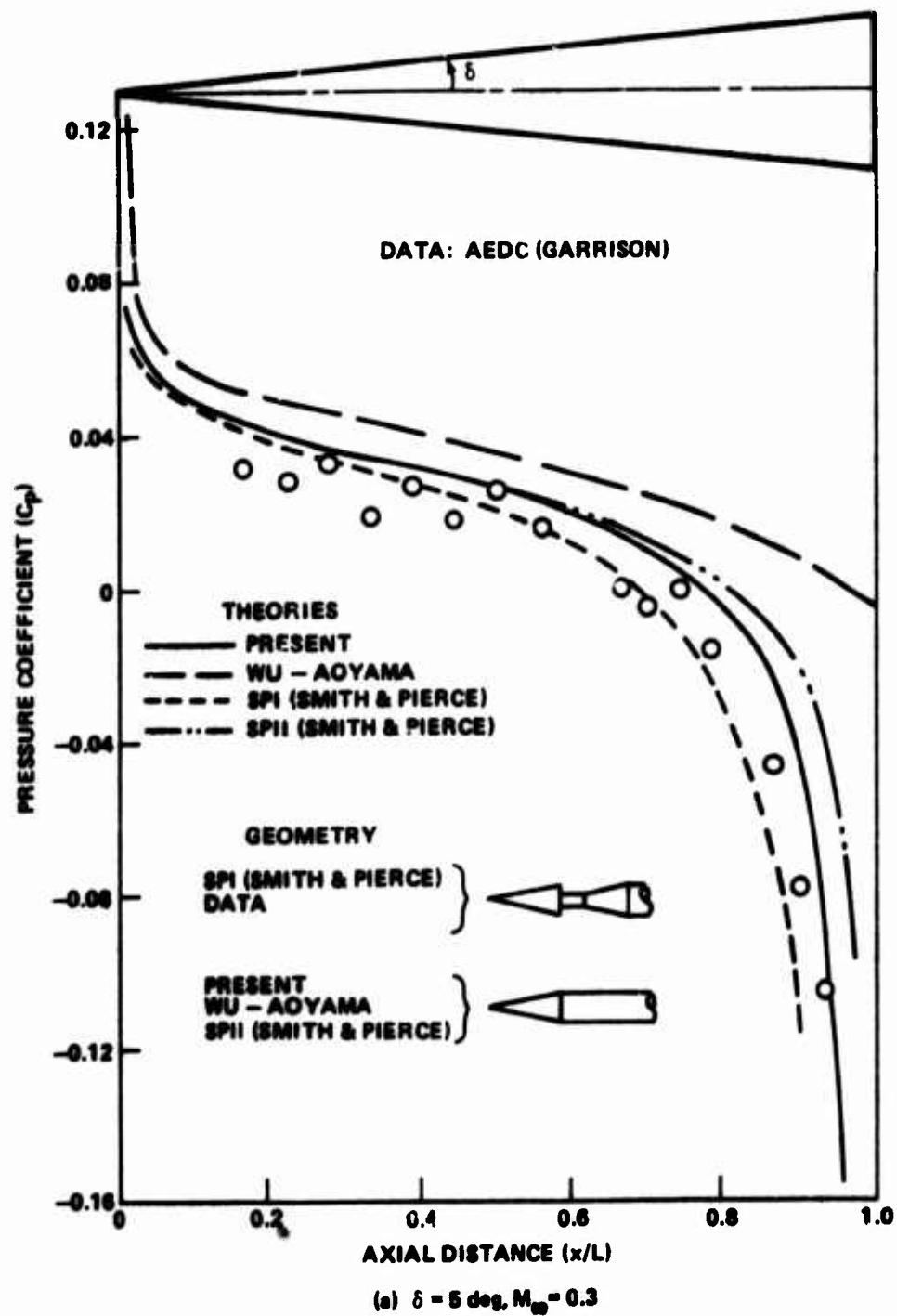


Figure 3. Comparison of various methods with data.

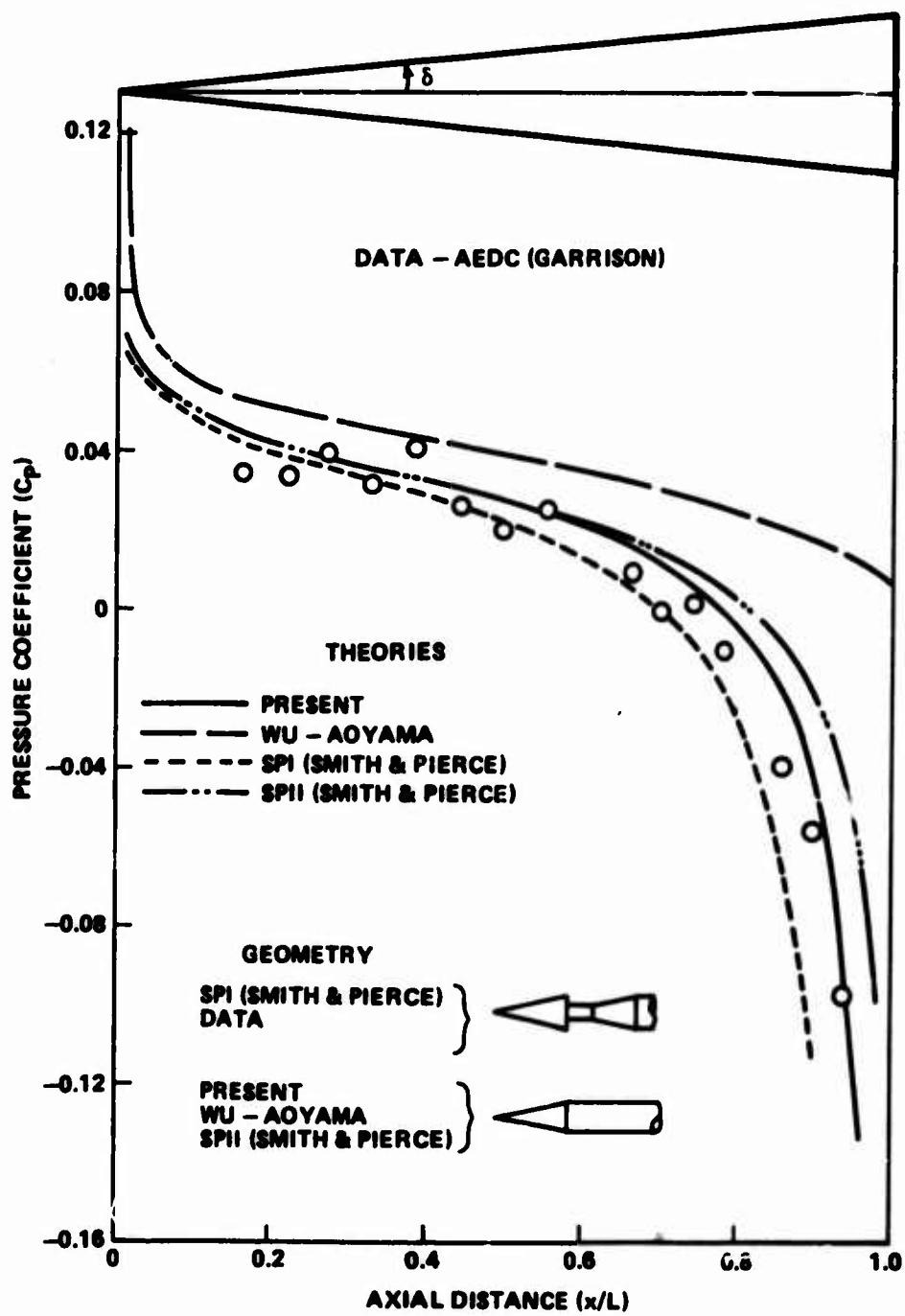
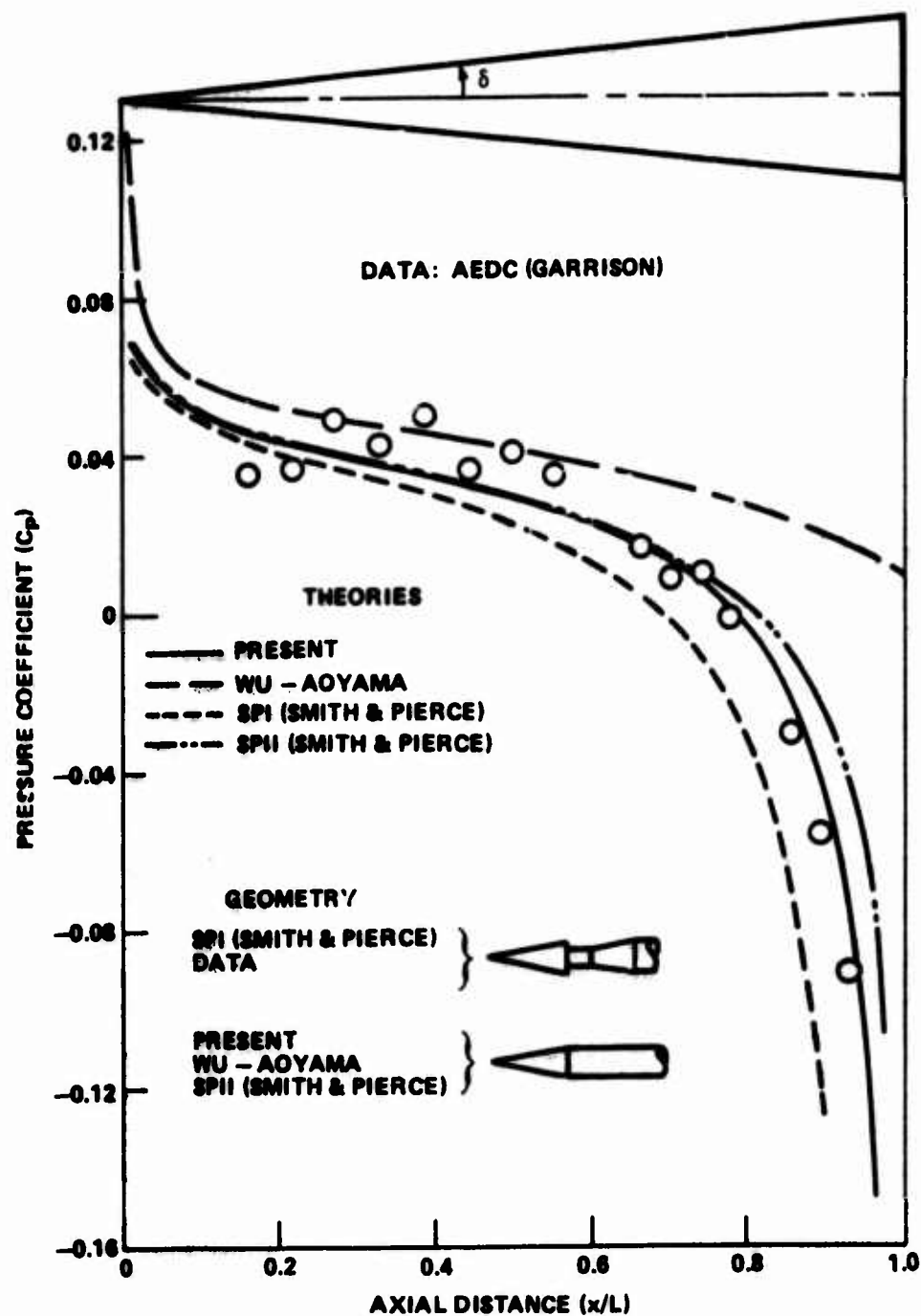
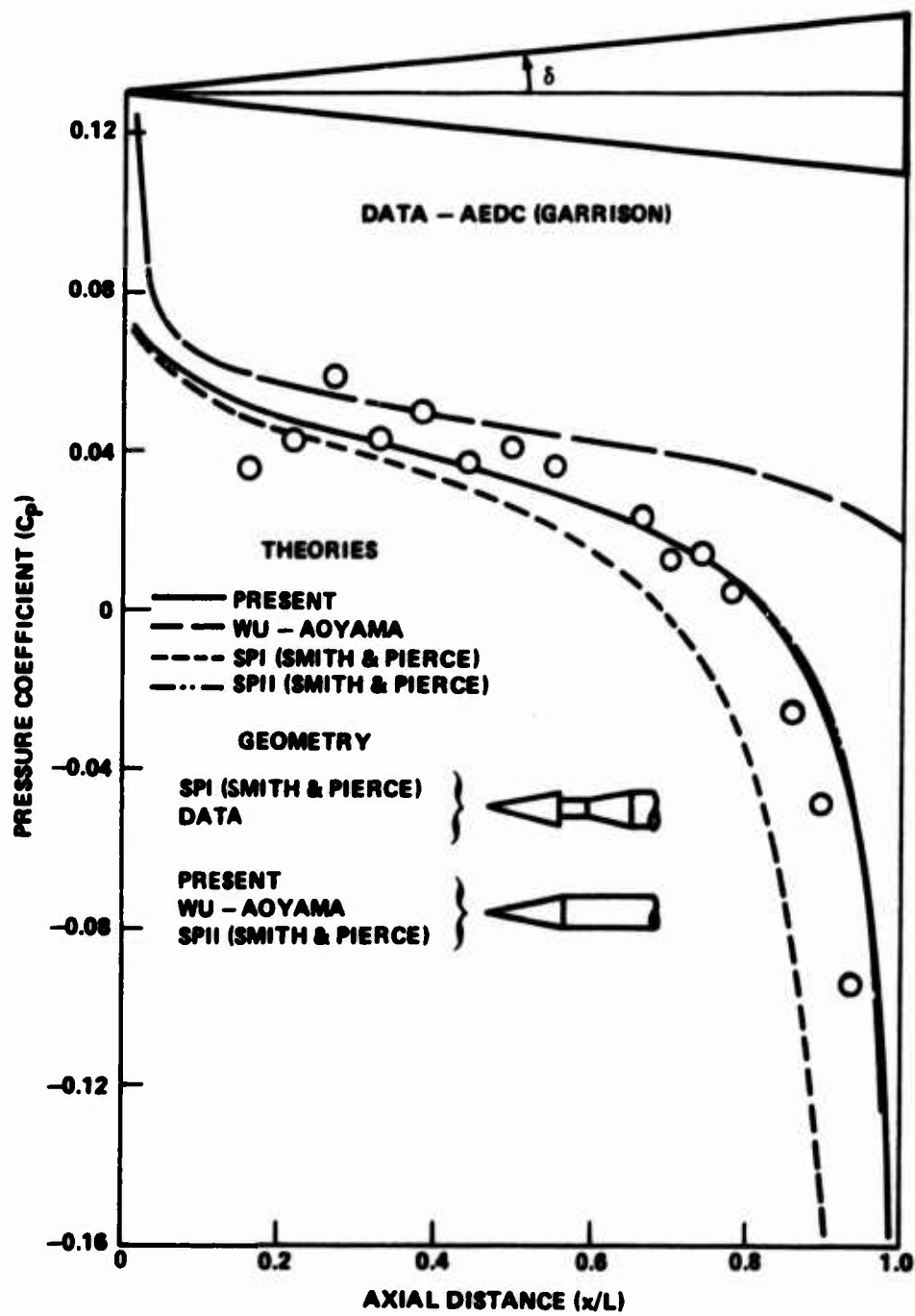


Figure 3. (Continued).



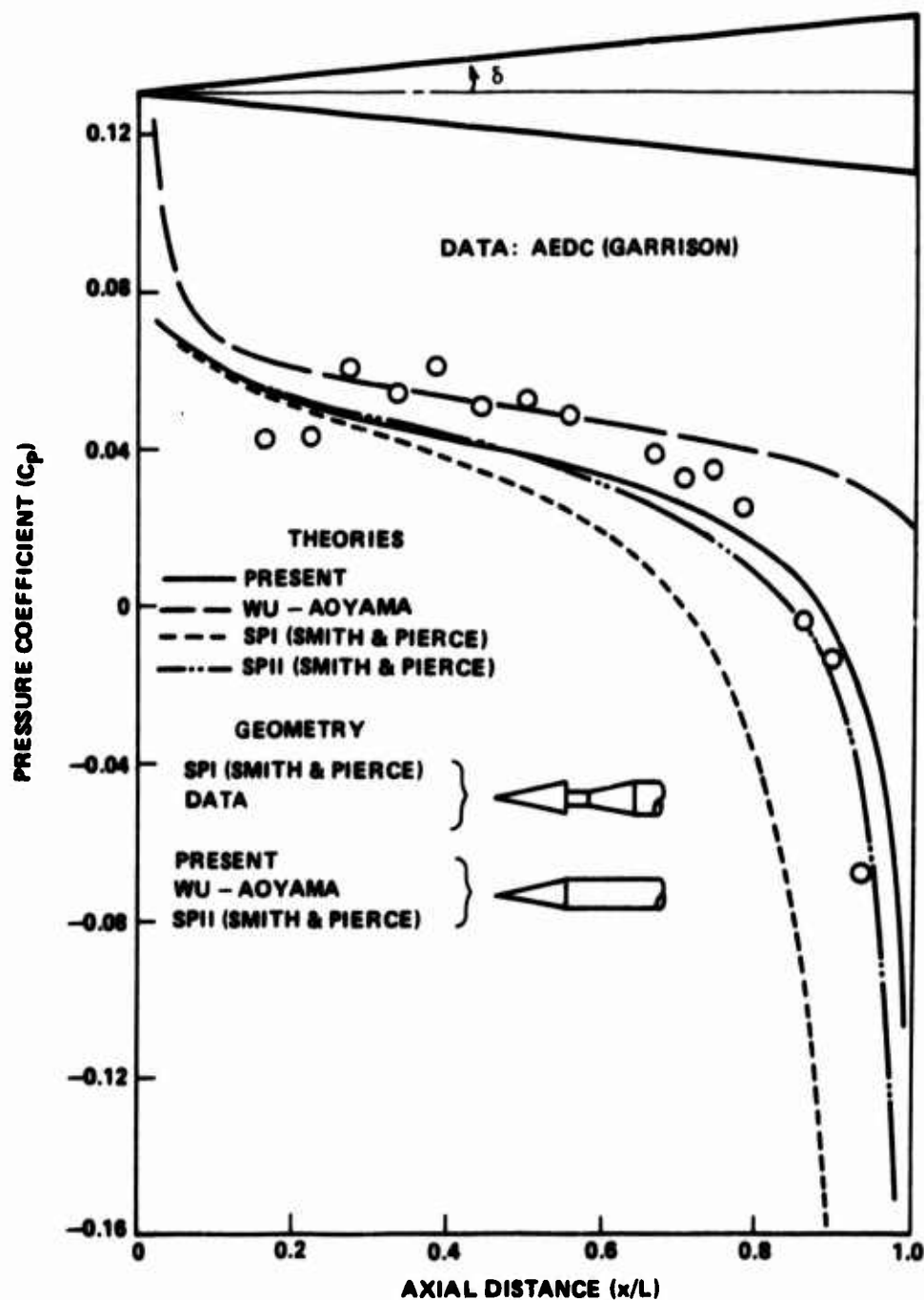
(c)  $\delta = 5 \text{ deg}$ ,  $M_\infty = 0.6$

Figure 3. (Continued).



(d)  $\delta = 5$  deg,  $M_\infty = 0.8$

Figure 3. (Continued).



(e)  $\delta = 5 \text{ deg}$ ,  $M_\infty = 0.9$

Figure 3. (Continued).

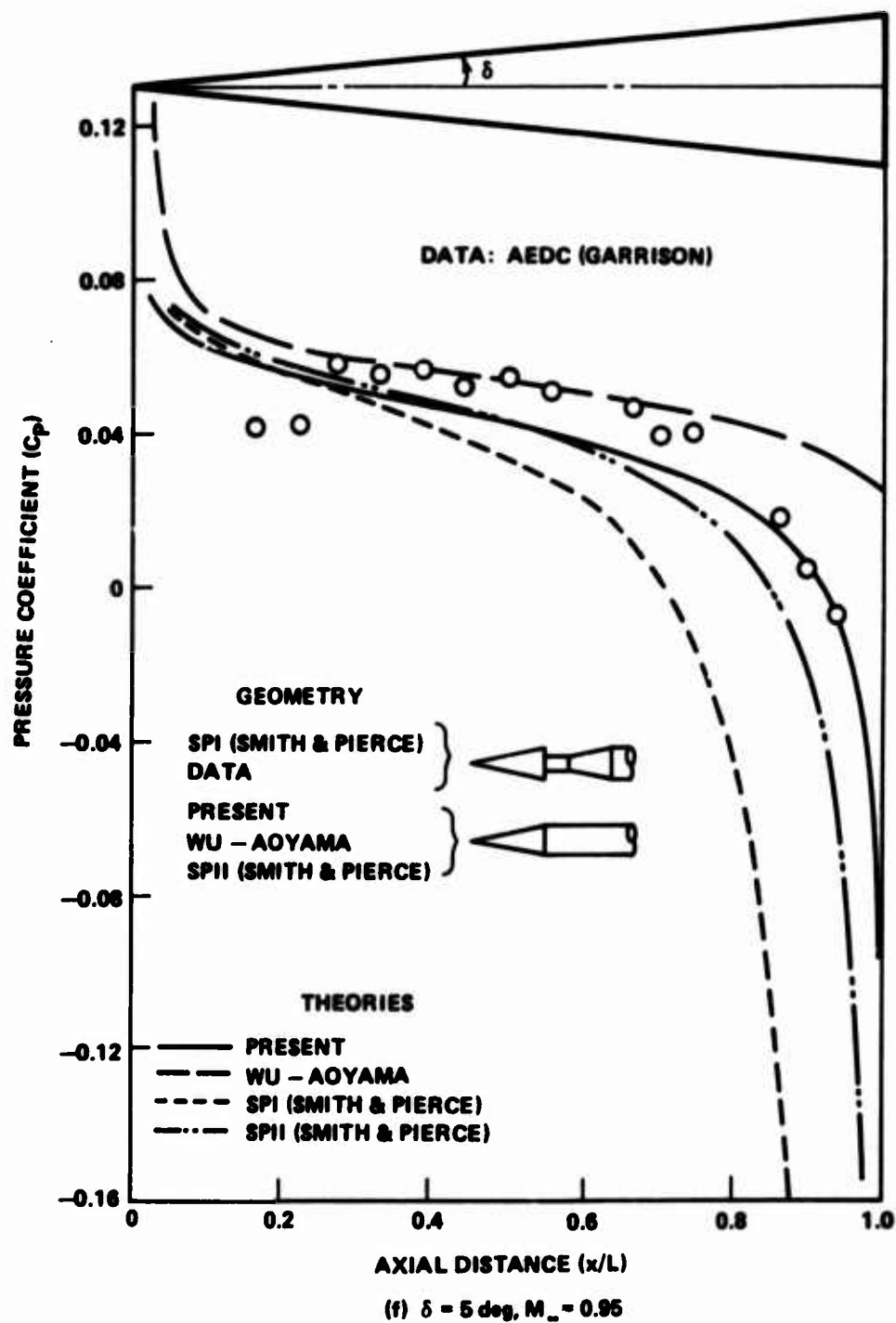
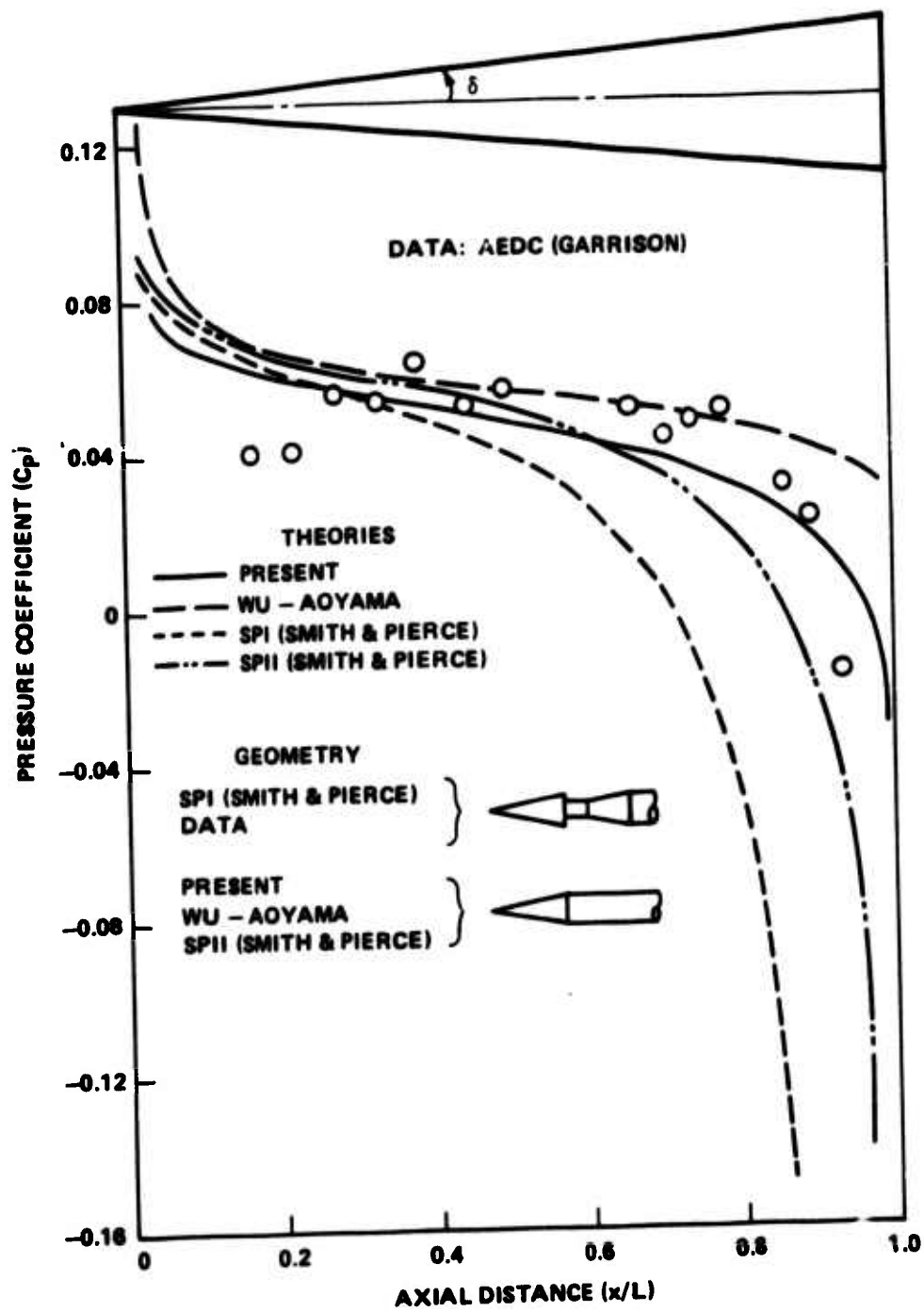
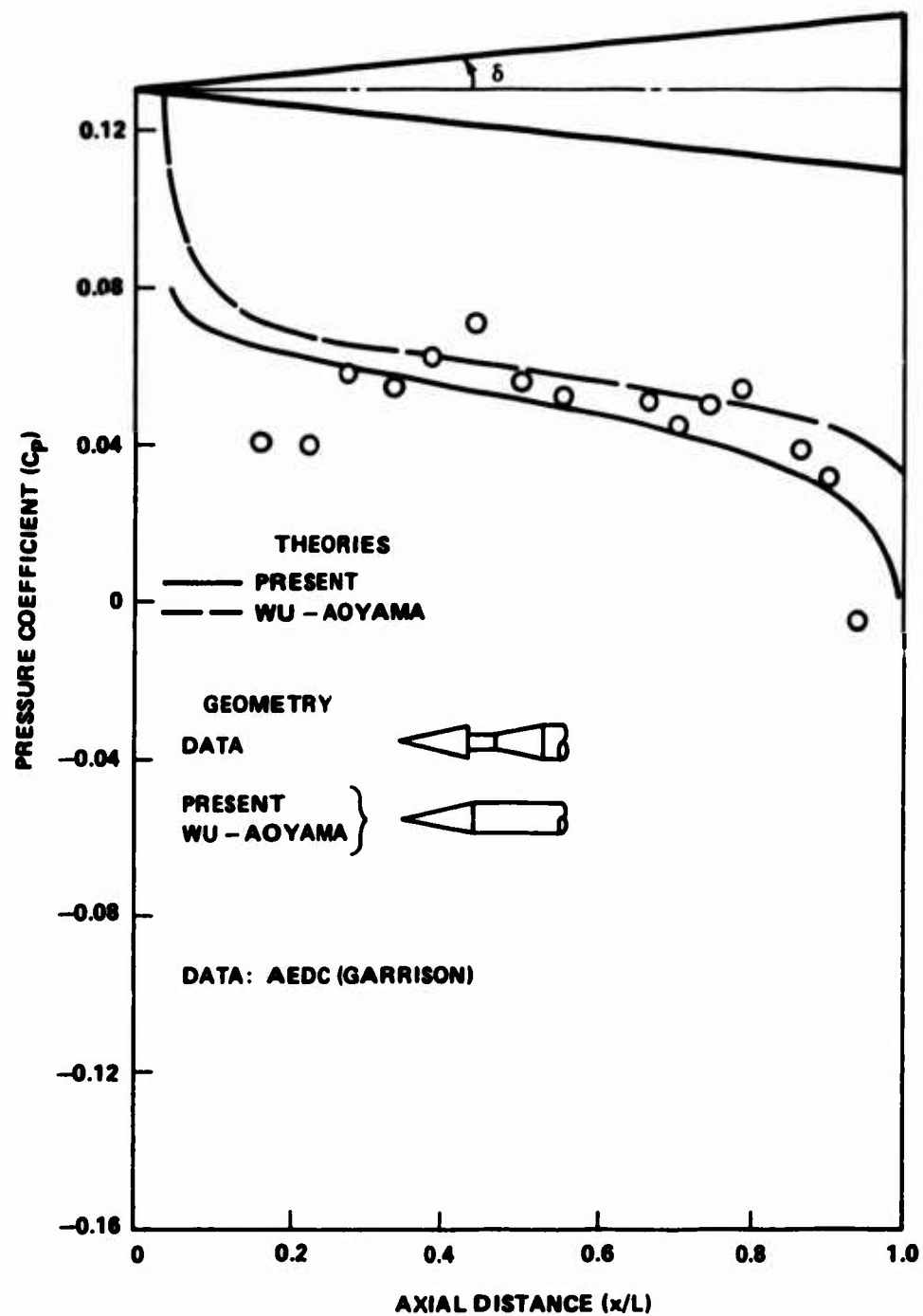


Figure 3. (Continued).



(g)  $\delta = 5 \text{ deg}$ ,  $M_\infty = 0.98$

Figure 3. (Continued).



(h)  $\delta = 5 \text{ deg}$ ,  $M_\infty = 1.0$

Figure 3. (Continued).

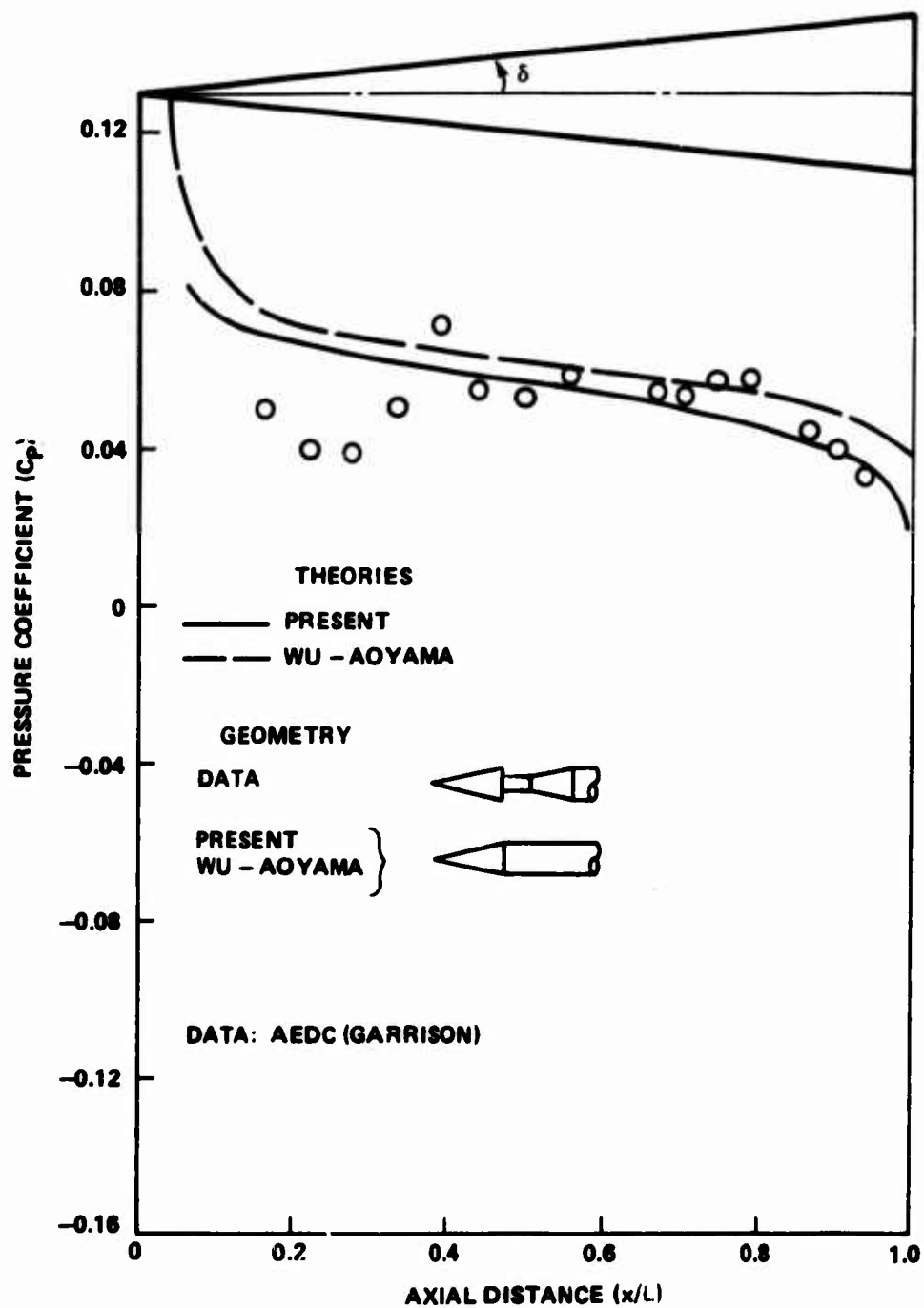
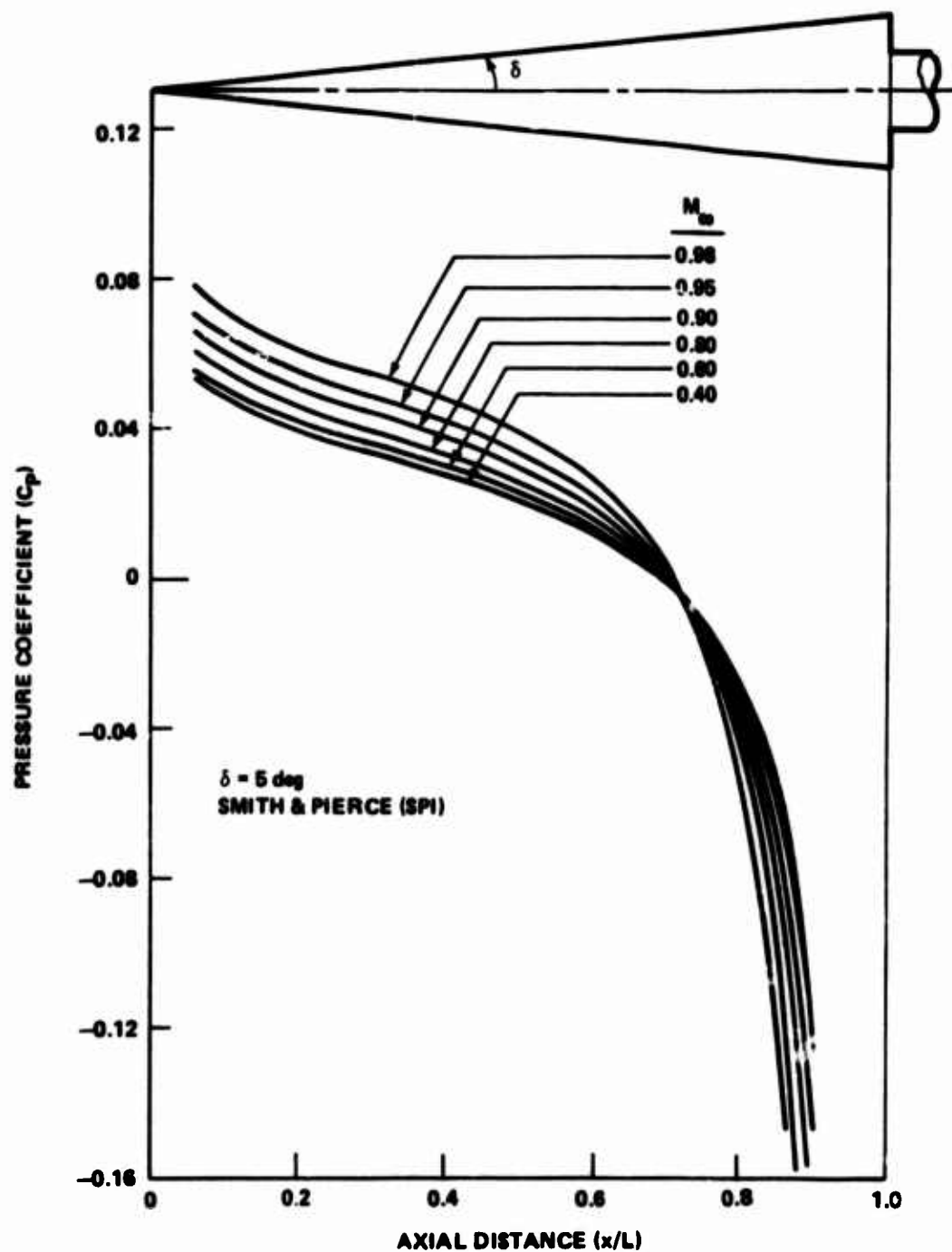
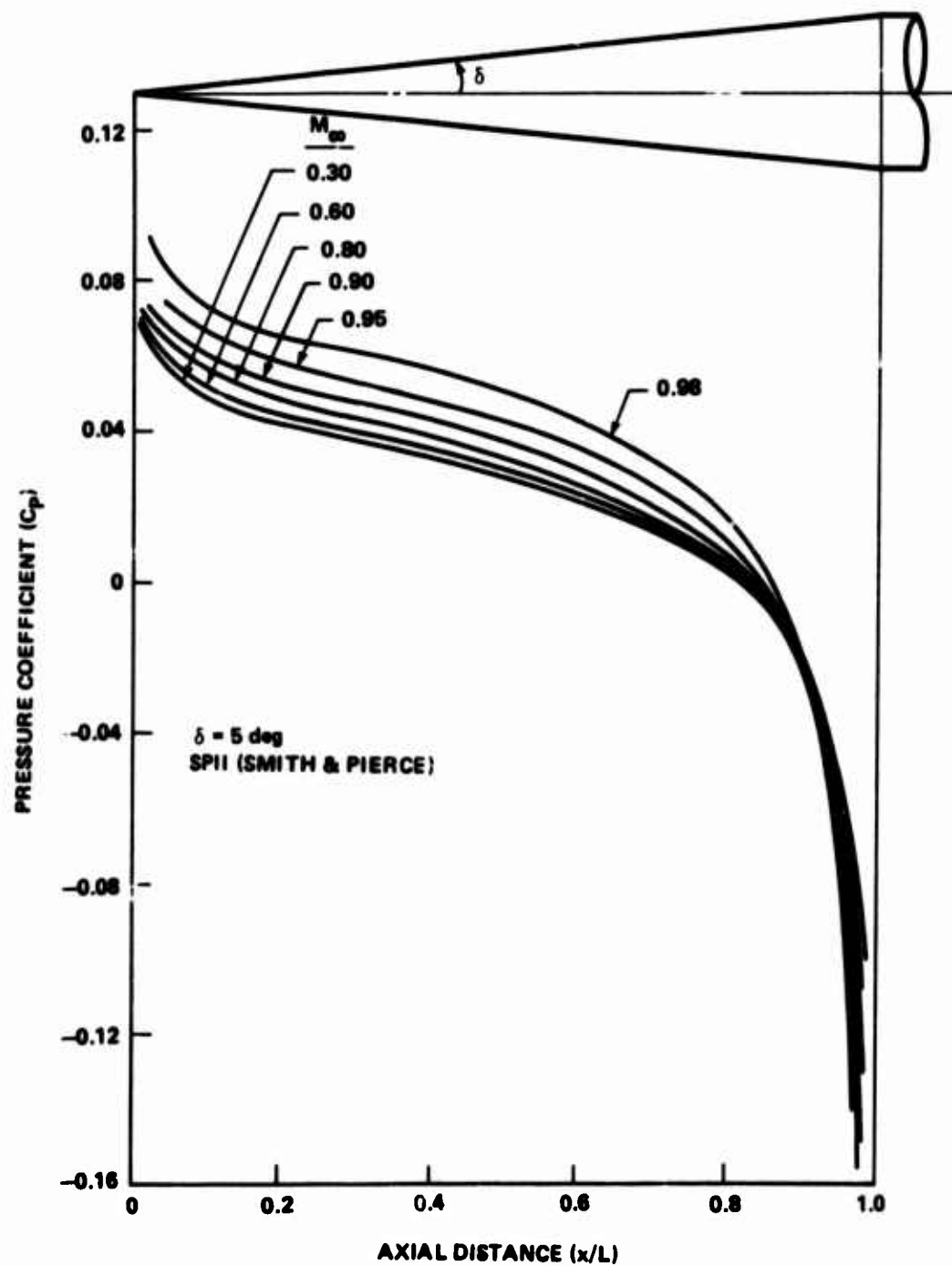


Figure 3. (Concluded).



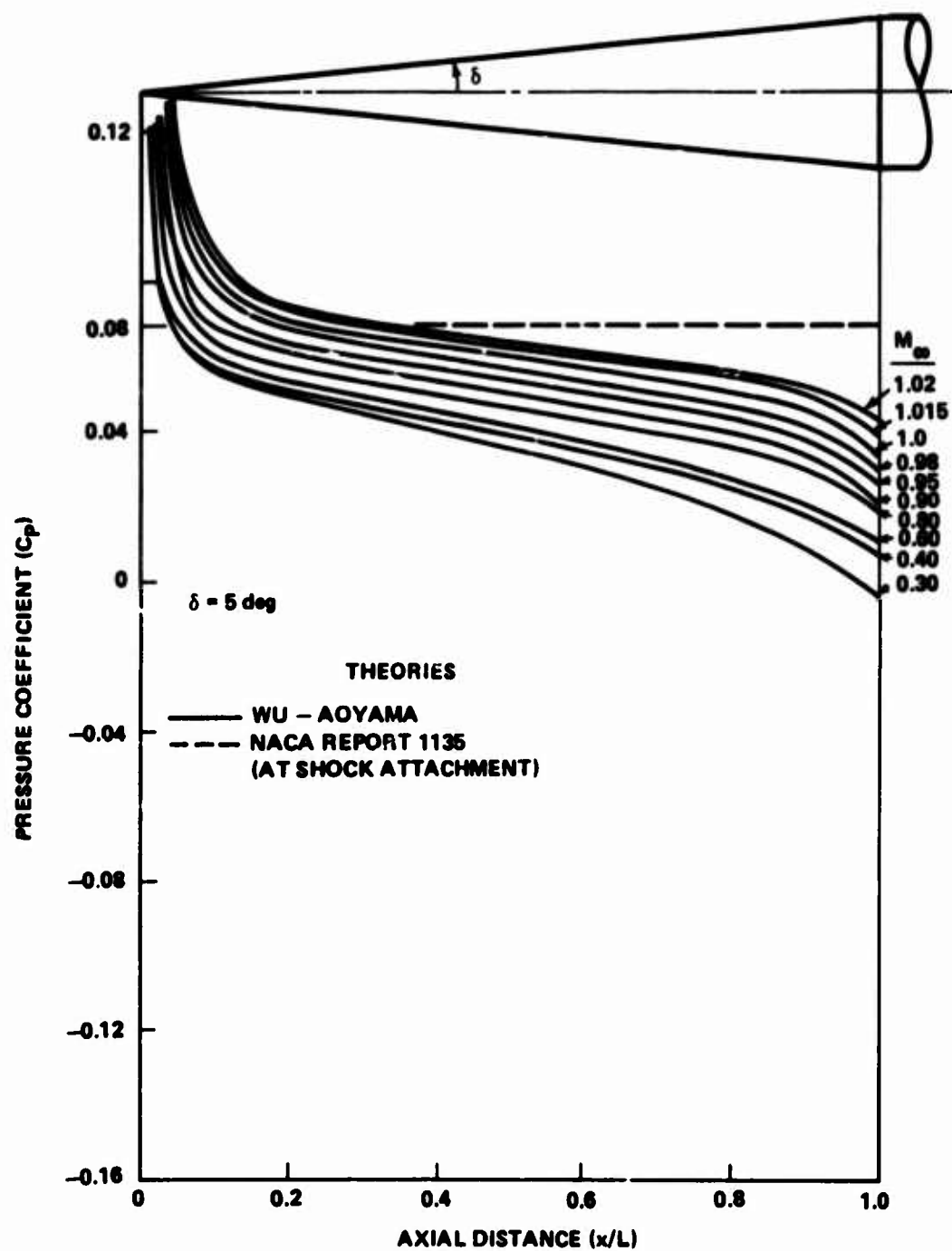
(a) SMITH AND PIERCE, SPI

Figure 4. Theoretical surface pressure distribution for a 5-degree half-angle cone at various Mach numbers.



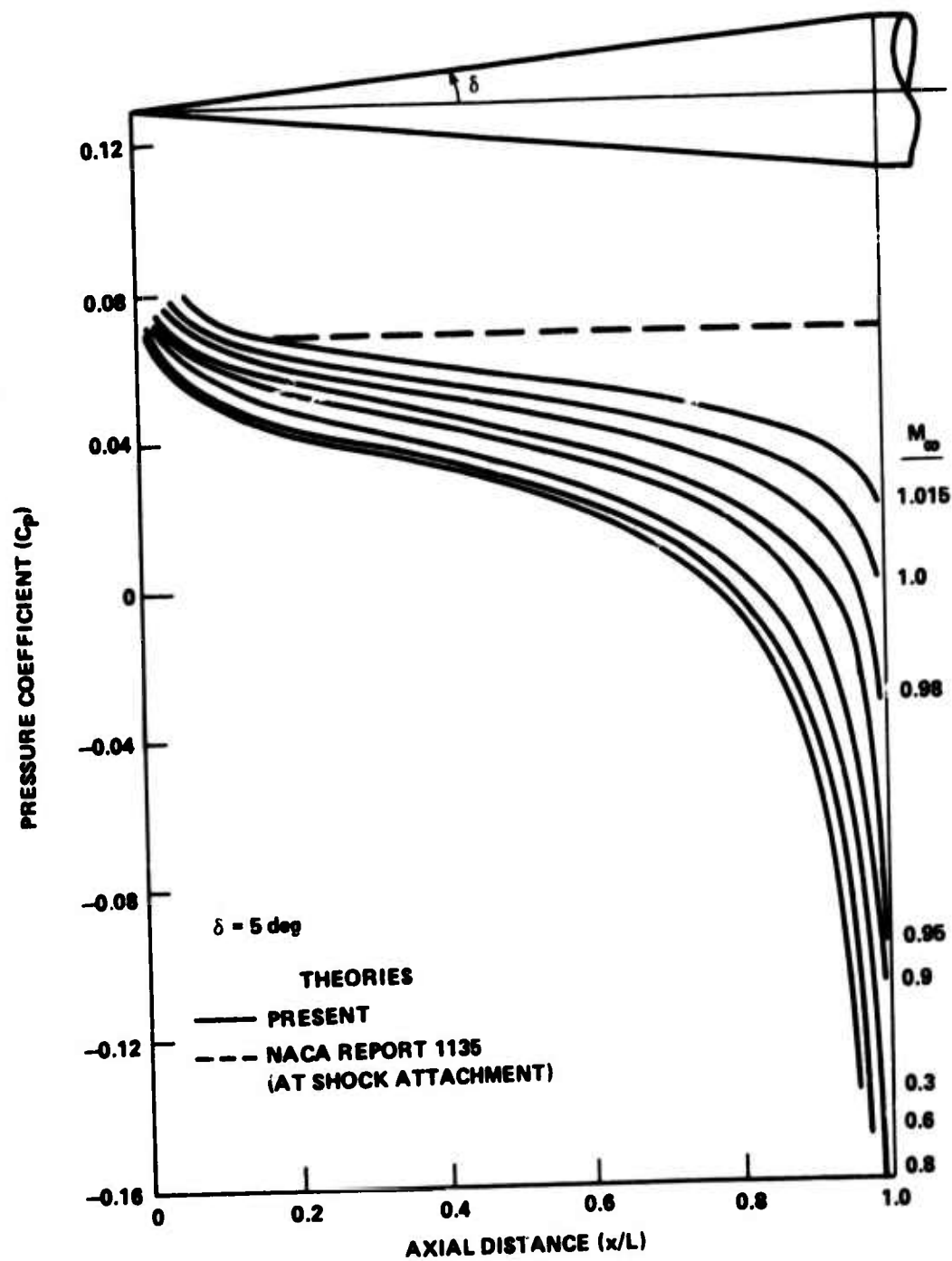
(b) SMITH AND PIERCE, SPII

Figure 4. (Continued).



(c) WU AND AOYAMA

Figure 4. (Continued).



(d) PRESENT METHOD

Figure 4. (Concluded).

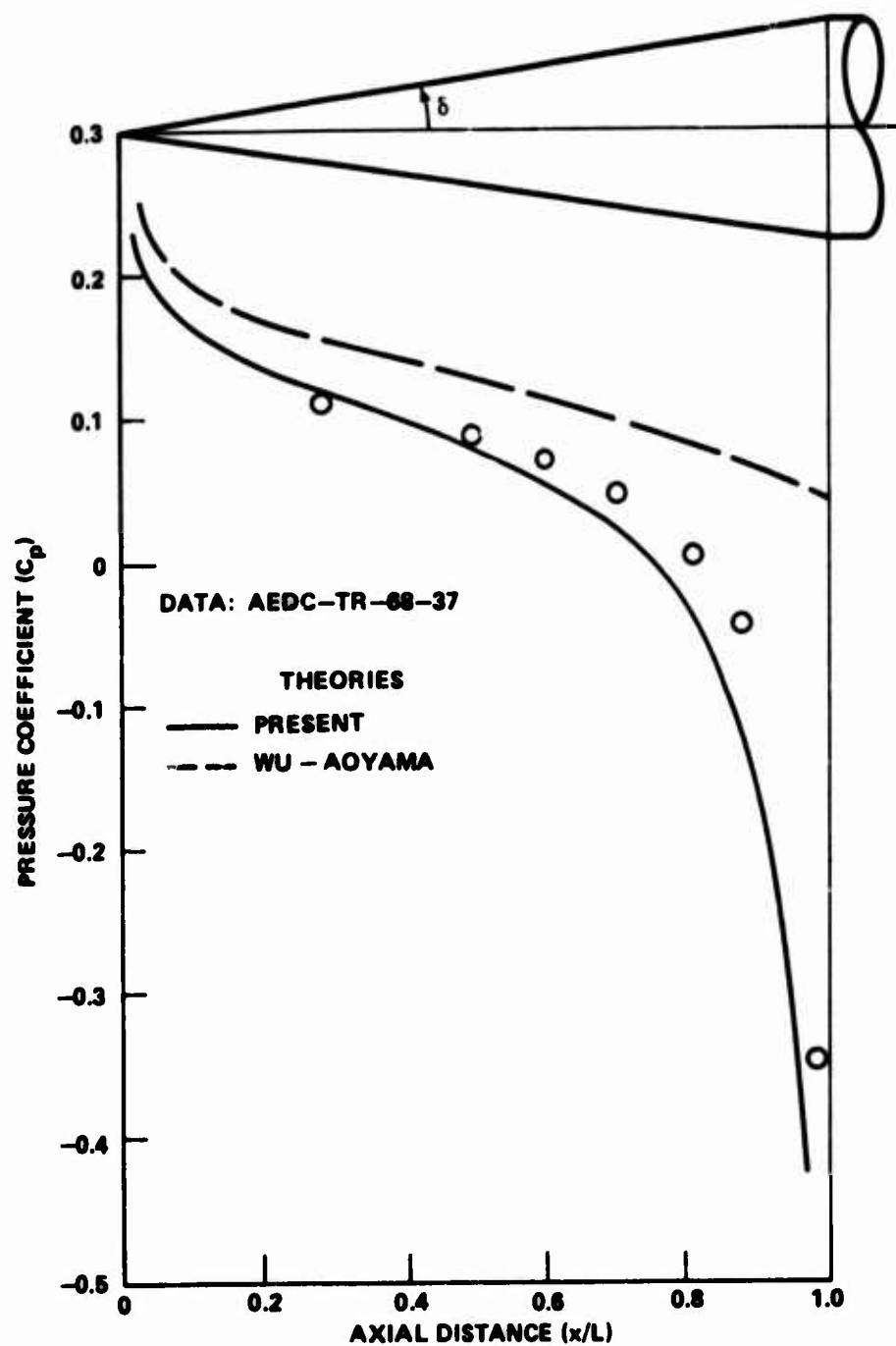
Figure 5 shows further comparisons of the present method with data and the previous Wu-Aoyama calculations. Again, the present solutions show acceptable agreement with data for the subsonic Mach numbers; however, the calculated values of both the present and the Wu-Aoyama procedures are somewhat lower than the data points for Mach numbers greater than one.

Figure 6 shows good agreement of the present method with data for a 15-degree half-angle blunted cone. Figure 7 demonstrates its applicability for the case of a blunted cone for a 6-degree angle of attack. Figure 8 is further proof that the method gives good results at moderate Mach numbers for small angles of attack.

It is interesting to note the variation of the pressure coefficient with Mach number at certain fixed axial locations on the cone surface. Figure 9 points out the advantages the present method has over the other calculated solutions. A comparison of the solutions for three different positions is shown in Figure 10.

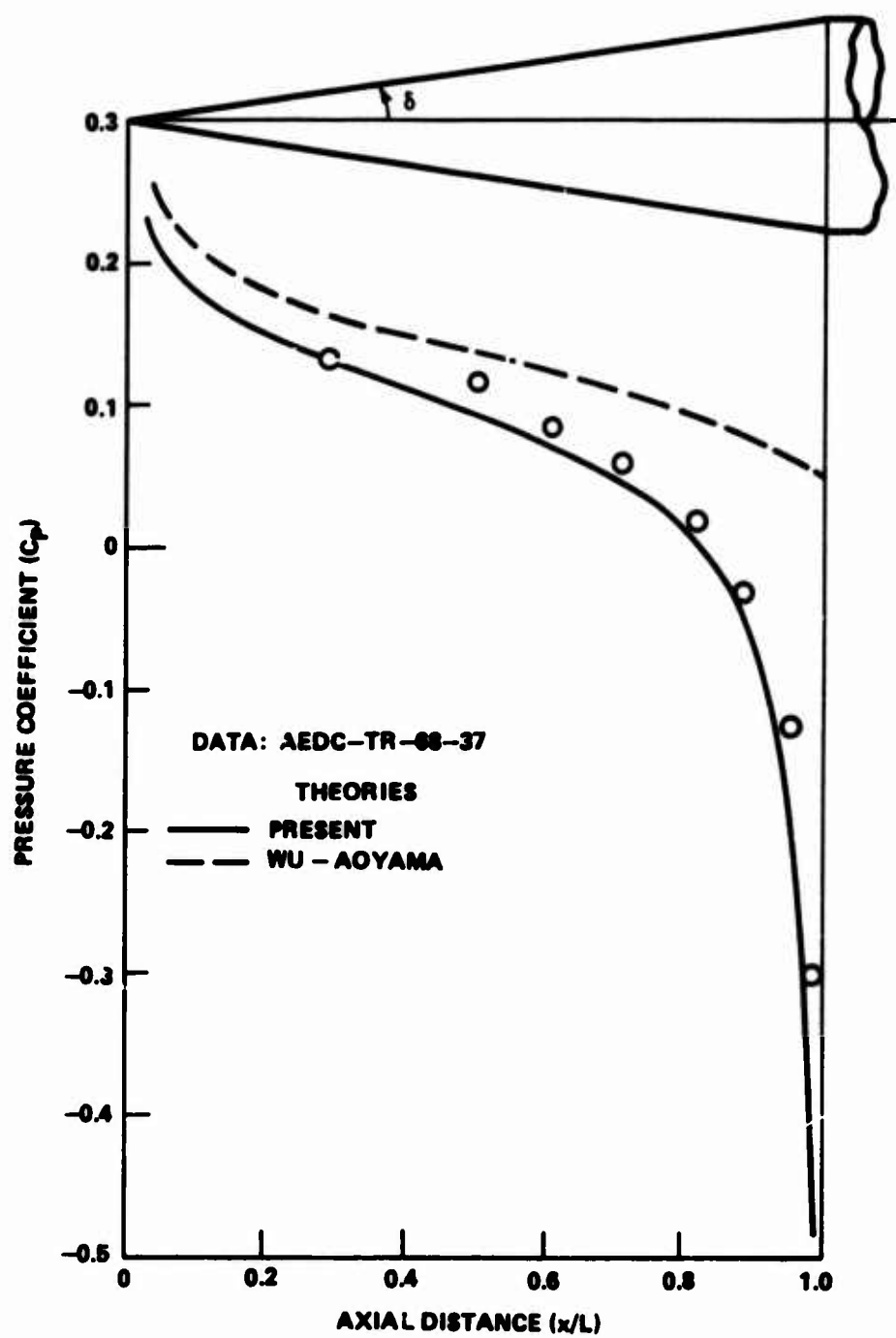
Also of interest is a comparison of the present solution with other transonic solutions, as shown in Figure 11. It must be noted that only the present and Wu-Aoyama solutions were specifically intended for Mach numbers other than one. The present method exhibits the best shape, although it seems to fall below the data points.

A drag coefficient versus Mach number curve is shown in Figure 12 for two different cone angles.



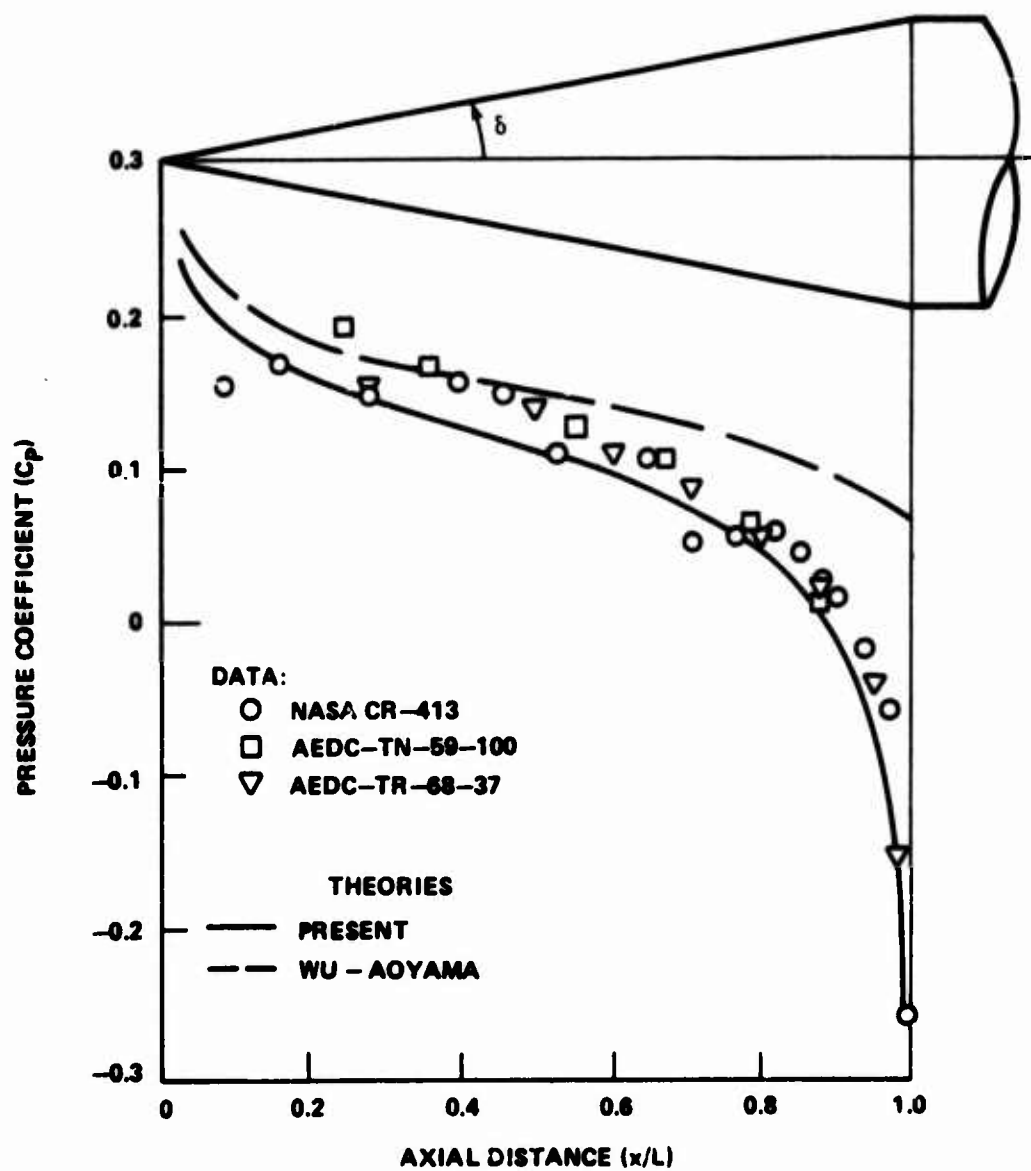
(a)  $\delta = 10 \text{ deg}$ ,  $M_\infty = 0.6$

Figure 5. Comparison of present method with data.



(b)  $\delta = 10$  deg,  $M_\infty = 0.8$

Figure 5. (Continued).



(c)  $\delta = 10^\circ$ ,  $M_\infty = 0.9$

Figure 5. (Continued).

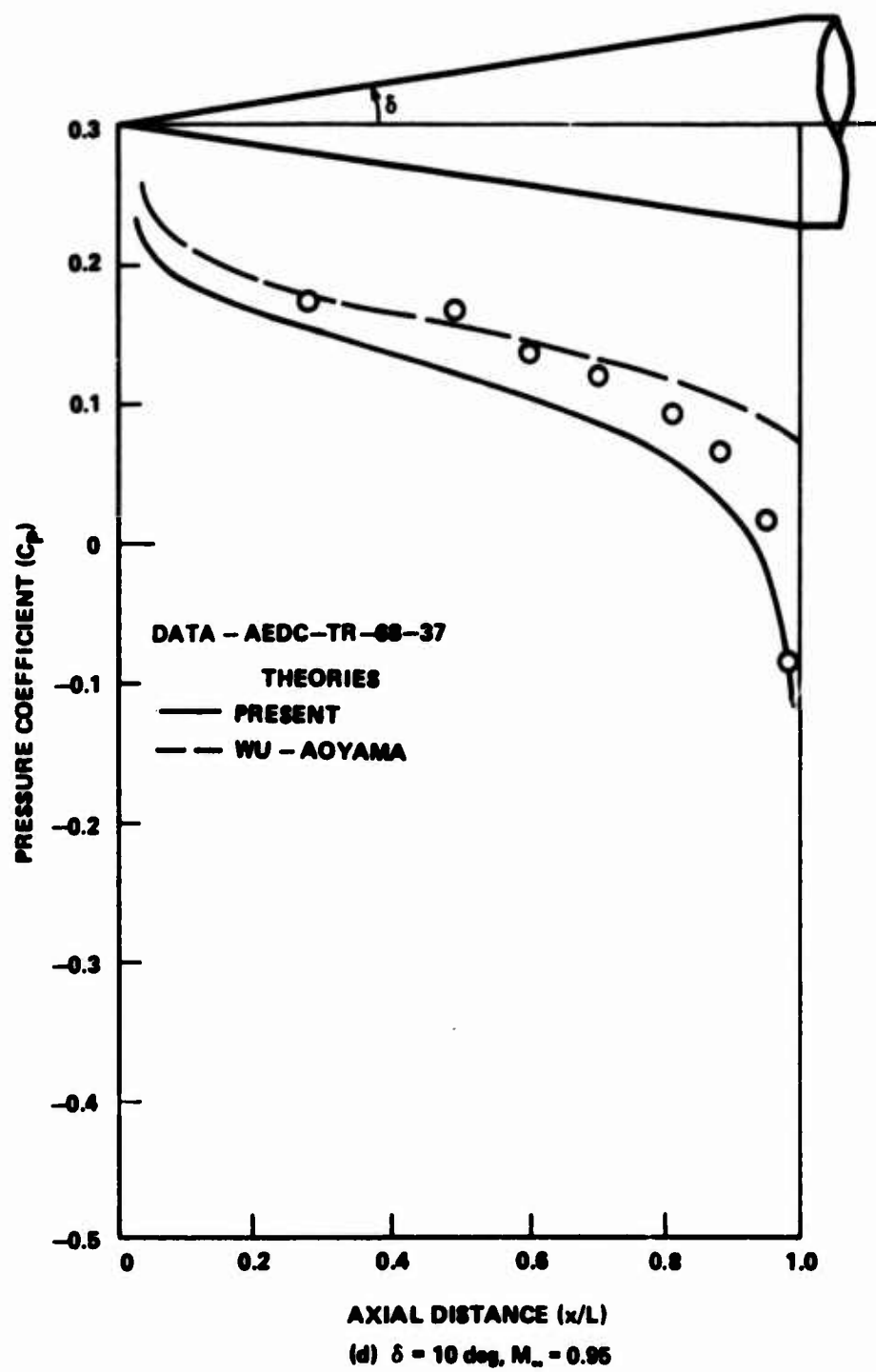
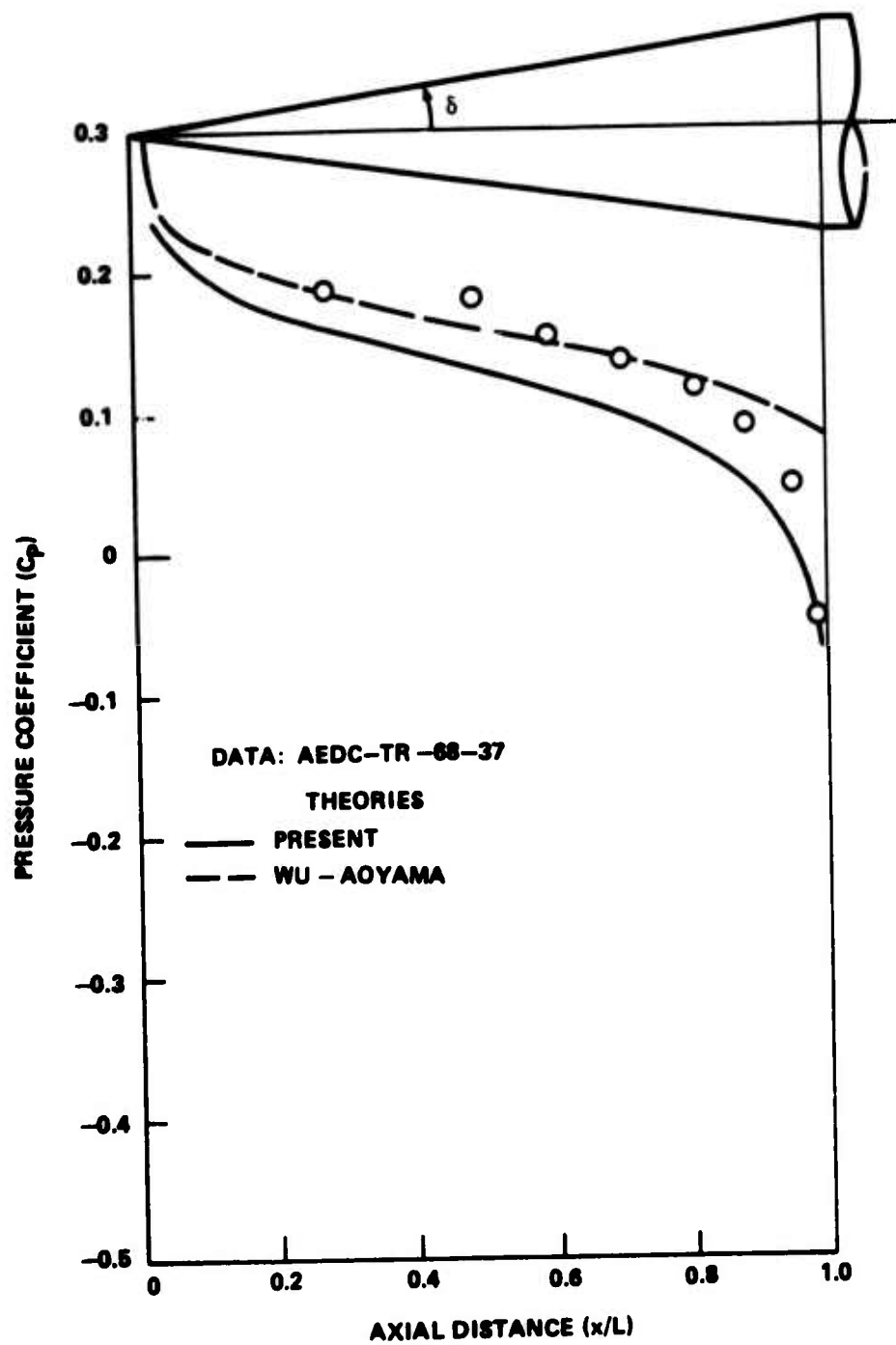
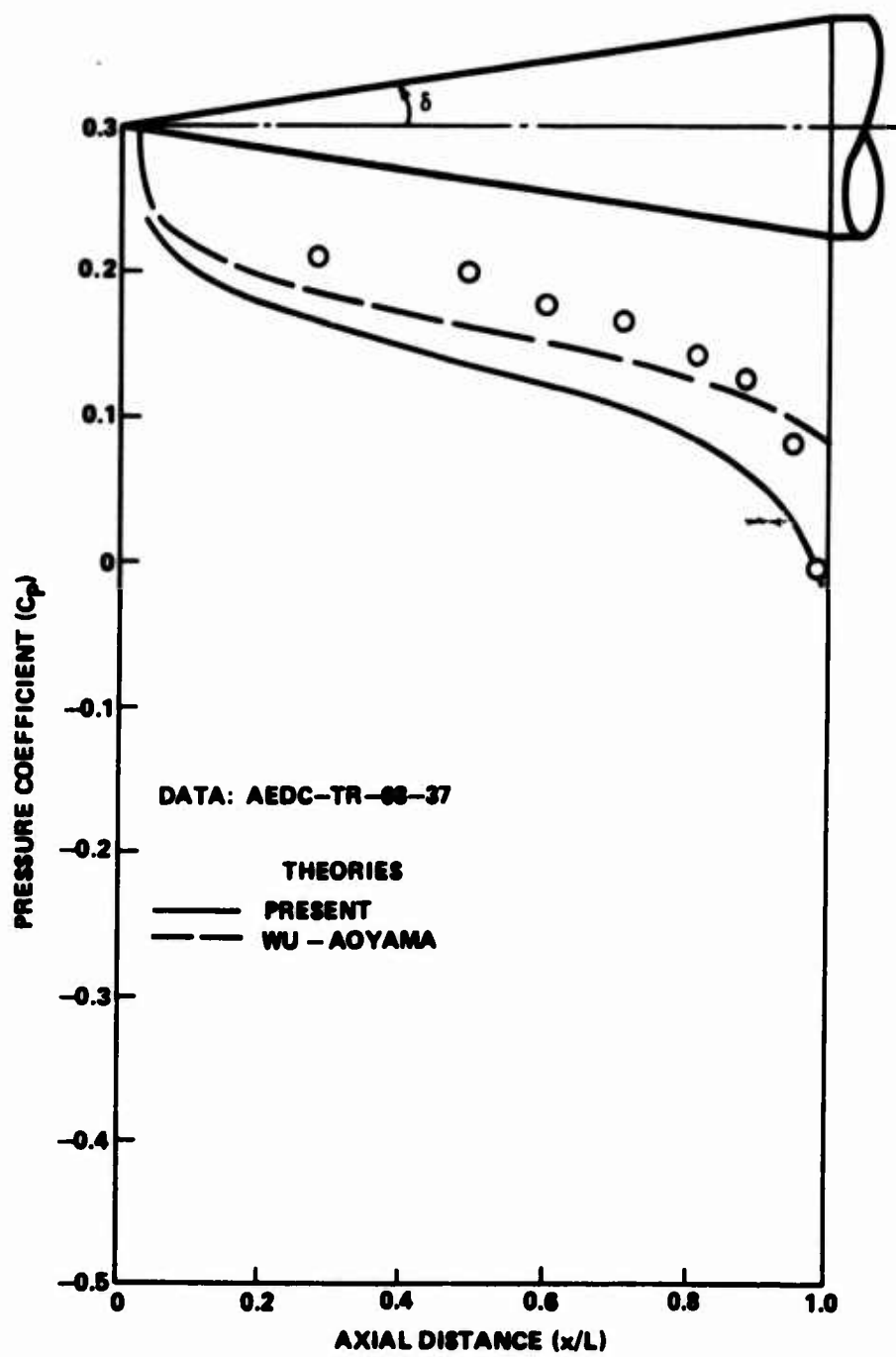


Figure 5. (Continued).



(a)  $\delta = 10^\circ$ ,  $M_\infty = 0.975$

Figure 5. (Continued).



(f)  $\delta = 10^\circ$ ,  $M_\infty = 1.0$

Figure 5. (Continued).

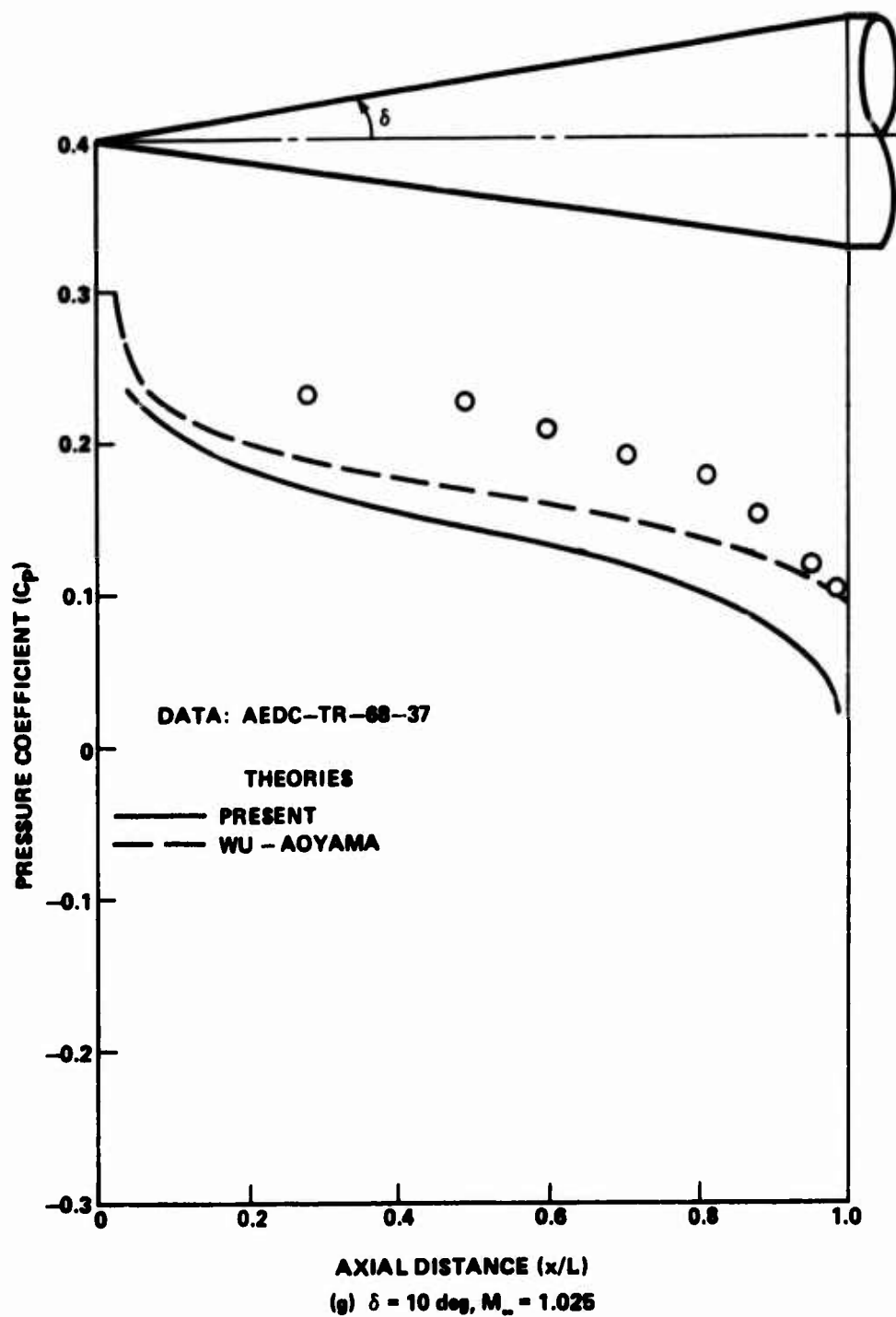
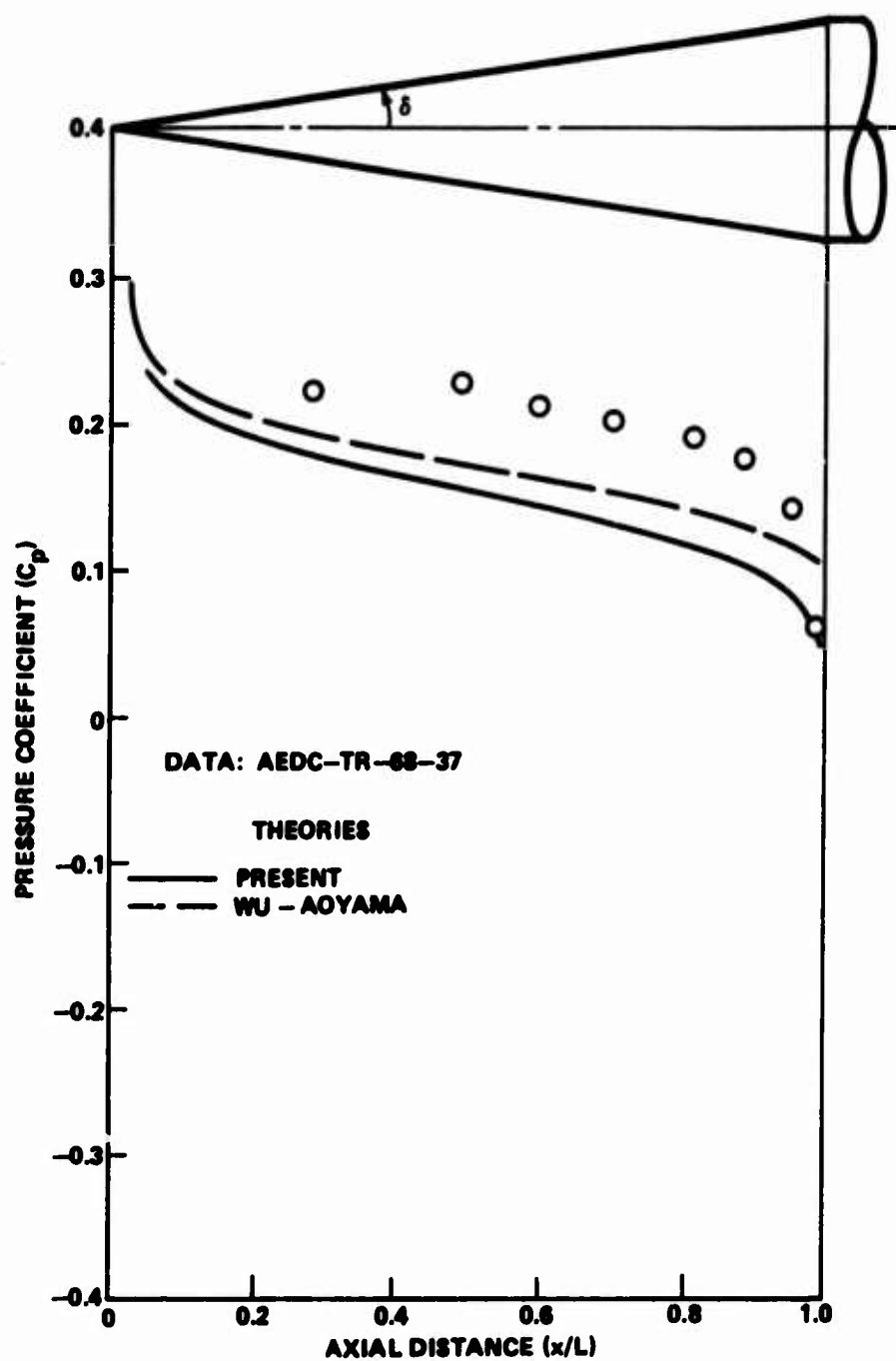


Figure 5. (Continued).



(h)  $\delta = 10^\circ$ ,  $M_\infty = 1.05$

Figure 5. (Concluded).

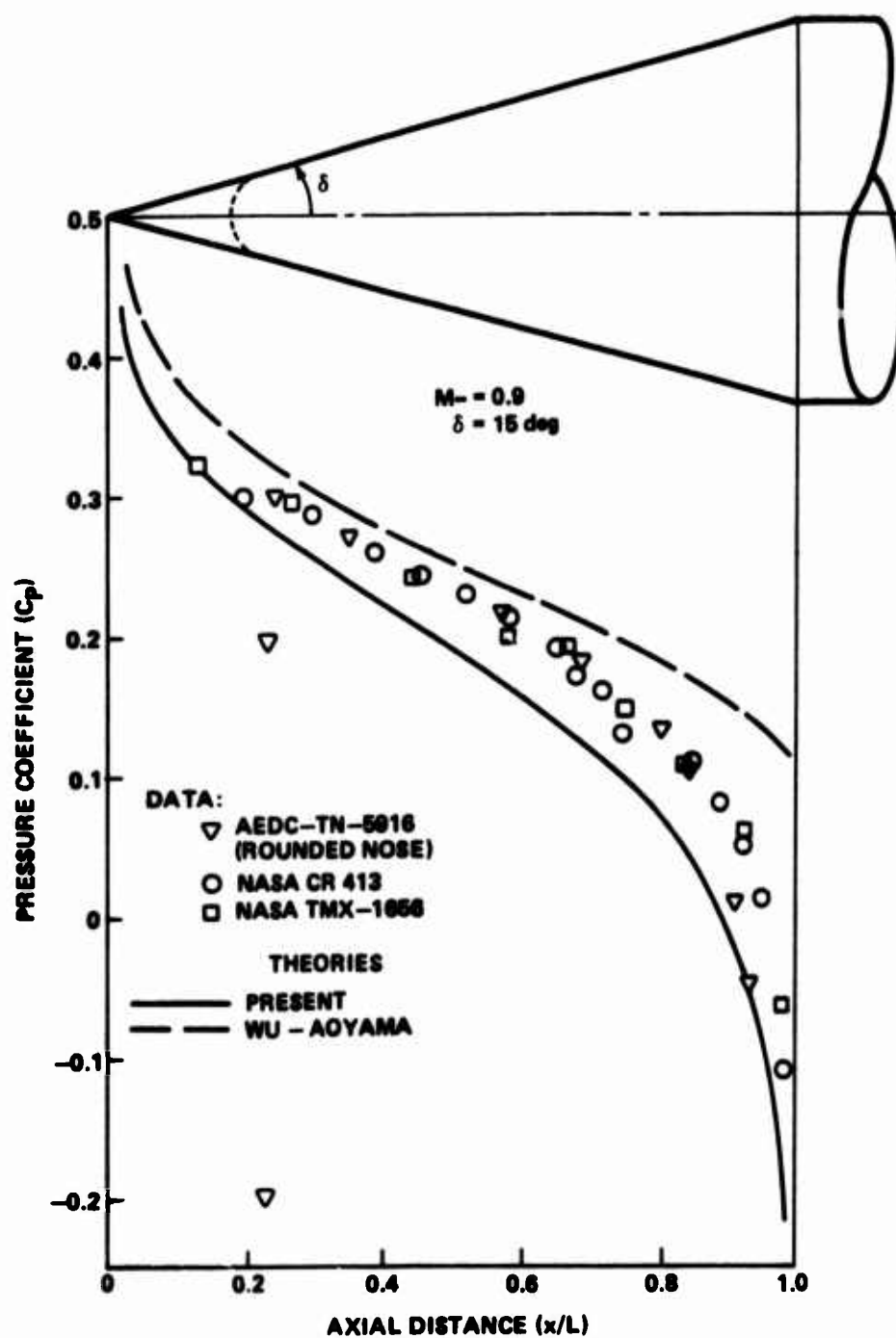


Figure 6. Comparison of present method with data for a blunted cone.

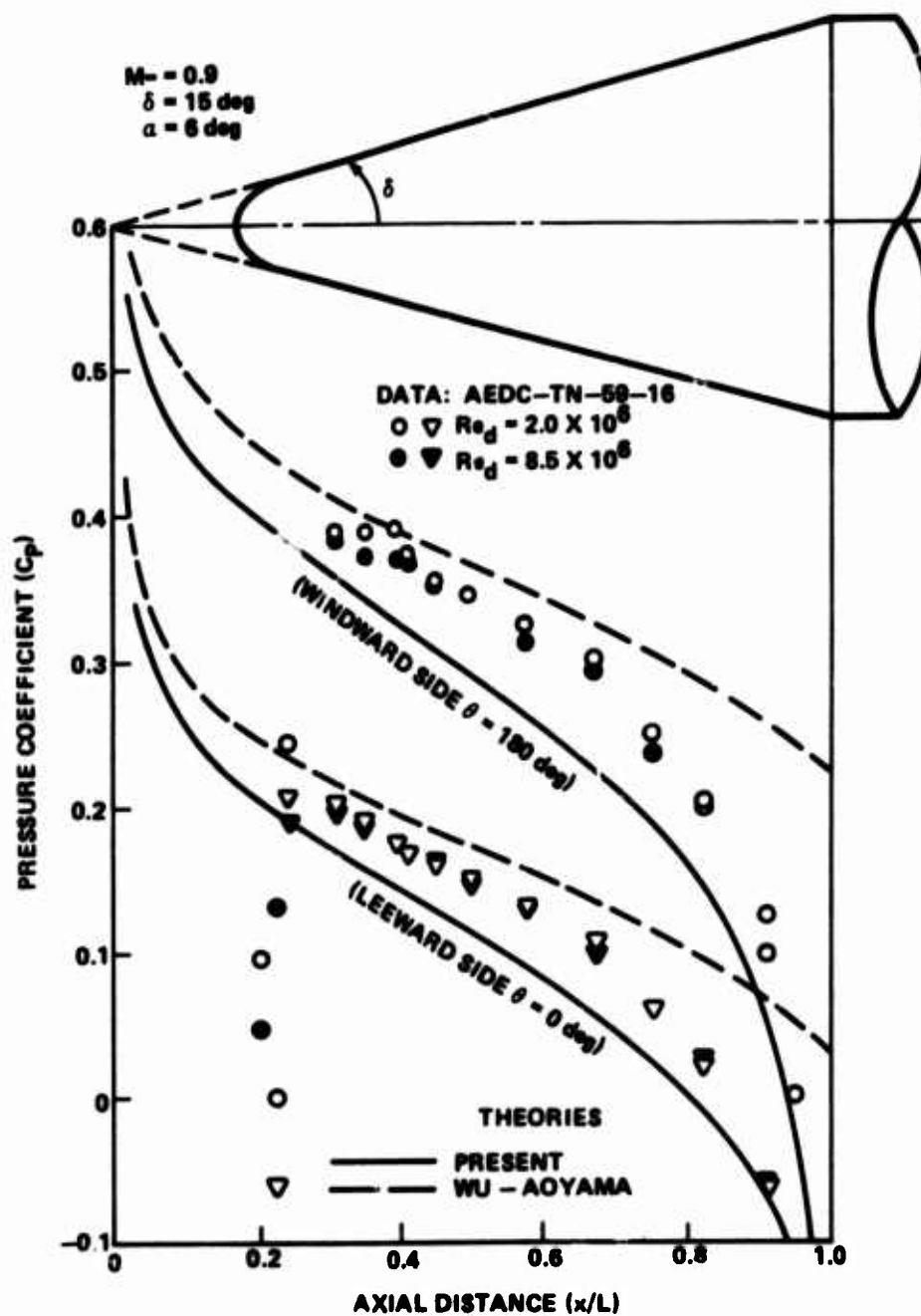


Figure 7. Surface pressure distribution for a blunted cone at a 6-degree angle of attack.

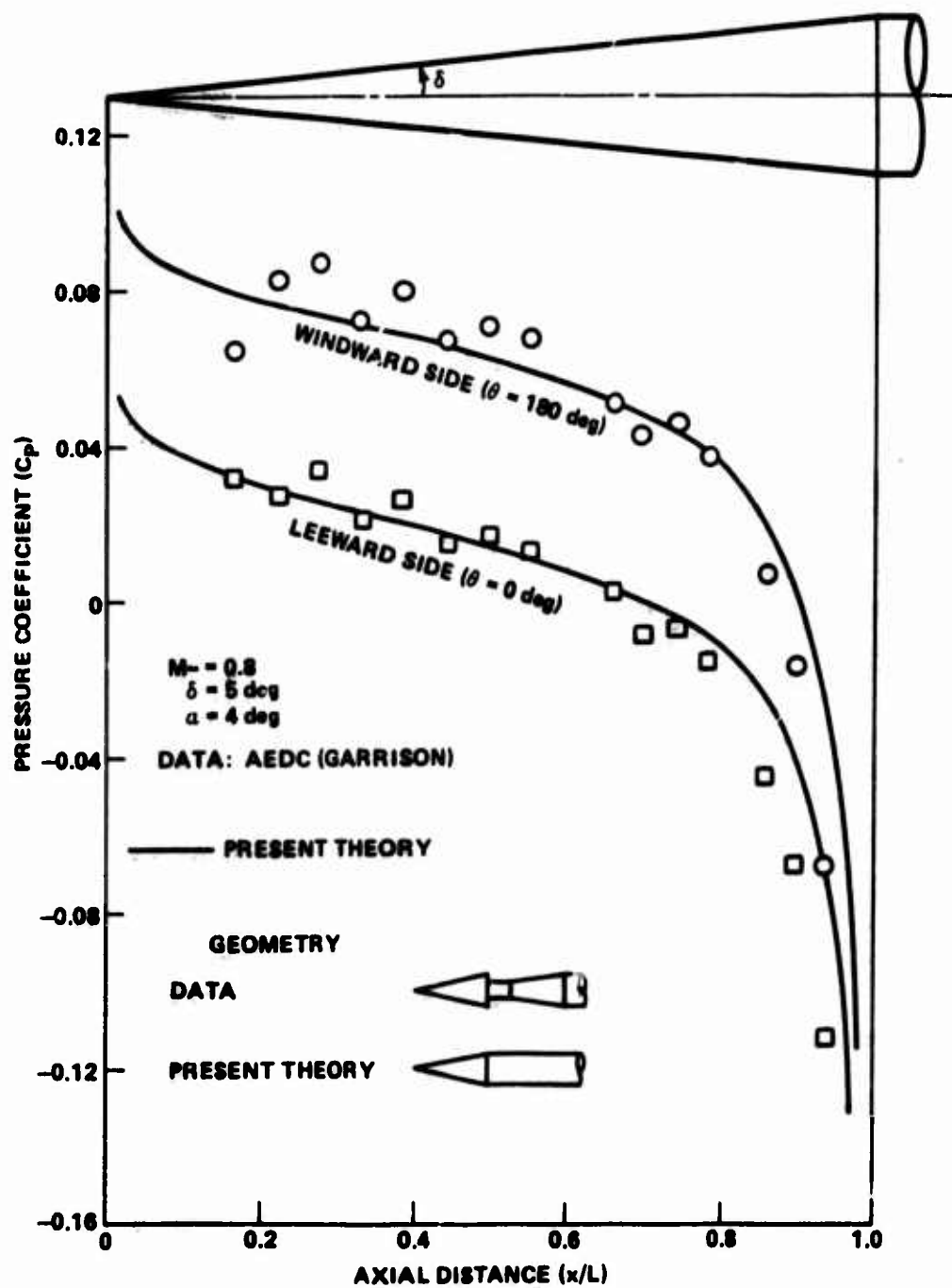


Figure 8. Surface pressure distribution for a sharp cone at a 4-degree angle of attack.

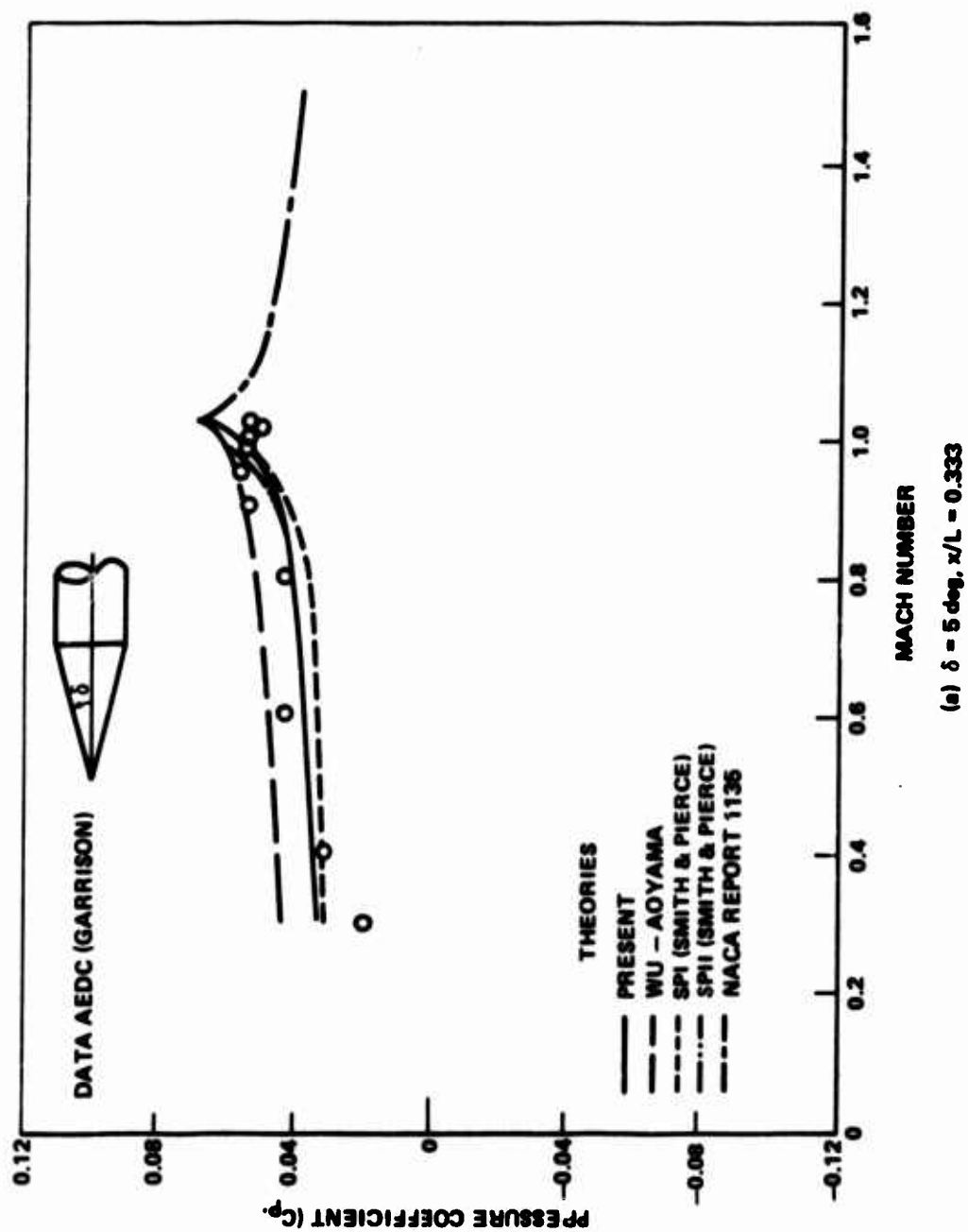


Figure 9. Variation of  $C_p$  with free-stream Mach number for a sharp cone.

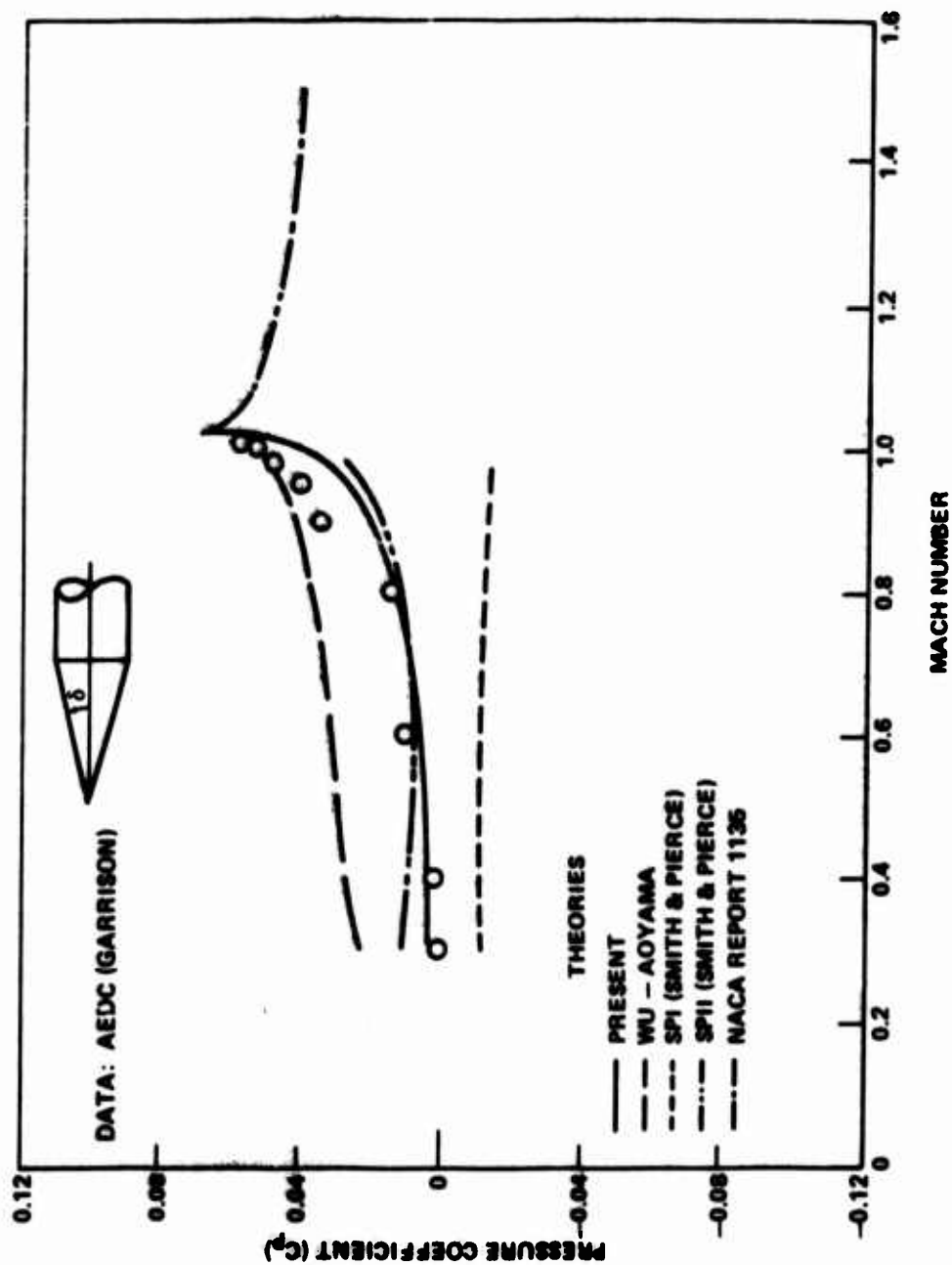
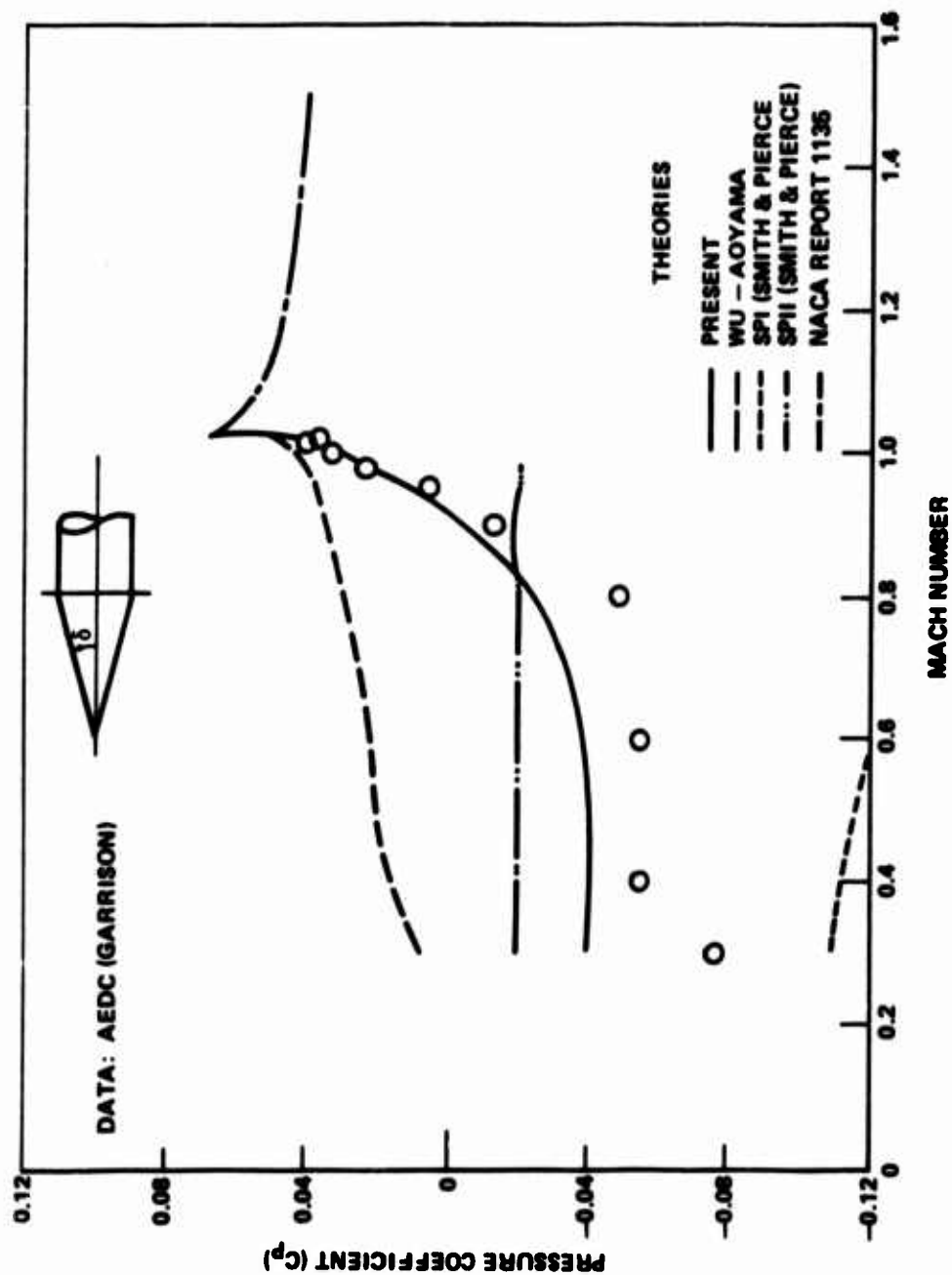


Figure 9. (Continued).



(c)  $\delta = 5 \text{ deg}$ ,  $x/L = 0.9$

Figure 9. (Concluded).

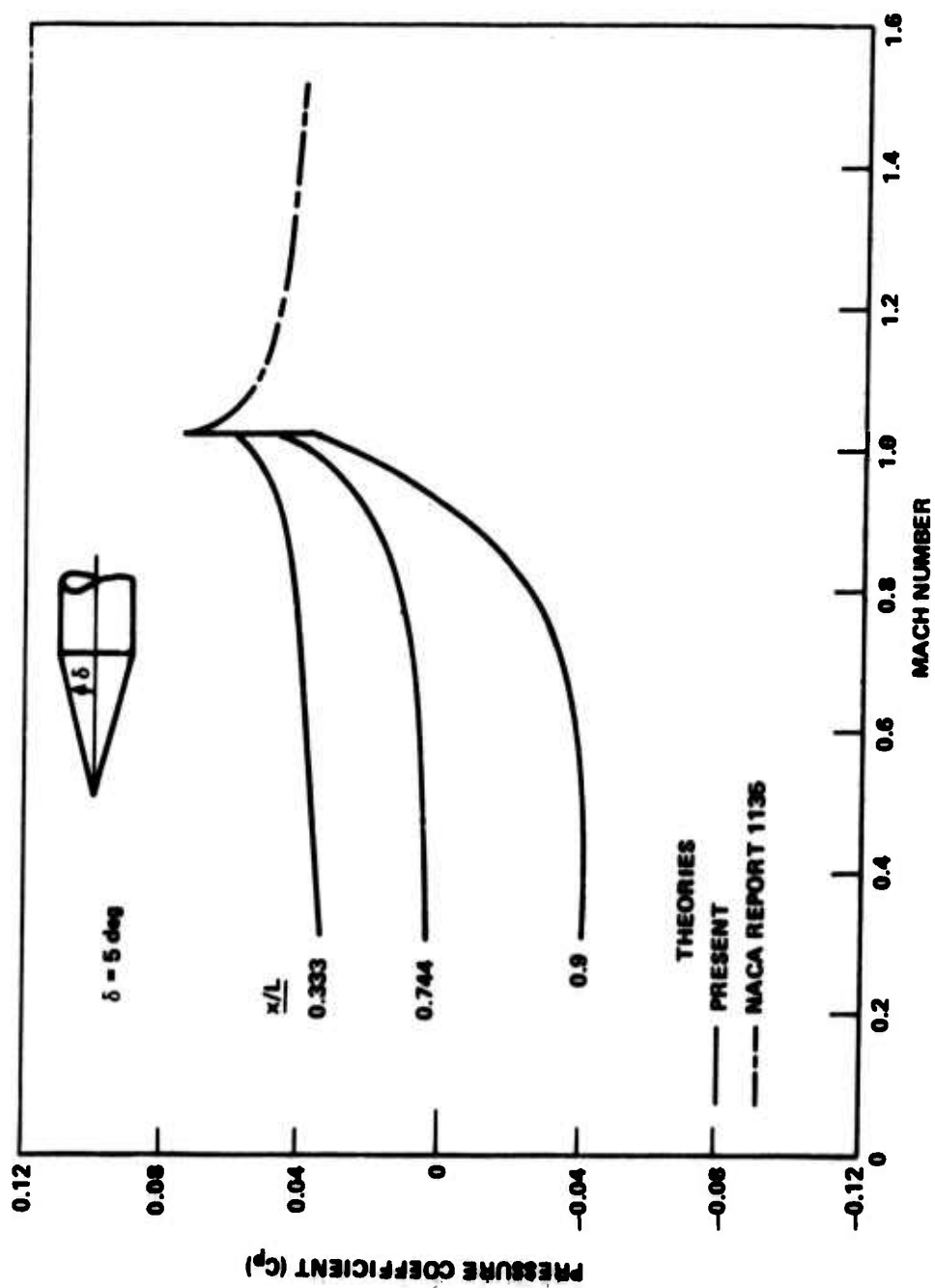


Figure 10. Variation of  $C_p$  with free-stream Mach number for several axis locations on a sharp cone.

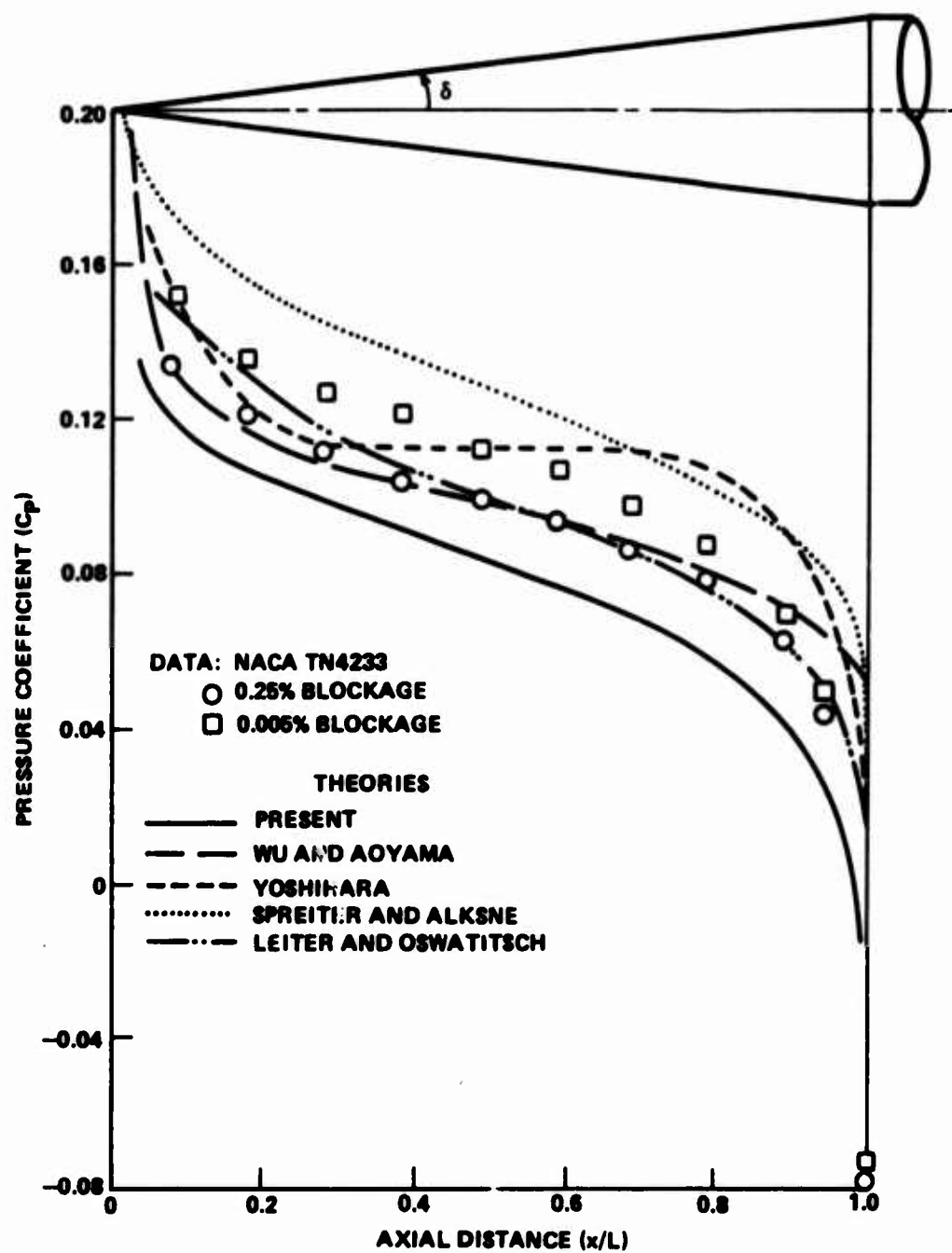


Figure 11. Comparison of various transonic methods with data ( $\delta = 7^\circ$ ,  $M_\infty = 1.0$ ).

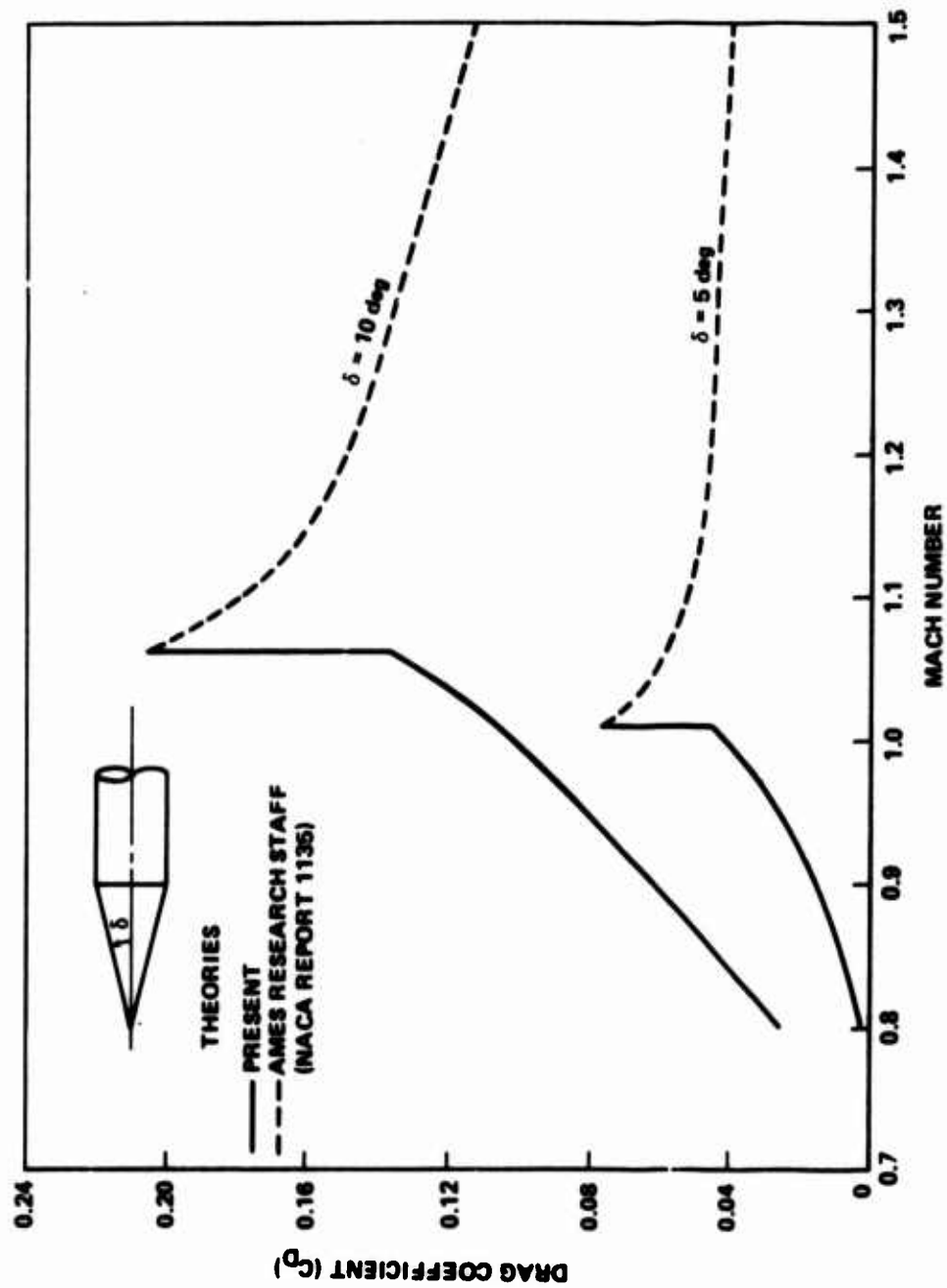


Figure 12. Comparison of pressure drag with Mach number (present method).

## Section V. CONCLUSIONS AND RECOMMENDATIONS

It can be concluded from this study that the present method provides the first real unified solution to the flow on the surface of a cone. It is applicable for the full range of Mach numbers right up to shock attachment. However, because the shape of the sonic line is not known a priori as a function of Mach number and cone angle, the total flow field solution cannot be computed. Although the solutions exhibit the correct tendencies with Mach number, the values calculated above  $M_\infty = 0.95$  are somewhat lower than the experimental results. This is due to the fact that the solution is only a first approximation. One recommendation would be to apply a successive approximation technique to solve for the complete velocity potential. This deviation may also be a result of forcing  $f(\xi)$  positive when solving the integral equation [Equation (68)]. Another recommendation would be to allow  $f(\xi)$  to assume negative values, iterate until the solution converged, even though the maximum value of  $\bar{x}(\xi)$  would be greater than one, and then compress the  $\bar{x}(\xi)$  scale about the center  $\bar{x}(\xi)$  such that  $0 \leq \bar{x}(\xi) \leq 1$ . Preliminary calculations indicate this would probably raise the pressure coefficient values all along the cone surface.

Different rearrangements of the terms of Equation (68), as discussed in Appendix A, might also be explored.

Consider also the possibility that viscous effects become important for these Mach numbers. Another recommendation would be to correct the present inviscid solutions for viscous effects in an effort to find better agreement with experimental data. Finally, it is recommended that the shape of the sonic line be studied in an attempt to obtain solutions for the whole flow field.

Although all of these recommendations relate to adjustments of the present method, the possibility that the experimental data are inaccurate for those upper transonic Mach numbers should not be completely ruled out either. It is a well-known fact that wind-tunnel wall interference effects, as well as compressibility effects, become very significant in this Mach number range.

## REFERENCES

1. Liepmann, H. W. and Roshko, A., Elements of Gas-Dynamics, New York, John Wiley and Sons, Inc., 1957.
2. Smith, A. M. O. and Pierce, Jesse, Exact Solution of the Neumann Problem, Calculation of Non-Circulatory Plane and Axially Symmetric Flows About or Within Arbitrary Boundaries, Douglas Aircraft Company Report No. ES26988, El Segundo, California, April 1958.
3. Van Dyke, M. D., Second-Order Slender Body Theory - Axisymmetric Flow, National Advisory Committee for Aeronautics, TN-4281, Washington, D.C., September 1958.
4. Ames Research Staff, Equations, Tables and Charts for Compressible Flow, National Advisory Committee for Aeronautics, Report No. 1135, Washington, D.C., 1953.
5. Yoshihara, H., On the Flow Over a Cone-Cylinder at Mach Number One, Wright Air Development Center, TR-52-295, Wright Air Field, Ohio, November 1952.
6. Leiter, E. and Oswatitsch, K., "Ermittlung Stationärer Schallnaher Strömungen im Absteigeverfahren aus dem Instationären," Zeitschrift für Angewandte Mathematik und Mechanik, 48:187-191, March 1968.
7. Spreiter, J. R. and Alksne, A. Y., Slender-Body Theory Based on Approximate Solution of the Transonic Equation, National Aeronautics and Space Administration, TR-R-2, Washington, D.C., 1959.
8. Wu, J. M., Aoyama, K., and Moulden, T. H., Transonic Flow Fields Around Various Bodies of Revolution, Including Preliminary Studies on Viscous Effects With and Without Plume, US Army Missile Command, Redstone Arsenal, Alabama, Report No. RD-TR-71-12, May 1971.
9. Wu, J. M. and Aoyama, K., Preliminary Review of Approximate Calculative Methods for Transonic Flow Around Bodies of Revolution, US Army Missile Command, Redstone Arsenal, Alabama, Report No. RD-TR-72-4, March 1972.
10. Aoyama, K., Analysis of Transonic Flow Field Around Bodies of Revolution, Ph.D. dissertation, The University of Tennessee, Knoxville, Tennessee, 1971.

## Appendix A. DETAILS OF THE NUMERICAL ITERATION PROCEDURE

Details of the numerical procedures used in the present analysis are described below.

Rewrite Equation (68) as:

$$f^3(\bar{\xi}) = A + \frac{\delta^2}{2} (\gamma + 1) M_\infty^2 [-B + C - D - E - F] \quad (A-1)$$

where

$$A = \left[ \left( 1 - M_\infty^2 \right) - 2\delta (\gamma + 1) M_\infty^2 \sin \alpha \cos \theta \right] f(\bar{\xi}) \quad ,$$

$$B = 2f(\bar{\xi}) \ln \left[ \frac{\delta \bar{x}(\bar{\xi})}{2\xi^{**} \sqrt{\bar{\xi}(1 - \bar{\xi})}} \right] \quad ,$$

$$C = \frac{(1 - 2\bar{\xi})\bar{x}(\bar{\xi})}{\xi^{**}\bar{\xi}(1 - \bar{\xi})} \quad ,$$

$$D = \int_0^1 \frac{f(\bar{k}) - f(\bar{t})}{|\bar{\xi} - \bar{t}|} d\bar{t} \quad ,$$

$$E = \frac{\bar{x}(\bar{\xi})}{\xi^{**}\bar{\xi}} \quad ,$$

$$F = \frac{1 - \bar{x}(\bar{\xi})}{\xi^{**}(1 - \bar{\xi})} \quad ,$$

and remember  $\bar{x}(\bar{\xi}) = \xi^{**} \int_0^{\bar{\xi}} f(\bar{t}) d\bar{t}$ .

The values of  $f(\bar{\xi})$ ,  $\xi^{**}$ , and  $\bar{x}(\bar{\xi})$  calculated by the original Wu-Aoyama method are used as the first approximation values in the present iteration scheme, and are substituted into Equation (A-1) to solve for new values of  $f(\bar{\xi})$ . A new value of  $\xi^{**}$  is then calculated according

to  $\xi^{**} = 1/\int_0^1 f(\bar{\xi})d\bar{\xi}$  using the new values of  $f(\bar{\xi})$ , and, finally, new values of  $\bar{x}(\bar{\xi})$  are calculated according to  $\bar{x}(\bar{\xi}) = \xi^{**} \int_0^{\bar{\xi}} f(\bar{\xi})d\bar{\xi}$ .

Several tests are then made to see if the new values of  $f(\bar{\xi})$  are acceptable and satisfy convergence. If they do not, then these new values of  $\xi^{**}$ ,  $f(\bar{\xi})$ , and  $\bar{x}(\bar{\xi})$  are substituted into Equation (A-1) to begin a second iteration. Successive iterations are performed until the solution converges.

A plot showing the relative magnitudes of the individual terms of Equation (A-1) is presented in Figure A-1. The terms were calculated during the first iteration using the Wu-Aoyama values of  $\bar{x}(\bar{\xi})$ ,  $\xi^{**}$ , and  $f(\bar{\xi})$ . It is easy to see that term B is dominant except near the shoulder ( $\bar{\xi} = 1$ ) where term C becomes dominant. Term A is not shown because it is small for the particular case being discussed and varies from 0.0175 at  $\bar{\xi} = 0.01$  to 0.0113 at  $\bar{\xi} = 0.99$ . At lower Mach numbers the value of term A would increase somewhat.

It should also be noted that the factor

$$\frac{\delta^2}{2} (\gamma + 1) M_\infty^2$$

is very dependent on the cone angle and the Mach number. Even so, very close to the shoulder, the right-hand side of Equation (A-1) becomes negative. This is caused by term C which has a tendency to blow up at  $\bar{\xi} = 1$ . This singularity is artificially eliminated in the computer program, as follows.

As long as the right-hand side of Equation (A-1) is positive, the value of  $f(\bar{\xi})$  is calculated according to Equation (A-1). However, when the right-hand side becomes negative, the value of each successive  $f(\bar{\xi})$  is forced to equal one-half the value of  $f(\bar{\xi})$  of the previous iteration. For example, if  $f(0.89) = 0.1$  and  $f(0.90) = -0.2$ , as calculated by Equation (A-1), then  $f(0.90)$  would be set equal to

$$0.5 f(0.90) \text{ previous iteration}$$

$$f(0.91) = 0.5 f(0.91) \text{ previous iteration}$$

etc., up to the shoulder. In effect, this procedure is simply limiting the effect that term C can have on the solution.

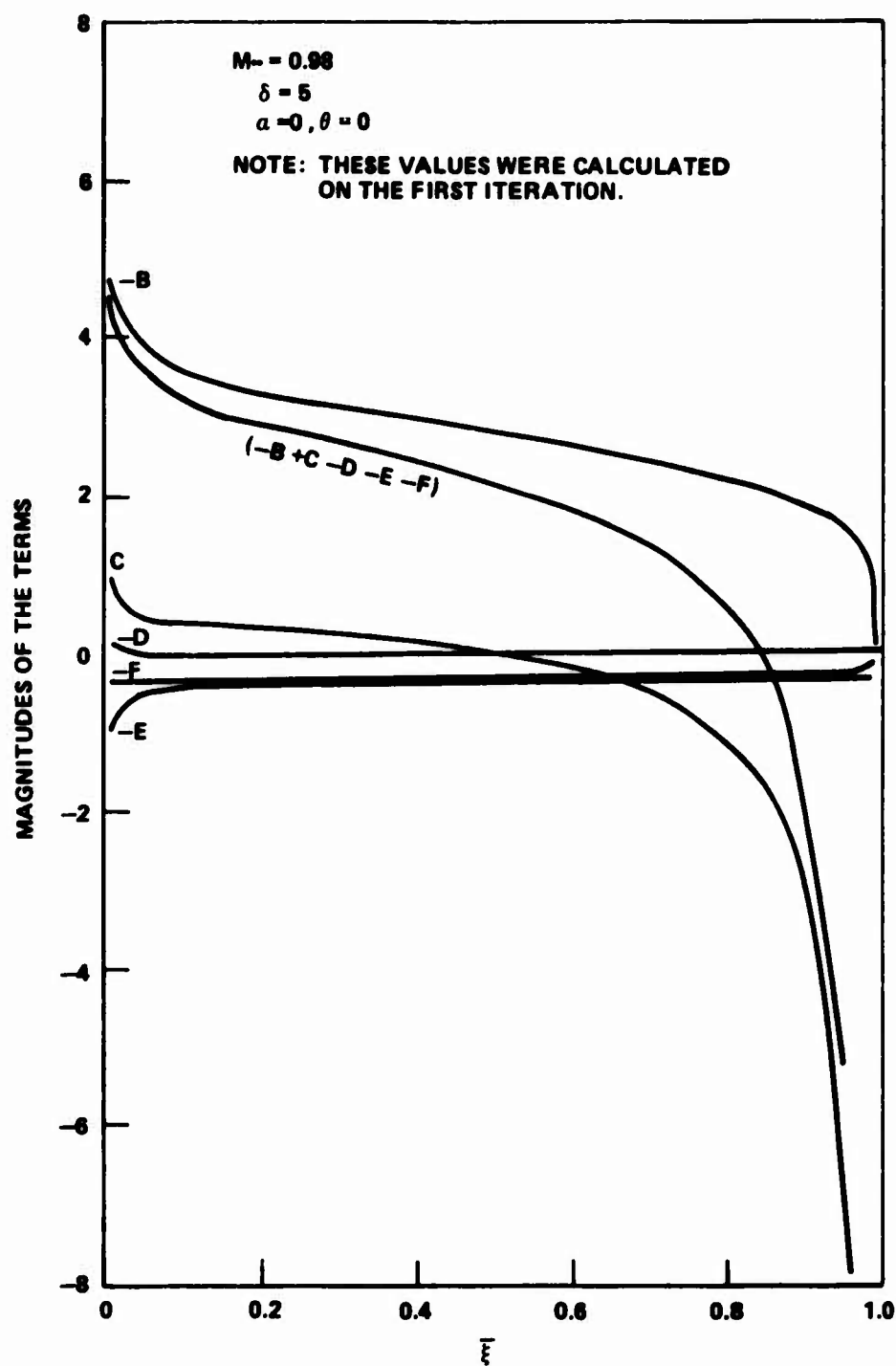


Figure A-1. Comparison of terms of integral Equation (A-1).

Now there are two tests for convergence:

1) Test No. 1: Whenever the maximum absolute difference between the new value of  $f(\xi)$  and the previous value of  $f(\xi)$  is less than or equal to 0.005, the iteration is halted. This works for the low Mach number cases. However, for Mach numbers in the transonic regime, it was found that the iterative solution developed an instability near the shoulder if the number of iterations became too large.

2) Test No. 2: Hence, the iteration was stopped as soon as the pressure coefficient values achieved a monotonically decreasing trend up to a value of  $x/L = 0.99$ . Figures A-2 and A-3 show typical plots of  $f(\xi)$  as calculated by the present method. A minimum of three iterations was always calculated after the Wu-Aoyama solution was obtained.

A solution was said to be nonconvergent if, after 10 iterations of the Wu-Aoyama preliminary calculations, test No. 1 had not been satisfied, or if after 25 iterations after the Wu-Aoyama solution was obtained, both tests No. 1 and No. 2 were still not satisfied.

Convergence was found to be very dependent on Mach number. Figure A-4 shows the maximum Mach numbers for which solutions converged.

Now the velocity,  $\phi_x$ , is calculated according to Equation (75) and, hence, values for the pressure coefficient,  $C_p$ , are obtained using Equation (76). Then the local Mach numbers at each location on the surface of the cone are calculated according to:

$$M = \left[ \left( \left( \frac{P_t}{P} \right)^{\frac{\gamma-1}{\gamma}} - 1 \right) \frac{2}{\gamma-1} \right]^{1/2}, \quad (A-2)$$

which was derived using the isentropic flow conditions where the total to static pressure ratio has been expressed in terms of the pressure coefficient as follows:

$$\frac{P_t}{P} = \frac{\frac{P_t}{P_\infty}}{1 + \frac{\gamma}{2} M_\infty^2 C_p}$$

and

$$\frac{P_t}{P_\infty} = \left[ 1 + \frac{\gamma-1}{2} M_\infty^2 \right]^{\frac{\gamma}{\gamma-1}}$$

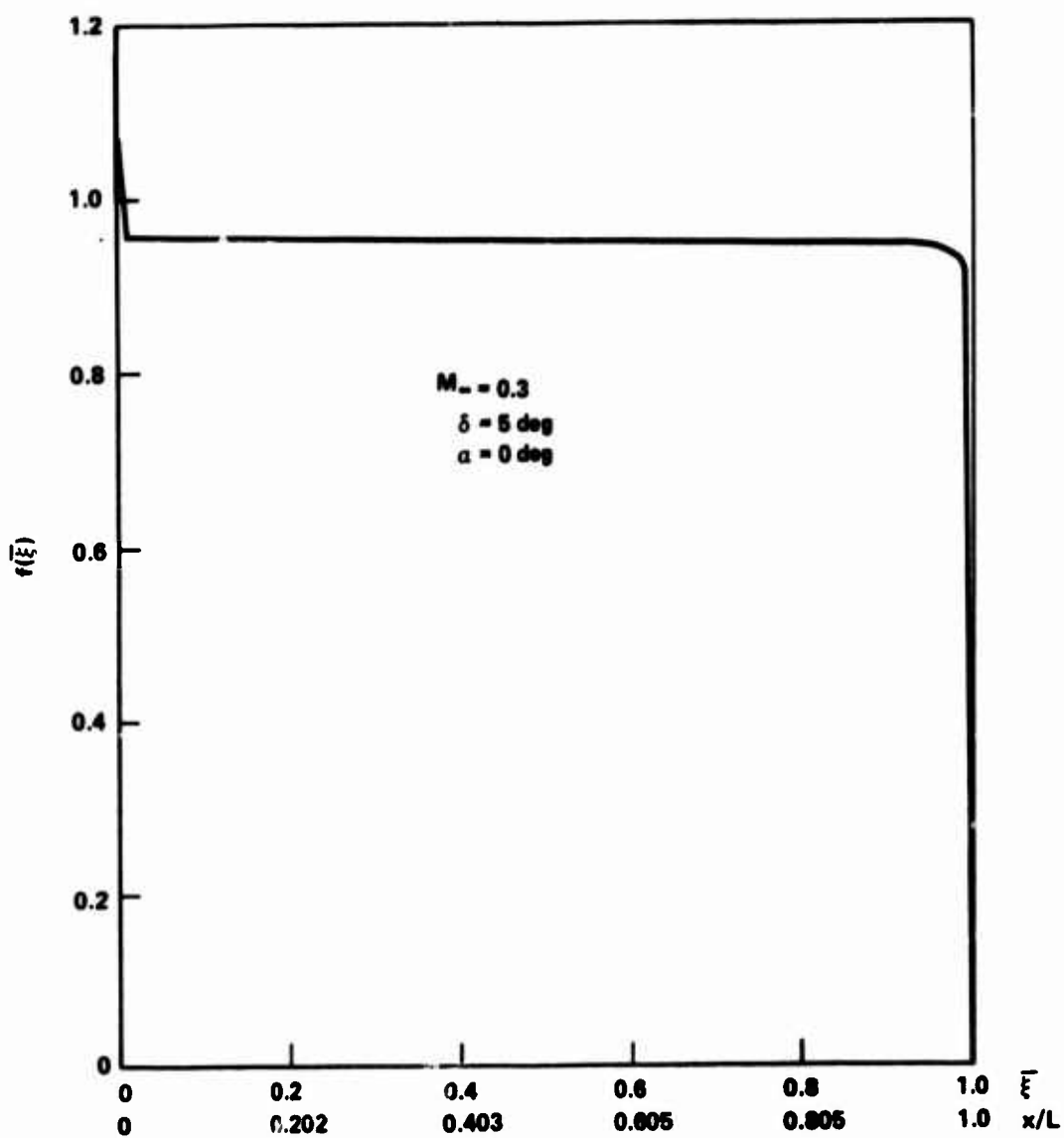


Figure A-2. Typical plot of  $f(\xi)$  for a subsonic Mach number.

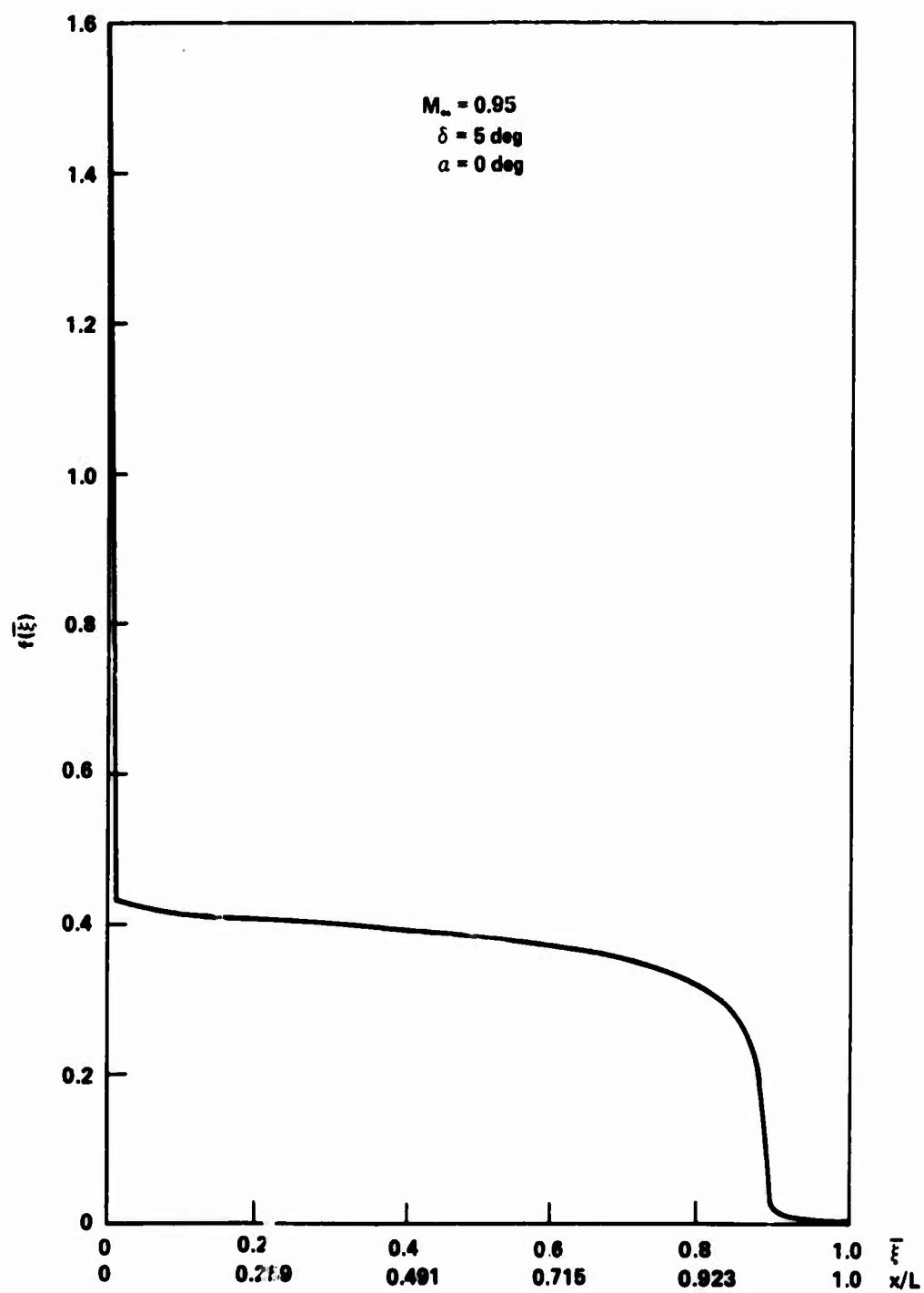


Figure A-3. Typical plot of  $f(\bar{\xi})$  for a transonic Mach number.

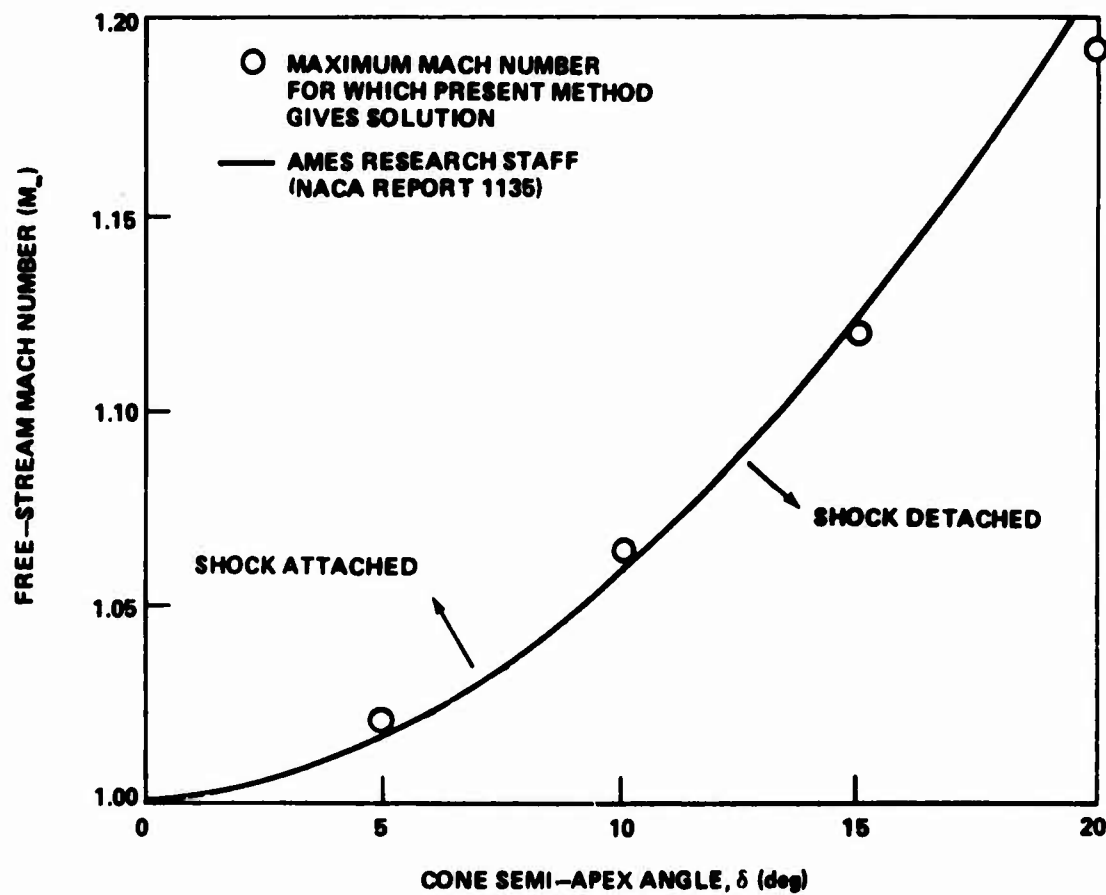


Figure A-4. Comparison of shock attachment Mach numbers of present method with supersonic flow theory.

Also, the free-stream to static pressure ratio is calculated for all points on the cone surface according to:

$$\frac{P_{\infty}}{P} = \frac{1}{C_p \frac{\gamma}{2} M_{\infty}^2 + 1} .$$

Finally, the pressure drag coefficient is calculated for the zero angle of attack cases according to:

$$C_{D1} = 2 \int_0^1 C_p \bar{x}(\bar{\xi}) \frac{d\bar{x}(\bar{\xi})}{d\bar{\xi}} d\bar{\xi}$$

where

$$\frac{d\bar{x}(\bar{\xi})}{d\bar{\xi}} = \xi^{**} f(\bar{\xi}) .$$

It should be noted that several different techniques were tried in order to cause the  $f(\bar{\xi})$  values to drop towards zero closer to the shoulder, as shown by the dotted line in Figure A-5. However, since  $\bar{x}(\bar{\xi})$ ,  $\xi^{**}$ , and  $f(\bar{\xi})$  are all dependent on one another, the only effect was that  $\xi^{**}$  assumed a different value for the new  $f(\bar{\xi})$  values and left the surface pressure distribution relatively unchanged.

Another trial included letting  $f(\bar{\xi})$  assume negative values. This resulted in values of  $\bar{x}$  greater than one. Although this technique was not pursued in this study, it was noted that a more thorough investigation may prove worthwhile.

The  $x/L$  values can be collapsed onto a compressed scale such that  $0 \leq x/L \leq 1$ , which might adjust the surface pressure coefficient values closer to those obtained by experiment.

Another technique that might be used is the rearrangement of the terms on the right-hand side of Equation (68) to see if the effect of the singularity at the shoulder can be minimized.

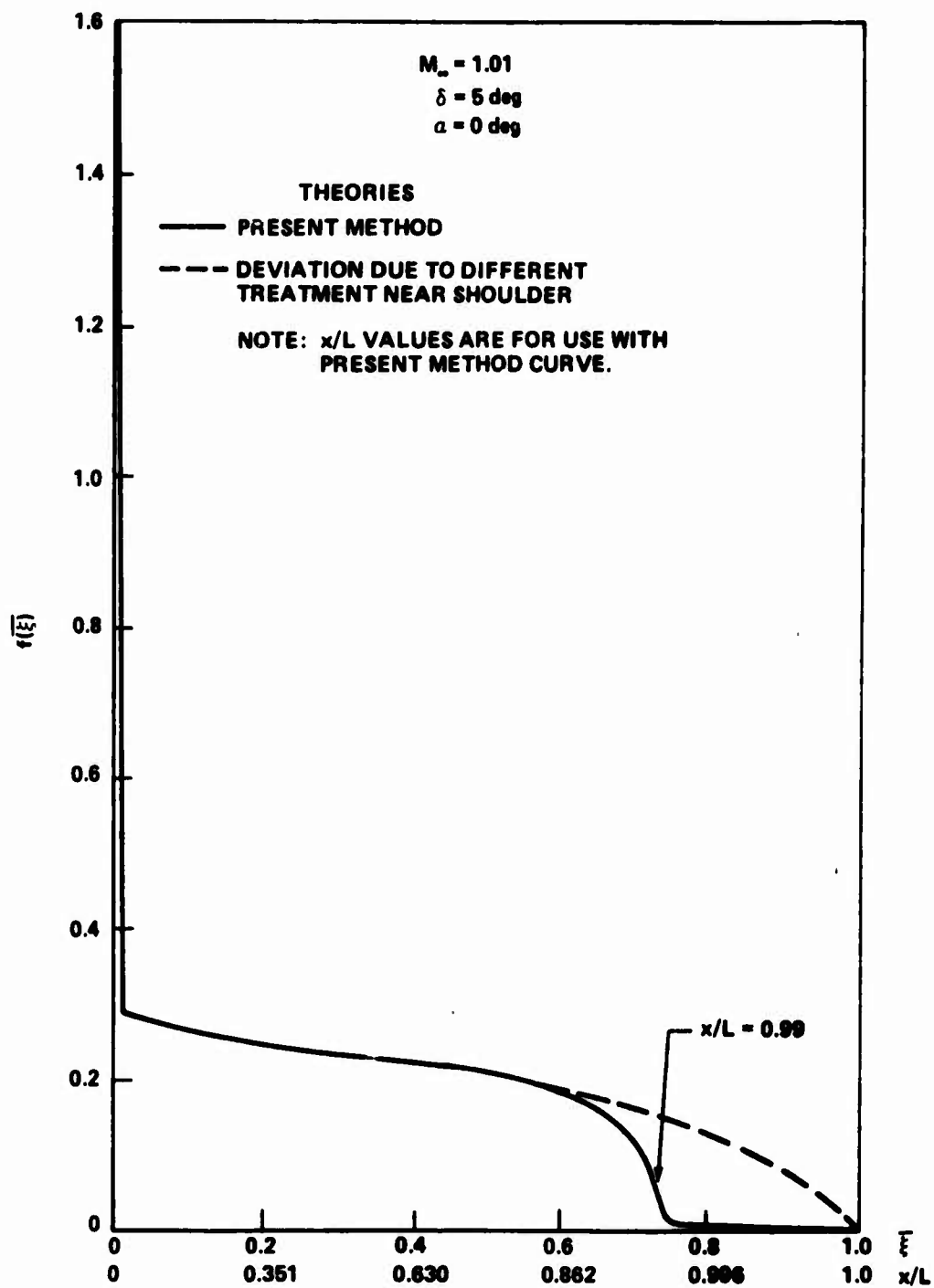


Figure A-5. Typical plot of  $f(\bar{\xi})$  near the shock attachment Mach number.

## Appendix B. COMPUTER PROGRAM AND SAMPLE OUTPUT

This appendix presents a listing of the computer program which calculates the surface pressure distribution on a cone according to the present method, followed by a sample output. The program was written for the IBM 370/155 computer at Arnold Engineering Development Center, Arnold Air Force Station, Tennessee. The drag coefficient is only printed for the case of zero angle of attack. To calculate the drag coefficient for the case of small angles of attack, simply add  $\alpha^2$  to the zero angle of attack value [see Equation (88)].

A list of symbols used in the output along with their meanings is presented in Table B-1.

TABLE B-1. COMPUTER PROGRAM SYMBOLS

Notation of Computer Output	Notation Used in Report
MACH INF	$M_{\infty}$
CONE SEMIVERTEX ANGLE	$\delta$
GAMMA	$\gamma$
ANGLE OF ATTACK	$\alpha$
AZIMUTH ANGLE	$\theta$
ITERATION	Total number of iterations performed (including those of the Wu-Aoyama calculations)
KSAI (SONIC)	$\xi^{**}$
DRAG COEFFICIENT	$C_{D1}$
KSAI	$\bar{\xi}$
X/L	$\bar{x}(\bar{\xi})$
F	$f(\bar{\xi})$
DF	$f(\bar{\xi}) _{\text{last iteration}} - f(\bar{\xi}) _{\text{previous iteration}}$
U	$\phi_{\bar{x}}$
CP	$C_p$
M	M
X/D	Ratio of axial position on cone to base diameter of cone
PI/P	$\frac{p_{\infty}}{p}$

```

0001 REAL MINF,MSIS,MAX
0002 DIMENSION Z(125), F(125), FM(125), D(125), V(125), X(125), CP(125)
0003 1. U(125), SC(125), ZM(125), SF(125), FM3(125), CD(125)
0004 DIMENSION AL(125),BL(125),CL(125),DL(125),EL(125),FL(125),GL(125)
0005 C
0006 THIRD = 1.0/3.0
0007 THETA=0.0
0008 ALFA = 0.0
0009 GAMMA=1.0
0010 SALISBURY=1.0
0011 GALT=0.0
0012 ZERO = 0.0
0013 C1 = -1.5
0014 C2 = 1.0
0015 C3 = -0.25
0016 C
0017 CONTINUE
0018 HEAD (5,21,END=99) MINF,DELTA,ALFA,THETA
0019 C
0020 MINF = FREE-STREAM MACH NUMBER
0021 DELTA = SKEWER ANGLE OF CONE IN DEGREE
0022 THETA = AZIMUTH ANGLE IN DEGREE
0023 ALFA=ANGLE OF ATTACK
0024 C
0025 WRITE (6,22)
0026 WRITE (6,25) MINF,DELTA,GAMMA
0027 WRITE (6,25) ALFA,THETA
0028 C
0029 ALFA=ALFA/57.29578
0030 TETA=THETA/57.29578
0031 DEL=DELTA/57.29578
0032 DEL=DELTA/57.29578
0033 DEL=DELTA/57.29578
0034 DEL=DELTA/57.29578
0035 SC16 = -2.0*SIN(ALFA)*COS(THETA)*DEL*GAM
0036 P1=1.0-0.5*GAM*(MINF**2)*DEL*GAM
0037 ITC=0
0038 IF (DEL*GAM) 2,3,3
0039 WRITE (6,25)
0040 GO TO 20
0041 C
0042 NO=NO+1
0043 GALT=0.5*GALT*DEL**2
0044 A=0.0
0045 H=0.0
0046 D(1)=0.0
0047 F(1)=0.0
0048 F(1)=0.0
0049 FM(1)=0.0
0050 FM(1)=0.0
0051 FM(1)=0.0
0052 U(1)=1.0
0053 U(1)=DEL*GAM
0054 X(1)=0.0
0055 X(1)=0.0

```

```

0045      V(1)=0.0
0046      V(101)=1.0
      C
0047      C FIRST ITERATION
      KSI=0.0/RM
      C
0048      DO 4 I=2,100
0049      A=0.01
0050      A(I) = RHO*ACSI(I).0 + A*(C1 + A*(C2 + C3*A(I)))
0051      F(I)=A*(1.0-A(I))
0052      V(I)=A
0053      C CONTINUE
0054      C
0055      A=0.0
0056      IF (I.E.1)
      C
0057      DO 9 I=2,100
0058      A=0.01
      C
0059      DO 6 J=1,101
0060      A=0.0
0061      SE(J)=F(J)/SQRT((V(I)-A)*0.02*(1.0+V(I)/KSI*0.02))
0062      C CONTINUE
      C
0063      CALL SERIM (M=SE, Z=101)
0064      F(I) = 0.0
0065      F(I) = Z(101)*GAM*SE(I) + SE(I) + SC(I)*F(I)
0066      IF (F(I) < 0.0) F(I) = F(I)*-1.0
0067      IF (F(I) < 0.0) F(I) = F(I)*0.5
0068      U(I)=F(I)-F(I)
0069      U(I)=(0.02*(F(I)-F(I)))/GAM
0070      C CONTINUE
      C
0071      CALL SERIM (M=FM, Z=101)
0072      KSI=1.0/Z(101)
      C
0073      DO 11 I=2,100
0074      CALL SERIM (M=FM, Z=11)
0075      A(I)=KSI*F(I)
0076      C CONTINUE
      C
0077      DO 16 I=1,101
0078      GAMF = A*(F(I))
0079      MAX = MAX(MAX, GAMF)
0080      F(I)=F(I)
0081      C CONTINUE
      C
0082      IF (MAX < 0.005) I=10.17
0083      IF (I.E.10) S=2.2
0084      C CONTINUE
      C
0085      ITER=0

```



74

0175	010X.00.12X.010.12X.010.01)
220	FORMAT (9F13.5,15)
0176	FORMAT /0.2X.1 MACH INF = 0.0.0.54. CONE SEMI-VENTX ANGLE = 0.
0177	079.41.01051.5X.00000 = 0.0.3.1)
001	FORMAT(/ 10X20.0N6 COEFFICIENT = 013.5 //)
0178	END

	1	2
0001	SUMROUTINE SEIN (M=2,N=10)	
0002	DIMENSION W(125),Z(125)	
0003	SUMZ=0	
0004	DO 1 I=2,N+1	
0005	SUM1=SUMZ	
0006	SUMZ=SUMZ+0.5*W(I)*W(I-1)	
0007	Z(I-1)=SUM1	
0008	Z(N+1)=SUMZ	
0009	RETURN	
0010	END	

# UNIFIED SUBSONIC - TRANSONIC FLOW SOLUTION FOR A CONE

MACH INF = 1.0000 CONE SEMI-VENTER ANGLE = 5.0000(DEG) GAMMA = 1.400

ANGLE OF ATTACK = 0.0 DEGREE AZIMUTH ANGLE = 0.0 DEGREE

ITERATION 7: KSAI(SONIC) = 0.00207

DRAG COEFFICIENT = 0.00011

KSAI	X/L	F	INF	U	CP	M	X/D	PI/P
0.0	0.0	1.5019	0.0	-1.0000	1.0000	0.0	0.0	0.0000
0.0100	0.0036	0.3220	-0.00251	-0.00002	0.00002	0.0	0.25924	0.01739
0.0200	0.0002	0.31419	-0.00222	-0.00013	0.00002	0.0	0.25924	0.00000
0.0300	0.0002	0.30425	-0.00193	-0.00005	0.00002	0.0	0.25924	0.00000
0.0400	0.0001	0.30580	-0.00171	-0.00004	0.00002	0.0	0.25924	0.00000
0.0500	0.0001	0.30306	-0.00155	-0.00003	0.00002	0.0	0.25924	0.00000
0.0600	0.0001	0.30073	-0.00144	-0.00002	0.00002	0.0	0.25924	0.00000
0.0700	0.0001	0.29868	-0.00136	-0.00002	0.00002	0.0	0.25924	0.00000
0.0800	0.0001	0.29682	-0.00130	-0.00002	0.00002	0.0	0.25924	0.00000
0.0900	0.0001	0.29512	-0.00126	-0.00002	0.00002	0.0	0.25924	0.00000
0.1000	0.0001	0.29356	-0.00123	-0.00002	0.00002	0.0	0.25924	0.00000
0.1100	0.0001	0.29205	-0.00121	-0.00002	0.00002	0.0	0.25924	0.00000
0.1200	0.0001	0.29064	-0.00120	-0.00002	0.00002	0.0	0.25924	0.00000
0.1300	0.0001	0.28930	-0.00119	-0.00002	0.00002	0.0	0.25924	0.00000
0.1400	0.0001	0.28800	-0.00119	-0.00002	0.00002	0.0	0.25924	0.00000
0.1500	0.0001	0.28675	-0.00119	-0.00002	0.00002	0.0	0.25924	0.00000
0.1600	0.0001	0.28554	-0.00120	-0.00002	0.00002	0.0	0.25924	0.00000
0.1700	0.0001	0.28437	-0.00121	-0.00002	0.00002	0.0	0.25924	0.00000
0.1800	0.0001	0.28322	-0.00122	-0.00002	0.00002	0.0	0.25924	0.00000
0.1900	0.0001	0.28209	-0.00123	-0.00002	0.00002	0.0	0.25924	0.00000
0.2000	0.0001	0.28099	-0.00125	-0.00002	0.00002	0.0	0.25924	0.00000
0.2100	0.0001	0.27990	-0.00126	-0.00002	0.00002	0.0	0.25924	0.00000
0.2200	0.0001	0.27882	-0.00128	-0.00002	0.00002	0.0	0.25924	0.00000
0.2300	0.0001	0.27776	-0.00130	-0.00002	0.00002	0.0	0.25924	0.00000
0.2400	0.0001	0.27670	-0.00132	-0.00002	0.00002	0.0	0.25924	0.00000
0.2500	0.0001	0.27566	-0.00136	-0.00002	0.00002	0.0	0.25924	0.00000
0.2600	0.0001	0.27461	-0.00136	-0.00002	0.00002	0.0	0.25924	0.00000
0.2700	0.0001	0.27357	-0.00139	-0.00002	0.00002	0.0	0.25924	0.00000
0.2800	0.0001	0.27253	-0.00141	-0.00002	0.00002	0.0	0.25924	0.00000
0.2900	0.0001	0.27149	-0.00144	-0.00002	0.00002	0.0	0.25924	0.00000
0.3000	0.0001	0.27045	-0.00147	-0.00002	0.00002	0.0	0.25924	0.00000
0.3100	0.0001	0.26940	-0.00150	-0.00002	0.00002	0.0	0.25924	0.00000
0.3200	0.0001	0.26835	-0.00153	-0.00002	0.00002	0.0	0.25924	0.00000
0.3300	0.0001	0.26729	-0.00156	-0.00002	0.00002	0.0	0.25924	0.00000
0.3400	0.0001	0.26622	-0.00159	-0.00002	0.00002	0.0	0.25924	0.00000
0.3500	0.0001	0.26515	-0.00163	-0.00002	0.00002	0.0	0.25924	0.00000
0.3600	0.0001	0.26406	-0.00167	-0.00002	0.00002	0.0	0.25924	0.00000

0.37000	0.54954	0.26296	-0.00171	-0.02041	0.05001	0.97021	3.00110	0.96610	38
0.38000	0.55324	0.26194	-0.00175	-0.02057	0.04952	0.97050	3.01100	0.96650	39
0.39000	0.55689	0.26070	-0.00179	-0.02082	0.04902	0.97079	3.02100	0.96690	40
0.40000	0.56049	0.25955	-0.00183	-0.02107	0.04852	0.97109	3.03100	0.96730	41
0.41000	0.56403	0.25830	-0.00187	-0.02132	0.04802	0.97139	3.04100	0.96770	42
0.42000	0.56751	0.25714	-0.00191	-0.02156	0.04750	0.97169	3.05100	0.96810	43
0.43000	0.57104	0.25596	-0.00195	-0.02180	0.04699	0.97200	3.06100	0.96850	44
0.44000	0.57461	0.25471	-0.00200	-0.02205	0.04645	0.97232	3.07100	0.96891	45
0.45000	0.57821	0.25344	-0.00204	-0.02230	0.04591	0.97264	3.08100	0.96932	46
0.46000	0.58184	0.25213	-0.00209	-0.02254	0.04536	0.97296	3.09100	0.96973	47
0.47000	0.58550	0.25079	-0.00213	-0.02278	0.04480	0.97328	3.10100	0.97014	48
0.48000	0.58918	0.24948	-0.00218	-0.02302	0.04422	0.97360	3.11100	0.97055	49
0.49000	0.59288	0.24818	-0.00222	-0.02326	0.04363	0.97392	3.12100	0.97096	50
0.50000	0.59660	0.24689	-0.00226	-0.02350	0.04302	0.97424	3.13100	0.97137	51
0.51000	0.60033	0.24561	-0.00230	-0.02374	0.04240	0.97456	3.14100	0.97178	52
0.52000	0.60407	0.24433	-0.00234	-0.02398	0.04177	0.97488	3.15100	0.97219	53
0.53000	0.60782	0.24306	-0.00238	-0.02422	0.04111	0.97520	3.16100	0.97260	54
0.54000	0.61158	0.24180	-0.00242	-0.02446	0.04043	0.97552	3.17100	0.97301	55
0.55000	0.61535	0.24054	-0.00246	-0.02470	0.03973	0.97584	3.18100	0.97342	56
0.56000	0.61912	0.23929	-0.00250	-0.02494	0.03900	0.97616	3.19100	0.97383	57
0.57000	0.62290	0.23803	-0.00254	-0.02518	0.03825	0.97648	3.20100	0.97424	58
0.58000	0.62668	0.23678	-0.00258	-0.02542	0.03749	0.97680	3.21100	0.97465	59
0.59000	0.63046	0.23553	-0.00262	-0.02566	0.03673	0.97712	3.22100	0.97506	60
0.60000	0.63424	0.23428	-0.00266	-0.02590	0.03596	0.97744	3.23100	0.97547	61
0.61000	0.63802	0.23303	-0.00270	-0.02614	0.03519	0.97776	3.24100	0.97588	62
0.62000	0.64180	0.23178	-0.00274	-0.02638	0.03442	0.97808	3.25100	0.97629	63
0.63000	0.64558	0.23053	-0.00278	-0.02662	0.03365	0.97840	3.26100	0.97670	64
0.64000	0.64936	0.22928	-0.00282	-0.02686	0.03288	0.97872	3.27100	0.97711	65
0.65000	0.65314	0.22803	-0.00286	-0.02710	0.03211	0.97904	3.28100	0.97752	66
0.66000	0.65692	0.22678	-0.00290	-0.02734	0.03134	0.97936	3.29100	0.97793	67
0.67000	0.66070	0.22553	-0.00294	-0.02758	0.03057	0.97968	3.30100	0.97834	68
0.68000	0.66448	0.22428	-0.00298	-0.02782	0.02980	0.98000	3.31100	0.97875	69
0.69000	0.66826	0.22303	-0.00302	-0.02806	0.02903	0.98032	3.32100	0.97916	70
0.70000	0.67204	0.22178	-0.00306	-0.02830	0.02826	0.98064	3.33100	0.97957	71
0.71000	0.67582	0.22053	-0.00310	-0.02854	0.02749	0.98096	3.34100	0.97998	72
0.72000	0.67960	0.21928	-0.00314	-0.02878	0.02672	0.98128	3.35100	0.98039	73
0.73000	0.68338	0.21803	-0.00318	-0.02902	0.02595	0.98160	3.36100	0.98080	74
0.74000	0.68716	0.21678	-0.00322	-0.02926	0.02518	0.98192	3.37100	0.98121	75
0.75000	0.69094	0.21553	-0.00326	-0.02950	0.02441	0.98224	3.38100	0.98162	76
0.76000	0.69472	0.21428	-0.00330	-0.02974	0.02364	0.98256	3.39100	0.98203	77
0.77000	0.69850	0.21303	-0.00334	-0.02998	0.02287	0.98288	3.40100	0.98244	78
0.78000	0.70228	0.21178	-0.00338	-0.03022	0.02210	0.98320	3.41100	0.98285	79
0.79000	0.70606	0.21053	-0.00342	-0.03046	0.02133	0.98352	3.42100	0.98326	80
0.80000	0.70984	0.20928	-0.00346	-0.03070	0.02056	0.98384	3.43100	0.98367	81
0.81000	0.71362	0.20803	-0.00350	-0.03094	0.01979	0.98416	3.44100	0.98408	82
0.82000	0.71740	0.20678	-0.00354	-0.03118	0.01902	0.98448	3.45100	0.98449	83
0.83000	0.72118	0.20553	-0.00358	-0.03142	0.01825	0.98480	3.46100	0.98490	84
0.84000	0.72496	0.20428	-0.00362	-0.03166	0.01748	0.98512	3.47100	0.98531	85
0.85000	0.72874	0.20303	-0.00366	-0.03190	0.01671	0.98544	3.48100	0.98572	86
0.86000	0.73252	0.20178	-0.00370	-0.03214	0.01594	0.98576	3.49100	0.98613	87
0.87000	0.73630	0.20053	-0.00374	-0.03238	0.01517	0.98608	3.50100	0.98654	88
0.88000	0.74008	0.19928	-0.00378	-0.03262	0.01440	0.98640	3.51100	0.98695	89
0.89000	0.74386	0.19803	-0.00382	-0.03286	0.01363	0.98672	3.52100	0.98736	90
0.90000	0.74764	0.19678	-0.00386	-0.03310	0.01286	0.98704	3.53100	0.98777	91
0.91000	0.75142	0.19553	-0.00390	-0.03334	0.01209	0.98736	3.54100	0.98818	92
0.92000	0.75520	0.19428	-0.00394	-0.03358	0.01132	0.98768	3.55100	0.98859	93
0.93000	0.75898	0.19303	-0.00398	-0.03382	0.01055	0.98800	3.56100	0.98900	94
0.94000	0.76276	0.19178	-0.00402	-0.03406	0.00978	0.98832	3.57100	0.98941	95
0.95000	0.76654	0.19053	-0.00406	-0.03430	0.00901	0.98864	3.58100	0.98982	96
0.96000	0.77032	0.18928	-0.00410	-0.03454	0.00824	0.98896	3.59100	0.99023	97
0.97000	0.77410	0.18803	-0.00414	-0.03478	0.00747	0.98928	3.60100	0.99064	98
0.98000	0.77788	0.18678	-0.00418	-0.03502	0.00670	0.98960	3.61100	0.99105	99
0.99000	0.78166	0.18553	-0.00422	-0.03526	0.00593	0.98992	3.62100	0.99146	100
1.00000	0.78544	0.18428	-0.00426	-0.03550	0.00516	0.99024	3.63100	0.99187	101

UNIFIED SUBSONIC - TRANSONIC FLOW SOLUTION FOR A CONE

MACH IN<sub>∞</sub> = 1.1800 CONE SEMI-VECTA ANGLE = 5.000010E01 GAMMA = 1.400

ANGLE OF ATTACK = 0.0 DEGREE AZIMUTH ANGLE = 0.0 DEGREE

SUPERSONIC FLOW NO CONVERGENCE

# SYMBOLS

A,B,C,D,E,F	Terms of Equation (A-1) as described in Appendix A
$C_D$	Pressure drag coefficient
$C_p$	Pressure coefficient
D	Pressure drag
F	Source strength
F	Function defined by Equation (43)
f	Transformation function defined by Equation (2)
G	Function defined by Equation (12)
I	Function defined by Equation (40)
K	Function defined by Equation (5b)
L	Length of cone
M	Mach number
p	Static pressure on cone surface
$p_t$	Total pressure
q	Dynamic pressure
R	Body radius
r	Radial coordinate
S	Projected area
s	Dummy variable
t	Dummy variable
$U_\infty$	Free-stream velocity
u	Perturbation velocity in axial direction, $\phi_x U_\infty$
v	Perturbation velocity in radial direction, $\phi_r U_\infty$
w	Perturbation velocity, $(\phi_\theta / \bar{r}) U_\infty$
x	Axial coordinate
$\alpha$	Angle of attack
$\beta$	$\sqrt{1 - M_\infty^2}$ = compressibility factor
$\gamma$	Ratio of specific heats

$\delta$	Half angle of cone
$\epsilon$	Small number defined in Equation (5b)
$\xi$	Independent variable defined by Equation (4)
$\theta$	Roll angle
$\phi$	Linearized perturbation velocity potential

#### Subscripts

a	Axial flow
c	Cross flow
l	Axial flow (drag calculations)
$\bar{r}$	Indicates differentiation with $\bar{r}$
t	Total condition
$\bar{x}$	Indicates differentiation with $\bar{x}$
0,1,2,3	Identification numbers
$\xi$	Indicates differentiation with $\xi$
$\theta$	Indicates differentiation with $\theta$
$\infty$	Free-stream condition

#### Superscripts

$(\bar{\quad})$	Indicates nondimensionalized quantity
*	Conditions at the sonic point on the cone surface
**	Conditions at the sonic point on the cone surface
$(\quad)'$	Differentiation

## BIBLIOGRAPHY

- Garrison, Dr. G. W., AEDC Transonic Acoustics Correlation Test, Unpublished data booklet, Project No. P/2176, Tunnel 1T, Arnold Engineering Development Center, Arnold Air Force Station, Tennessee, April 1971. Also see R. C. Lock, M. S. Thesis, University of Tennessee Space Institute, Tullahoma, Tennessee, December 1973.
- Hamner, R. L. and Leff, A. D., Linear Aerodynamic Loads on Cone-Cylinders at Mach Numbers from 0.7 to 2.0, National Aeronautics and Space Administration, Washington, D.C., Contractor Report 413, March 1966.
- Hartley, M. S. and Jacocks, J. L., Static Pressure Distributions on Various Bodies of Revolution at Mach Numbers from 0.6 to 1.6, Arnold Engineering Development Center, Arnold Air Force Station, Tennessee, TR-68-37, March 1968.
- Jackson, F. M. and Sloan, E. H., Calibration of the AEDC-FWT 1-Foot Transonic Tunnel, Arnold Engineering Development Center, Arnold Air Force Station, Tennessee, TR-68-4, February 1968.
- Mitchell, G. A., Effect of Model Forebody Shape on Perforated Tunnel Wall Interference, National Aeronautics and Space Administration, Washington, D.C., TM-X-1656, April 1968.
- Nichols, J. H., Determination of Optimum Operating Parameters for the PWT 16-ft Transonic Circuit Utilizing One Percent Bodies of Revolution, Arnold Engineering Development Center, Arnold Air Force Station, Tennessee, TN-59-100, September 1959.
- Page, W. A., Experimental Study of the Equivalence of Transonic Flow About Slender Cone-Cylinders of Circular and Elliptic Cross Section, National Advisory Committee for Aeronautics, Washington, D.C., TN-4233, April 1958.
- Rittenhouse, L. E. and Kaupp, H. Jr., An Investigation of the Influence of Several Shape Parameters on the Aerodynamics of Ballistic Re-Entry Configurations, Arnold Engineering Development Center, Arnold Air Force Station, Tennessee, TN-59-16, May 1959.
- Test Facilities Handbook, Arnold Air Force Station, Tennessee, Arnold Engineering Development Center, Eight edition, Vol. 5, 1969.